ADAPTIVE RADAR RECEIVERS FOR TARGET DETECTION IN THE PRESENCE OF CLUTTER

A Thesis Submitted
in Partial Fulfilment of the Requirements
for the Degree of
MASTER OF TECHNOLOGY

By

SRIKANT VISWESWARIAH

to the

DEPARTMENT OF ELECTRICAL ENGINEERING

INDIAN INSTITUTE OF TECHNOLOGY, KANPUR

OCTOBER, 1980

POST GRADUATE OFFICE
Submitted on 27.10.80

CERTIFICATE

This is to certify that the thesis entitled 'ADAPTIVE RADAR RECEIVERS FOR TARGET DETECTION IN THE PRESENCE OF CLUTTER' by Srikant Visweswariah has been carried out under my supervision and that it has not been submitted elsewhere for a degree.

Dr. P.R.K. Rao
Professor
Department of Electrical Engineering
Indian Institute of Technology
Kanpur

Kanpur
Oct. 1980.

PO[illegible]
This thesis [illegible]
for the award of the degree of
Master of [illegible]
in accordance with
regulations [illegible]
Institute of [illegible]
Dated 6.11.80

GENERAL LIBRARY
A 66003
19 MAY 1981

EE-1980-M-VIS-ADA

ACKNOWLEDGEMENTS

I would like to express my thanks to Dr. P.R.K. Rao for his guidance and encouragement during the course of this work. He devoted much of his valuable time for long sessions of discussion with me. It has been a privilege to have worked with him and I will always remember this association with gratitude.

I would also like to thank Dr. S.K. Mullick for useful discussions on the maximum entropy method of spectral analysis.

I am also grateful to my service, the Indian Air Force, for having provided me the opportunity to work towards my M.Tech. degree at I.I.T.Kanpur.

My thanks are also due to Mr. K.N. Tewari for his efficient typing of the thesis.

SRIKANT VISWESWARIAH

TABLE OF CONTENTS

			Page
LIST OF FIGURES			vi
LIST OF TABLES			vii
ABSTRACT			viii
CHAPTER 1		INTRODUCTION	1
	1.1	Background and Previous Related Work	1
	1.2	Organisation of the Thesis	6
CHAPTER 2		THE RADAR DETECTION PROBLEM AND A REVIEW OF THE MAXIMUM ENTROPY METHOD OF SPECTRAL ANALYSIS	10
	2.1	Detection as a Hypothesis Testing Problem	10
	2.2	Target Models for Pulsed Radars	12
	2.3	Modelling of Clutter Returns	15
	2.4	Mathematical Statement of the Problem	18
	2.5	Maximum Entropy Method of Spectral Analysis	25
CHAPTER 3		OPTIMUM RECEIVER FORMULATION	37
	3.1	Integral Equation Approach to the Optimum Receiver	37
	3.2	Performance of the Optimum Receiver	47
CHAPTER 4		STRUCTURED OPTIMUM RECEIVER FORMULATION	53
	4.1	Matched Filter Structure Imposition	54
	4.2	Structured Optimum Receiver for Swerling 1 Target Models	58

4.3 Performance of Structured Optimum Receiver for Swerling 1 Target Models 69

4.4 Performance Evaluation of the Structured Optimum Receiver by Simulation and Numerical Computation 71

CHAPTER 5 STRUCTURED RECEIVER FORMULATION 94

5.1 Structured Receiver Based on the Whitening Filter Concept of MEM 96

5.2 Performance of the Structured Receiver with Coherent Detection 103

5.3 A Generalised Procedure to Calculate P_D and P_F for Receivers where the Sufficient Statistic is obtained by a Summation of Modulus Squared Correlated Jointly Complex Gaussian Random Variables 106

5.4 Performance Evaluation of the Structured Receiver by Simulation and Numerical Computation 118

CHAPTER 6 CONCLUSIONS 137

REFERENCES 143

APPENDIX A 148

APPENDIX B 153

LIST OF FIGURES

Fig.No.	Caption	Page
3.1	Optimum Receiver for Swerling 1 Target Models (Complex Operations).	48
4.1	Matched Filter Structured Optimum Receiver (Complex Operations).	55
4.2	Structured Optimum Receiver for Swerling 1 Target Models (Complex Operations).	65
4.3	Alternate Realisation of the Structured Optimum Receiver (Complex Operations).	67
4.4-4.16	Receiver Operating Characteristic for Structured Optimum and Matched Filter Receivers.	81-93
5.1	Interference Whitening Filter Obtained by MEM (Complex Operations).	97
5.2	Structured Receiver A1 (Complex Operations).	101
5.3	Structured Receiver A2 (Complex Operations).	101
5.4	Structured Receiver B1 (Complex Operations)	102
5.5	Structured Receiver B2 (Complex Operations)	102
5.6	General Configuration of the Receiver (Complex Operations) for which P_D and P_F Expressions are obtained	107
5.7	MTI using a Double Line Canceller (Complex Operations).	124
5.8-5.20	Receiver Operating Characteristic for Structured and MTI Receivers	124-136
A1.1	MEM Recursive Algorithm for a Complex - Valued Time Series.	152

LIST OF TABLES

Table No.	Caption	Page
1	Performance Results of Structured Optimum and Matched Filter Receivers	78

ABSTRACT

This thesis considers the design and performance of adaptive radar receivers in the presence of clutter with slowly time varying statistics.

An optimum radar receiver for detecting a Swerling 1 target in the presence of clutter is derived. Considering the complexity involved in the implementation of such a receiver in a changing clutter environment, two suboptimum receivers are proposed and expressions for their probability of detection performance are derived. These receivers are adaptive in that the slowly time varying clutter statistics are taken into account through the maximum entropy method of spectral analysis of the received signal.

Simulation results show that the first of these receivers, termed the Structured Optimum Receiver, can operate satisfactorily with as few as 16 hits per scan. The performance of this receiver which is always superior to that of the conventional matched filter receiver is compared with that achievable with a received signal without clutter. In the wide range of situations considered, the degradation in performance is small except for low target Doppler shifts and large clutter spectral widths.

The second receiver, termed the Structured Receiver, can easily be implemented relative to the structured optimum receiver particularly if noncoherent detection is employed. The performance of this receiver under both coherent and noncoherent detection modes is compared with that of a moving target indicator (MTI) receiver.

CHAPTER 1

INTRODUCTION

1.1 Background and Previous Related Work

In radar systems, the receiver's ability to detect target echoes is limited not only by additive thermal noise but also by another type of interference called clutter. Clutter is defined as a conglomeration of unwanted radar echoes and arises from the back scattering of electromagnetic energy from possibly extended and fluctuating reflectors. Clutter signals differ from thermal noise in that they are caused by the radar's own transmission. Also what constitute clutter producing reflectors clearly depends on which class of targets a particular radar is intended to detect. In general, clutter signals are statistical in nature and the statistical modelling of radar returns from ground, sea etc. have been the subject of many publications [1-5]. Although several models have been proposed, none can be considered to adequately explain the observed returns. In a clutter model [5] most often used for theoretical analysis, the complex envelope of the clutter signal is considered to be a sample function of a zero-mean complex Gaussian random process. Under wide-sense stationarity and uncorrelated scattering assumptions, the statistics of clutter may then be described by an associated scattering function which

gives a measure of the distribution of the returned clutter energy in the delay-Doppler domain [5]. Although, in practice, these statistics change with time, they may be modelled as quasi time-invariant.

Radar targets are also modelled statistically and various target models have been proposed for different situations by Marcum [6-7], Swerling [8-9], Weinstock [10] and Mitchell [11]. In these models, the radar cross-section of a target is treated as a random variable. The various models differ in their prescription of the probability density function and fluctuation rate of the radar cross-section of the target. For example, the radar cross-section of a Swerling 1 target model is slowly fluctuating and has an exponential density function.

In most of the previous related work on the design of radar receivers for clutter rejection, it has been assumed that the statistics of clutter are a priori known. Also, in addition to receiver design alone, considerable emphasis has been placed on the choice of the transmitted waveform and joint transmitter/ receiver design. In fact, receiver design is very closely linked to signal (or transmitter) design.

There are three principal approaches [5] to the design of receivers for processing of radar echoes in the combined presence of clutter and thermal noise. The first

approach is to find the optimum receiver (optimum in terms of a certain specified performance criterion) for a given clutter scattering function. However, finding this optimum receiver for any arbitrary clutter scattering function is extremely difficult. Moreover, the optimum receiver may turn out to be too complicated to be realised in practice.

Another approach is to design a conventional matched filter receiver assuming that only white thermal noise is present. The degradation in performance due to clutter is then minimised by signal design. For any given clutter scattering function, this consists of minimising the common volume of the scattering function and the shifted signal ambiguity function in the delay-Doppler plane. The best signal will depend on the target's location in the delay-Doppler plane as well as on the scattering function of clutter. In general, receivers designed using this approach are suboptimum in performance.

The third approach is to structure the receiver so that it is implementable - and then, within the constraints imposed by that structure, optimise the performance of such a receiver. In general, the performance of such a receiver will also be suboptimum. However, this structured approach is attractive as it permits design of a receiver that works better than the conventional matched filter receiver (second approach), but can be constrained to

be less complicated than the optimum receiver. In addition to receiver optimisation using the structured approach, joint transmitter/receiver optimisation can be done for a class of transmitter signals/receivers.

The design of optimum receivers for clutter rejection were first investigated by Urkowitz [12] and Manasse [13]. Both assumed a range invariant scattering function with a Doppler spread which was small compared to the signal bandwidth. Urkowitz ignored thermal noise and proposed the inverse filter for clutter rejection. Manasse considered the presence of thermal noise and showed the dependence of the signal to interference (thermal noise plus clutter) ratio at the output of the receiver on the signal bandwidth. He found the best signal to be a wideband signal. Westerfield et.al. [14] considered the approach of designing a conventional matched filter, and then optimising its performance in the presence of clutter by signal design. Stutt and Spafford [15] proposed a 'best' mismatched filter or receiver where the signal to clutter rati is maximised. Rummler [16], Spafford [17], Delong and Hofstetter [18] also investigated the signal and receiver design problem for a slowly fluctuating point target assuming that the scattering function of clutter is a priori known. Most of these investigations were carried

out for a class of transmitter signals/receivers. Delong and Hofstetter [18] and Spafford [17] also proposed steps for joint optimisation of both the transmitter signal and the receiver for a class of transmitter signals/receivers. More related work on the design of radar receivers and transmitter signals can be found in [19-25].

However, in most practical radar systems, because of lack of knowledge of the statistics of clutter, the moving target indicator (MTI) receiver is used to distinguish moving targets in clutter. MTI receivers are simple to implement and are based on the reasoning that ground and sea clutter returns have a very small Doppler spread and can be filtered out or cancelled in delay line cancellers. MTI receivers are obviously suboptimum and their design ignores the presence of thermal noise. A variation of the MTI called the moving target detector (MTD) has been developed at the Massachusetts Institute of Technology [26-27]. In the MTD, fast Fourier transform (FFT) techniques are used to estimate the spectrum of the received signal and filter out clutter returns.

In this thesis, an optimum radar receiver for detecting a Swerling 1 target in the presence of clutter is obtained and it is found that implementing this receiver in a changing clutter environment is extremely difficult. In view of this, this thesis primarily deals

with the design and study of two adaptive structured radar receivers for the detection of a Swerling 1 target in the presence of clutter. These receivers are adaptive in the sense that their parameters are adjusted or updated in response to changes in the statistics of clutter. The quasi time-invariant nature of the statistics of clutter is taken into account through the maximum entropy method of spectral analysis of the received signal during those scans when there is no target or a decision to that effect is made.

1.2 Organisation of the Thesis

This thesis is organised as follows. In this thesis the various bandpass signals, systems and random processes are described in terms of complex envelope notation [5].

In Chapter 2, the radar target detection problem in the presence of clutter is posed as a hypothesis testing problem. Various target models in the context of pulsed radars are considered. The complex envelope of the clutter signal is modelled as a zero-mean complex Gaussian random process. Some of the receiver structures obtained in later chapters as solutions to the target detection problem posed in this chapter, require spectral estimators as subsystems in order to be adaptive to the changing clutter environment. As the maximum entropy method (MEM) of spectral estimation

is most non-committal in its processing of the observations made, we have considered it appropriate to use the MEM for estimation of the required statistics of clutter. Accordingly, in Chapter 2, the MEM of spectral analysis of a stationary time series is briefly reviewed.

In Chapter 3, the optimum receiver for Swerling 1 target models and expressions for its performance are derived. It is found that optimum receivers which continually estimate the required clutter statistics and then update their parameters are difficult to implement with present day technology. In view of this, suboptimum receivers, which are simpler to implement and whose parameters can be determined adaptively using the MEM, are proposed and evaluated in Chapters 4 and 5.

In Chapter 4, a structure is imposed on the receiver and within the constraints imposed by that structure, an optimum receiver is obtained for Swerling 1 target models. Expressions for the performance of such a receiver, termed Structured Optimum Receiver, are derived. A study is made of how the MEM can be used to estimate the required statistics of clutter during those scans when no target is present in the range bin of interest, thereby enabling the parameters of the structured optimum receiver to be determined adaptively. The performance of such a receiver is evaluated by computer simulation and

numerical computation for both the cases when the required clutter statistics are a priori known and when the MEM is used to estimate the required statistics of clutter. These performances are compared with the performance of a conventional matched filter receiver. A large number of receiver operating characteristic (ROC) graphs indicating the performance of the structured optimum receiver for varying conditions of clutter power, clutter spectral width, target Doppler shift etc. are including in this chapter.

In Chapter 5, an adaptive suboptimum receiver, termed Structured Receiver, which in many instances is simpler to implement than the structured optimum receiver, is proposed. This receiver is based on interpreting MEM as an attempt to determine the structure of a whitening filter for a time series. This chapter also discusses how the structured receiver can be used for both coherent and noncoherent detection. Expressions for the performance of structured receivers for both coherent and non-coherent detection modes are derived. The performance of these receivers are evaluated by computer simulation and numerical computation and compared with the performance of a double delay line canceller MTI receiver. Again a large number of ROC graphs indicating the performance of these structured receivers for varying conditions of clutter power, target Doppler shift, clutter spectral width etc. are included in this chapter.

Chapter 6 concludes the thesis with some suggestions for future work.

Appendix A describes the computer simulation scheme used in the performance evaluation of the structured optimum and structured receivers. Appendix B gives a listing of the main program and the subroutines used in the performance evaluation of the structured optimum, structured, matched filter and MTI receivers.

CHAPTER 2

THE RADAR DETECTION PROBLEM AND A REVIEW OF THE MAXIMUM ENTROPY METHOD OF SPECTRAL ANALYSIS

The first part of this chapter formulates the radar target detection problem in the presence of clutter and thermal noise. Section 2.1 considers the radar detection problem as a binary hypothesis testing problem. Section 2.2 enumerates various target models in the context of pulsed radars. This is followed by a discussion on the modelling of clutter in Section 2.3. The pulsed radar detection problem is stated in mathematical terms in Section 2.4.

Some of the receiver structures obtained in later chapters as solutions to the radar detection problem posed here, require spectral estimators as subsystems. As maximum entropy method (MEM) of spectral analysis is most non-committal in its processing of the observations made, we have considered it appropriate to use the MEM for estimation of clutter spectra. Accordingly, in the second part of this chapter, we briefly review the maximum entropy method of spectral analysis of a stationary time series.

2.1 Detection as a Hypothesis Testing Problem

A radar target detection problem may be posed as a binary hypothesis testing problem, which may be stated

as one of finding a decision function of the observations

$$R(t) = R_1(t) \qquad T_i \leq t \leq T_f \qquad : H_1$$

$$R(t) = R_0(t) \qquad T_i \leq t \leq T_f \qquad : H_0$$

which optimises a specified criterion of performance. $R_1(t)$ contains both signal and noise while $R_0(t)$ contains only noise. The nature of assumptions made concerning the statistical information of the received waveforms on hypotheses H_1 and H_0 determines the complexity of the decision function in respect of cost, ease of implementation, sensitivity to small changes in the assumed apriori information and performance. In radar it is difficult to assign a priori probabilities for the occurrence of H_1 or H_0, nor is it possible to assign realistic cost functions for the decisions made. Therefore the Neyman-Pearson criterion is most often used in arriving at a decision function. This criterion maximises the probability of detection of a target (P_D) subject to the constraint that the probability of false alarm (P_F) is equal to or less than a certain prespecified number. It can be shown [28–30] that this criterion leads to the likelihood ratio test as the optimum test. This test is defined by

$$\frac{p_{R/H_1}(R/H_1)}{p_{R/H_0}(R/H_0)} = \Lambda(R) \underset{H_0}{\overset{H_1}{\gtrless}} \lambda \qquad (2.1)$$

where $p_{R/H_1}(R/H_1)$ and $p_{R/H_0}(R/H_0)$ are the multidimensional

conditional probability density functions of the observations given that H_1 and H_0 are true respectively. $\Lambda(R)$ is the likelihood ratio and λ is the threshold for comparison.

Thus the optimum receiver processes the observations to find the likelihood ratio $\Lambda(R)$ and then compares $\Lambda(R)$ with a threshold in order to make a decision. If we denote the probability density function of Λ when H_0 is true as $p_{\Lambda/H_0}(\Lambda/H_0)$, and when H_1 is true as $p_{\Lambda/H_1}(\Lambda/H_1)$, then

$$P_F = \int_{\lambda}^{\infty} p_{\Lambda/H_0}(\Lambda/H_0)\, d\Lambda \quad \text{and} \quad P_D = \int_{\lambda}^{\infty} p_{\Lambda/H_1}(\Lambda/H_1)\, d\Lambda \qquad (2.2)$$

The threshold λ is obtained by setting P_F equal to the maximum permissible value of false alarm probability and solving (2.2).

2.2 Target Models for Pulsed Radars

Numerous target models have been proposed for different situations [6-11]. Marcum [6] assumed that the target can be modelled as a nonfluctuating or constant reflector. However, in general, the radar cross-section of a target is a statistical variable. Swerling in his classic paper [8] proposed four different models of target fluctuation. These four fluctuation models are commonly referred to as Swerling 1, 2, 3 and 4 models respectively. They are as follows:

Swerling 1 model

The amplitude of the entire reflected pulse sequence from the target during a particular scan is a single random variable with a Rayleigh density function. In addition, there will be phase coherence between the various pulses in the returned sequence except that the initial phase of the sequence will be a statistically independent random variable uniformly distributed over 2π radians. The density function for the target cross-section (σ) will therefore be given by

$$p(\sigma) = \frac{1}{\bar{\sigma}} \exp(-\sigma/\bar{\sigma}) \qquad (\sigma \geq 0) \qquad (2.3)$$

where $\bar{\sigma}$ is the average cross-section. In complex envelope notation, the complex envelope of the entire pulse sequence is multiplied by a single zero-mean complex Gaussian random variable as it gets reflected from the target. However, the complex multipliers in different scans are statistically independent. This type of fluctuation is called scan to scan fluctuation.

Swerling 2 model

Here the amplitude of each reflected pulse in the sequence is a different statistically independent Rayleigh distributed random variable. In addition, the initial phase of each pulse will be a different statistically independent uniformly distributed random variable. The density function for the target cross-section is again

given by (2.3). In complex envelope notation, the complex envelope of each pulse in the sequence is multiplied by different statistically independent zero-mean complex Gaussian random variables as the sequence gets reflected from the target. This type of fluctuation is called pulse to pulse fluctuation.

Swerling 3 model

This is scan to scan fluctuation and the density function for the target cross-section (σ) is given by

$$p(\sigma) = \frac{4\sigma}{\bar{\sigma}^2} \exp(-2\sigma/\bar{\sigma}) \qquad (\sigma \geq 0) \qquad (2.4)$$

Swerling 4 model

This is pulse to pulse fluctuation and the density function for the target cross-section is given by (2.4).

It would be well to indicate in which situations the various models may apply. The density function given in (2.3) is observed when the target consists of many independent scattering elements, of which no single one predominates. Most available observational data on aircraft targets indicate agreement with the exponential density. The density function given in (2.4) corresponds to that of a target having one main scattering element that predominates, together with many smaller independent elements. One such target may be a spherical satellite with extensions. The scan to scan fluctuation model would apply to targets such

as jet aircrafts or missiles, or for radars having a fairly high pulse repetition rate. The pulse to pulse fluctuation model would apply to propeller driven aircrafts if the propellers contribute a large portion of the echoing area, or for radars having a low pulse repetition rate.

The above four fluctuation models of Swerling have been found to bracket a wide range of practical cases, particularly for aircraft targets. In 1970, Swerling [9] extended his original models to cover more cases of interest by considering three families of radar cross-section models; the chi-square family, the Rice family and the log-normal family.

In this thesis, however, only Swerling 1 target models are considered. Also the targets are assumed to be small compared to the radar resolution cell, that is, they are point targets.

2.3 Modelling of Clutter Returns

In this thesis, it is assumed that ground, sea and weather returns constitute clutter. The statistical modelling of ground and sea returns have been the subject of many publications [1-5, 31,32,33] and although several models exist none can be considered to adequately explain observed returns. The clutter model [5] most often used for theoretical analysis is that of a large number of independent scatterers,

with no single one predominating, within the radar resolution cell. The phases of the returns from each scatterer are assumed to be random and uniformly distributed over 2π radians. Also each phase angle is statistically independent of the other. In general, clutter producing targets or clutter targets are extended fluctuating targets. More specifically, let $\sqrt{E_t}\,\tilde{f}(t)$ be the complex envelope of the transmitted signal. The reflected signal from any range interval $(\lambda, \lambda + d\lambda)$ will be the superposition of a large number of reflections with random phases. If the phases are statistically independent and none of the scatterers predominate, central limit theorem based arguments can be used to characterise the reflection coefficient as a zero-mean complex Gaussian random variable. If the orientation and composition of the reflectors change with time, the reflection coefficient must be modelled as a random process. The reflected signal from any range interval $(\lambda, \lambda + d\lambda)$ can be written as

$$\tilde{n}_c(t, \lambda) = \sqrt{E_t}\,\tilde{f}(t - \lambda)\,\tilde{b}(t - \tfrac{\lambda}{2}, \lambda)\,d\lambda \qquad (2.5)$$

where $\tilde{b}(t, \lambda)$ is a zero-mean complex Gaussian process whose independent variables are both time and space. The return from the entire extended target is a superposition of the returns from the incremental intervals and is given by

$$\tilde{n}_c(t) = \int_{-\infty}^{\infty} \sqrt{E_t}\,\tilde{f}(t - \lambda)\,\tilde{b}(t - \tfrac{\lambda}{2}, \lambda)\,d\lambda \qquad (2.6)$$

The complex envelope of the clutter return $\tilde{n}_c(t)$ is a sample

function of a zero-mean complex Gaussian process. It can be seen that the covariance function of $\tilde{n}_c(t)$ is signal dependent. Under the assumptions of uncorrelated scattering from different range intervals and wide sense stationarity of $\tilde{b}(t, \lambda)$, the covariance function of $\tilde{b}(t, \lambda)$ can be written as

$$E[\tilde{b}(t,\lambda)\ \tilde{b}^*(u, \lambda_1)] = \tilde{K}_{DR}(t-u, \lambda)\ \delta(t - \lambda_1) \qquad (2.7)$$

where $\delta(t)$ denotes a unit impulse function and $E[\ .\ ]$ denotes an ensemble average. In actual practice $\tilde{b}(t, \lambda)$ will not be wide sense stationary. However, assuming $\tilde{b}(t, \lambda)$ to be wide sense stationary over a short interval of time or over several scans is realistic enough.

Assuming that the clutter extends from zero range to range LT seconds, (2.6) can be written as

$$\tilde{n}_c(t) = \int_0^{LT} \sqrt{E_t}\ \tilde{f}(t - \lambda)\ \tilde{b}(t - \frac{\lambda}{2}, \lambda)\ d\lambda \qquad (2.8)$$

Now assume that the complex envelope of the transmitted signal is bandlimited to $W_S/2$ around its carrier frequency, or

$$\tilde{F}(f) = 0 \quad \text{for } |f| > W_S/2 \qquad (2.9)$$

where $\tilde{F}(f)$ is the Fourier transform of $\tilde{f}(t)$.

Also let $T = \frac{1}{W}$ where $W \geq W_S$. The criterion for choosing T will be explained later.

Following Kailath [34] and Van Trees [5] the clutter return $\tilde{n}_c(t)$ in (2.8) can be written as the output of a tapped-delay line filter with taps spaced T seconds apart, when the input to the filter is $\tilde{f}(t)$. Or

$$\tilde{n}_c(t) = \sum_{k=0}^{L} \sqrt{E_t}\, \tilde{b}_k(t)\, \tilde{f}(t-kT) \qquad (2.10)$$

The tap gains $\tilde{b}_k(t)$'s are zero-mean complex Gaussian random processes and if $\tilde{K}_{DR}(t-u, \lambda)$ in (2.7) is essentially constant with respect to λ over an interval T seconds long, then

$$E[\tilde{b}_k(t)\, \tilde{b}^*_\ell(u)] = \begin{cases} \frac{1}{T}\, \tilde{K}_{DR}(t-u, kT), & k = \ell \\ 0, & k \neq \ell \end{cases} \qquad (2.11)$$

In the case of moving weather clutter, the clutter return will be centered around a mean Doppler frequency. If ω_{WT} is the mean Doppler frequency shift of the returned signal due to the motion of weather, then using the above arguments, the complex envelope of the clutter signal is given by

$$\tilde{n}_c(t) = \sum_{k=0}^{L} \sqrt{E_t}\, \tilde{b}_k(t)\, \exp(j\omega_{WT}\, t)\, \tilde{f}(t-kT) \qquad (2.12)$$

In this thesis (2.10) will be used to represent the complex envelope of the returned clutter signal. However, (2.12) could also have been used to represent the complex envelope of the returned clutter signal.

2.4 Mathematical Statement of the Problem

Let the transmitted signal be given by

$$S_t(t) = \sqrt{2}\, \mathrm{Re}[\sqrt{E_t}\, \tilde{f}(t)\, \exp(j\omega_c t)] \qquad (2.13)$$

where ω_c is the carrier frequency and $\int_{-\infty}^{\infty} |f(t)|^2\, dt = 1$. E_t is the energy in the signal. When a target is at range $R(t)$ and moving inwards with velocity V ($R(t) = R_o - Vt$), the

received signal from the target is given by

$$S_r(t) = \sqrt{2}\,\mathrm{Re}[\sqrt{E_t}\,\tilde{B}\,\tilde{f}(t - \tau(t))\exp[j\omega_c(t-\tau(t))]\,] \quad (2.14)$$

where $\tau(t)$ is the round trip delay time. $\tilde{B}$ is a zero-mean complex Gaussian random variable if a Swerling 1 or Swerling 2 target is assumed. A signal received at time t would have been reflected from the target at time $(t- (\tau(t)/2))$. At that time the target range would be

$$R(t - \frac{\tau(t)}{2}) = R_o - V(t - \frac{\tau(t)}{2}) \quad (2.15)$$

By definition

$$\tau(t) = \frac{2R(\ t - \frac{\tau(t)}{2})}{c} \quad (2.16)$$

where c is the velocity of light.

Substituting (2.16) in (2.15) and solving for $\tau(t)$ we obtain

$$\tau(t) = \frac{2R_o/c}{1+ V/c} - \frac{2(V/c)t}{1+ V/c} \quad (2.17)$$

For target velocities of interest, $V/c \ll 1$. Then

$$\tau(t) = 2(R_o/c) - 2(V/c)t \quad (2.18)$$

Let $\tau_d = 2R_o/c$ be the nominal range delay. The received signal is given by

$$S_r(t) = \sqrt{2}\,\mathrm{Re}[\sqrt{E_t}\,\tilde{B}\,\tilde{f}(t - \tau_d + \frac{2V}{c}t)\exp[j\omega_c(t+ \frac{2V}{c}t-\tau_d)]] \quad (2.19)$$

If $W_S T_o << \frac{c}{2V}$, where W_S is the bandwidth of $\tilde{f}(t)$ and T_o is the duration of $f(t)$, we can ignore the compression or stretching of the time scale of the complex envelope. The Doppler frequency shift is given by

$$\omega_D = \omega_c(2V/c) \qquad (2.20)$$

Absorbing the $\exp(-j\omega_c\tau_d)$ phase term in the phase of $\tilde{B}$, the received signal is given by

$$S_r(t) = \sqrt{2}\ \mathrm{Re}[\sqrt{E_t}\ \tilde{B}\ \tilde{f}(t - \tau_d)\ \exp(j\omega_c t + j\omega_D t)] \qquad (2.21)$$

The complex envelope of the received signal $\{\tilde{S}_r(t)\}$ from a target at nominal range delay τ_d is given by

$$\tilde{S}_r(t) = \sqrt{E_t}\ \tilde{B}\ \tilde{f}(t - \tau_d)\ \exp(j\omega_D t) \qquad (2.22)$$

If $E[\,|\tilde{B}|^2] = 2\sigma_B^2$, the expected value of the received signal energy is equal to $2E_t\sigma_B^2$. The additive receiver thermal noise $w(t)$ will be modelled as a zero-mean bandpass white Gaussian process[5]. It can be represented as

$$w(t) = \sqrt{2}\ \mathrm{Re}[\tilde{w}(t)\ \exp(j\omega_c t)] \qquad (2.23)$$

where ω_c is the carrier frequency and $\tilde{w}(t)$ is the complex envelope and is a zero-mean complex Gaussian process. If the bandwidth of $w(t)$ is larger than the other bandwidths in the system of interest, $\tilde{w}(t)$ can be represented as a complex white noise process.

Let $\tilde{r}(t)$ be the complex envelope of the received signal in the presence of clutter and thermal noise.

Using the notation developed in the earlier sections, the radar detection problem - to detect a target at range delay τ_d and Doppler ω_d in the presence of clutter and thermal noise - can now be stated as the following binary hypothesis testing problem:

$$\begin{aligned} \tilde{r}(t) &= \tilde{S}_r(t) + \tilde{n}_c(t) + \tilde{w}(t) \quad : H_1 \\ \tilde{r}(t) &= \tilde{n}_c(t) + \tilde{w}(t) \quad : H_o \end{aligned} \qquad T_i \leq t \leq T_f \qquad (2.24)$$

Substituting for $\tilde{S}_r(t)$ from (2.22) and for $\tilde{n}_c(t)$ from (2.10) we get,

$$\begin{aligned} \tilde{r}(t) = \sqrt{E_t}\, \tilde{B}\, \tilde{f}(t-\tau_d) \exp(j\omega_D t) + \sqrt{E_t} \sum_{k=o}^{L} \tilde{b}_k(t)\tilde{f}(t-kT) \\ + \tilde{w}(t) \quad : H_1 \\ \tilde{r}(t) = \sqrt{E_t} \sum_{k=o}^{L} \tilde{b}_k(t)\tilde{f}(t-kT) \\ + \tilde{w}(t) \quad : H_o \end{aligned}$$

$$T_i \leq t \leq T_f$$

Also

$$E[\tilde{B}] = E[\tilde{b}_k(t)] = E[\tilde{w}(t)] = 0, \quad E[\tilde{w}(t)\tilde{w}^*(u)] = N_o\delta(t-u)$$

$$E[|\tilde{B}|^2] = 2\sigma_B^2 , \quad E[\tilde{b}_k(t)\tilde{b}_\ell^*(u)] = \begin{cases} \tilde{K}_{DR}(t-u, kT), & k = \ell \\ 0, & k \neq \ell \end{cases}$$

$$-\infty < t, u < \infty \qquad (2.25)$$

This hypothesis testing problem will now be modified in the following way:

In a particular scan let M $\tilde{f}(t)$, waveforms or pulses be transmitted with a repetition rate of $1/T_p$. Let $T_p >> T_o$ where T_o is the duration of $f(t)$. We assume that the $\tilde{b}_k(t)$'s are so narrow band that during the time a pulse - $\tilde{f}(t)$ - is illuminating it, the $\tilde{b}_k(t)$'s are random variables. This means the sample functions of $\tilde{b}_k(t)$'s are so slowly varying that during the time a pulse is being reflected (T_o seconds), $\tilde{b}_k(t) \approx \tilde{b}_k$. However, when M pulses are being transmitted during a particular scan, for each pulse, the $\tilde{b}_k(t)$'s may be different random variables. For example, for the first $\tilde{f}(t)$, $\tilde{b}_k(t) \approx \tilde{b}_{ko}$, for the second pulse in the pulse train $\tilde{f}(t-T_p)$, $\tilde{b}_k(t) \approx \tilde{b}_{k1}$ and so on. It essentially means that the reflection coefficient $\tilde{b}(t-\frac{\lambda}{2}, \lambda)$ in any given range interval $(\lambda, \lambda + d\lambda)$ will be a random variable for the duration T_o when the waveform $\tilde{f}(t)$ is being reflected from that interval. In the context of pulsed radars, and ground, sea and weather clutter, this is a very realistic assumption.

If the complex envelope of the transmitted signal is given by

$$\tilde{S}_t(t) = \sqrt{E_t} \sum_{m=0}^{M-1} \tilde{f}(t - mT_p) \qquad (2.26)$$

where

$$\int_{-\infty}^{\infty} \tilde{f}(t-nT_p)\, \tilde{f}^*(t-mT_p)dt = \delta_{nm} \quad \text{as} \quad T_p >> T_o$$

the hypothesis testing problem becomes,

$$\tilde{r}(t) = \sqrt{E_t} \sum_{m=o}^{M-1} \tilde{B}_m \tilde{f}(t-\tau_d-mT_p)\exp(j\omega_D t)$$

$$+ \sqrt{E_t} \sum_{m=o}^{M-1} \sum_{k=o}^{L} \tilde{b}_{mk} \tilde{f}(t-kT-mT_p)+\tilde{w}(t) \qquad :H_1$$

$$\tilde{r}(t) = \sqrt{E_t} \sum_{m=o}^{M-1} \sum_{k=o}^{L} \tilde{b}_{mk} \tilde{f}(t-kT-mT_p)+\tilde{w}(t) \qquad :H_o$$

$$T_i \leq t \leq T_f \qquad (2.27)$$

where $\tilde{b}_{mk}$'s are jointly complex Gaussian random variables with

$$E[\tilde{b}_{mk}] = 0,\ E[\,|\tilde{b}_{mk}|^2] = 2\sigma^2_{b_k},\ E[\tilde{b}_{mk}\,\tilde{b}^*_{nj}] = \tilde{R}_{\tilde{b}_k}(m-n)\delta_{kj}$$

where δ_{kj} is a Kronecker delta function. (2.28)

This hypothesis testing problem will again be modified in the following way: Let the entire range duration of interest be divided into range bins and let the length of each range bin be T seconds. Let there be in all (N+1) range bins. Now instead of testing for a target at a particular range delay τ_d, we will test for a target in a particular range bin by testing at the centre of the bin. Now T should be small enough so that there is little degradation in performance even if the target is at $\pm T/2$ from the centre of a range bin. If we let τ_d be in the nth range bin, we can replace τ_d by nT in (2.28). Without loss of generality we will assume n = o and test for a target in the zero'th range bin.

We also impose the following conditions on the waveform:

$$\int_{-\infty}^{\infty} \tilde{f}(t-kT-mT_p)\tilde{f}^*(t-jT-nT_p)dt = 0 \quad \text{for } j,k = 0,\ldots,N$$

when $m \neq n$

and

$$\int_{-\infty}^{\infty} \tilde{f}(t-kT-mT_p)\, \exp(j\omega_D t)\, \tilde{f}^*(t-jT-nT_p)\,dt = 0$$

$$\text{for } j,k = 0,1,\ldots,N$$

$$\text{when } m \neq n \qquad (2.29)$$

Then the hypothesis testing problem becomes

$$\tilde{r}(t) = \sqrt{E_t} \sum_{m=0}^{M-1} \tilde{B}_m\, \tilde{f}(t-mT_p)\, \exp(j\omega_D t) + \sqrt{E_t} \sum_{m=0}^{M-1} \sum_{k=0}^{L} \tilde{b}_{mk}\, \tilde{f}(t-kT-mT_p) + \tilde{w}(t) \qquad :H_1$$

$$\tilde{r}(t) = \sqrt{E_t} \sum_{m=0}^{M-1} \sum_{k=0}^{L} \tilde{b}_{mk}\, \tilde{f}(t-kT-mT_p) + \tilde{w}(t) \qquad :H_0$$

$$T_i \leq t \leq T_f \qquad (2.30)$$

Let $E[|\tilde{B}_m|^2] = 2\sigma_B^2$ for $m = 0,1,\ldots,M-1$.

For a Swerling 1 target,

$$\tilde{B}_m = \tilde{B} \qquad \text{for } m = 0,1,\ldots, M-1. \qquad (2.31)$$

For a Swerling 2 target

$$E[\tilde{B}_m\, \tilde{B}_n^*] = 2\sigma_B^2\, \delta_{mn} \qquad (2.32)$$

In Chapters 3 - 5, various receiver structures are obtained as solutions to this hypothesis testing problem. Some of them involve the use of the maximum entropy method(MEM)

the entropy H_N is defined as

$$H_N = - \int_{-\infty}^{\infty} \cdots \int_{-\infty}^{\infty} p[X(1),\ldots X(N)] \times \log p[X(1), \ldots X(N)]\, dX(1), \ldots dX(N) \quad (2.33)$$

where $p[.]$ represents the N dimensional joint probability density of the random variables X(1), ... X(N). Jaynes contends that the probability density function $p[.]$ that is in agreement with the 'testable' available data but is maximally non-committal about unavailable information is the one that maximises entropy. To apply this method to power spectrum estimation, we observe that power spectrum representation implies second order characterisation of a stationary random process. Shannon [45] showed that of all the processes over $(-\infty, \infty)$ having the same first and second order moments, the Gaussian process has the maximum entropy. Thus the MEM constrains the process to be modelled as Gaussian. Now let $X_N = [X(1), X(2),\ldots, X(N)]^T$ where the superscript T denotes transpose of a vector or a matrix. Then assuming the process to be real and zero-mean, the joint probability density of these observations can be written as

$$p(X_N) = \frac{1}{(2\pi)^{N/2}\ \mathrm{Det}(T_N)} \exp(-\tfrac{1}{2}\, X_N^T\, T_N^{-1}\, X_N) \quad (2.34)$$

where Det(.) denotes the determinant of a matrix and T_N denotes the (N x N) autocovariance matrix given below,

$$T_N \triangleq \begin{bmatrix} R(0) & R(1) & \cdots & R(N-1) \\ R(1) & R(0) & \cdots & R(N-2) \\ \vdots & \vdots & & \vdots \\ R(N-1) & R(N-2) & \cdots & R(0) \end{bmatrix}$$

and (2.35)

$$R(p) = E[X(m)\ X(m-p)]$$

Substituting (2.34) in (2.33) the entropy H_N can be shown to be [46]

$$H_N = \tfrac{1}{2} \log[\mathrm{Det}(T_N)] + \text{Constant} \qquad (2.36)$$

For increasing N, H_N diverges, so instead entropy density h as defined below is maximised

$$h = \lim_{N \to \infty} \frac{H_N}{N} \qquad (2.37)$$

If initially it is assumed that the autocovariance function R(k) for $|k| < N$ are known, the MEM strategy results in the extrapolation of the autocovariance function R(k) for $|k| \geq N$ such that

$$\frac{\partial h}{\partial R(k)} = 0 \qquad \text{for } |k| \geq N \qquad (2.38)$$

subject to the constraints inposed by the known R(k)'s for $|k| < N$. That is, R(k)'s for $|k| \geq N$ are chosen so as maximize the entropy density h in (2.37) without perturbing the autocovariance values already known. The autocovariance

matrix T_N is symmetric and the elements along any diagonal are identical. This Toeplitz structure is instrumental in establishing a relation between the power spectral density S(f) of the process and the entropy density h. The following relation between the determinant of T_N and the power spectral density S(f) of the process can be established [46],

$$\lim_{N\to\infty} [\mathrm{Det}(T_N)]^{1/N} = 2f_N \exp\left[(1/2f_N) \int_{-f_N}^{f_N} \log S(f)\, df\right]$$

$$\text{provided} \quad \mathrm{Det}(T_N) \neq 0 \qquad (2.39)$$

where $f_N = 1/2\Delta t$ and Δt is the time interval between successive observations. After certain manipulations using (2.36), (2.37), (2.38) and (2.39), it has been shown by [46] that the power spectral density S(f) that maximises the entropy density h is given by

$$S(f) = \frac{P_{N-1}\, \Delta t}{\left|1 + \sum_{k=1}^{N-1} \alpha_k \exp(-j2\pi fk\,\Delta t)\right|^2} \quad ; \; -f_N \leq f \leq f_N \qquad (2.40)$$

where the coefficients $\alpha_1, \alpha_2, \ldots, \alpha_{N-1}$ and P_{N-1} are obtained by solving

$$R(j) + \sum_{k=1}^{N-1} \alpha_k R(j-k) = P_{N-n}\, \delta_{jo} \quad ; \quad j = 0,1,\ldots,N-1 \qquad (2.41)$$

Equation (2.41) can also be written as

$$\sum_{k=o}^{N-1} \alpha_k R(j-k) = P_{N-1}\, \delta_{jo} \quad ; \quad j = 0,1,\ldots,N-1 \qquad (2.42)$$

with $\alpha_o = 1$.

Thus to obtain the power spectral density, only α_k's and P_{N-1} need to be determined. The Toeplitz structure of the covariance matrix T_N allows (2.42) to be solved in a recursive manner as suggested by Levinson [47].

Here it need be pointed out that the Autoregressive (AR) modelling approach and the prediction filtering approach lead to the same spectral estimator. It has been shown by [48] that MEM spectral analysis is equivalent to fitting an AR model to the random process. This brings out an interesting fact, that the respresentation of a random process by an AR model is that representation that exhibits the maximum entropy. The equivalence between the prediction filtering approach when the present value of a random sample is estimated by a linear combination of some past values, and MEM has been shown by [39]. The MEM approach can also be viewed as an attempt to find a filter structure that whitens the observed time series [35]. The whitening filter transfer function H(f) in this case is given by,

$$H(f) = 1 + \sum_{k=1}^{N-1} \alpha_k \exp(-j2\pi fk\,\Delta t) \qquad (2.43)$$

The above results for MEM spectral analysis is also valid for a complex-valued time series [49]. It was also assumed that in solving (2.42) the R(k)'s for $k < N$ were known. Burg [36] suggested a method of obtaining α_k's in (2.42) directly from the data samples without prior knowledge of the autocovariance

function. Based on this method, Anderson [50] and Haykin [49] have developed a fast recursive procedure for MEM spectral analysis of a real-valued and complex-valued time series respectively. A brief summary of the recursive procedure developed by Haykin [49] is given below.

Recursive Procedure for MEM Spectral Analysis of a Complex Valued Time Series:

Equation (2.42) corresponds to fitting an AR model of order N-1 or finding a prediction error filter of length N. P_{N-1} is the output power of the prediction error filter. Rather than finding the N-1 coefficients of this error filter, the coefficients of a prediction error filter of length 2 are first found. The coefficients of the prediction error filter of length 3 are recursively evaluated from these and so on. The equations to be solved then are,

$$\sum_{k=0}^{m} \alpha_{mk} R(j-k) = P_m \delta_{j,0} \quad ; \quad j = 0,1,\ldots,m$$

$$\text{and } \alpha_{mo} = 1 \text{ for any } m \qquad (2.44)$$

where m denotes the order of the AR model being fitted and m+1 gives the length of the prediction error filter whose coefficients are being found. Equation (2.44) is now solved recursively by increasing the matrix dimension from m to m+1. The initial value for P_m when $m = 0$ is given by

$$P_o \triangleq R(o) = \frac{1}{N} \sum_{i=1}^{N} |X(i)|^2 \qquad (2.45)$$

The corresponding prediction error filter is trivial with a single weight equal to unity. After solving (2.44) for (m-1)th order of filter, the next step for m involves the determination of m+2 unknowns (R(m), α_{m1}, α_{m2} ... α_{mm}, P_m) from the m+1 equations (2.44). The additional condition required to solve for the unknowns is obtained by minimizing the average output power or the circular error power with respect to α_{mm}. This circular error power π_m is obtained by averaging the power from forward filtering and that from backward filtering, i.e., when the filter is conjugated, and the samples are run reversed in time. According to Haykin and Kesler [49], this circular error power π_m is given by

$$\pi_m = \frac{1}{2(N-m)} \sum_{k=1}^{N-m} \left[\left| X(k) + \sum_{j=1}^{m} \alpha^*_{mj} \, X(k+j) \right|^2 + \left| X(k+m) + \sum_{j=1}^{m} \alpha_{mj} \, X(k+m-j) \right|^2 \right] \qquad (2.46)$$

Minimising π_m with respect to α_{mm} and writing down the results [49] we get

$$\alpha_{mm} = \frac{-2 \sum_{k=1}^{N-m} B^*_{mk} \, C_{mk}}{\sum_{k=1}^{N-m} \left[|C_{mk}|^2 + |B_{mk}|^2 \right]} \qquad (2.47)$$

where B_{mk} and C_{mk} are given by the following pair of recursive equations,

$$B_{mk} = B_{(m-1)k} + \alpha^{*}_{(m-1)(m-1)}\, C_{(m-1)k}$$

$$C_{mk} = C_{(m-1)(k+1)} + \alpha_{(m-1)(m-1)}\, B_{(m-1)(k+1)} \qquad (2.48)$$

The iteration starts with m = 1 and

$$B_{1k} = X(k)$$

$$C_{1k} = X(k+1) \qquad (2.49)$$

The other coefficients of the (m+1) long prediction error filter are calculated by

$$\alpha_{mk} = \alpha_{(m-1)k} + \alpha_{mm}\, \alpha^{*}_{(m-1)(m-k)} \; ; \quad k=1,2,\ldots,(m-1) \qquad (2.50)$$

and the prediction error powers are given by,

$$P_m = P_{(m-1)}\,(1 - |\alpha_{mm}|^2) \qquad (2.51)$$

The autocovariance function R(m) at each step m is obtained by,

$$R(m) = -\sum_{k=1}^{m} \alpha_{mk}\, R(m-k) \qquad (2.52)$$

The whole recursion is to be carried out upto and including a certain value of m = MAX. Proper choice of MAX.is an important part of MEM spectral analysis. Various criteria for the choice of MAX have been suggested [51-54]. Ulrych and Bishop [42] observed that spurious details were introduced into the spectrum when excessively large values of MAX were used. Small values of

MAX tend to smoothen out the resulting spectrum, thus annihilating some significant detail. However, the Final Prediction Error (FPE) criterion introduced by Akaike [51-53] is the most widely used criterian to choose MAX. If α_{mk}'s are a set of AR coefficients based on a certain sample realisation of a time series, Akaike's FPE measures the error that is incurred on the average when these coefficients are used as the model for other sample realisations of the same time series. For zero-mean processes, the following estimate of FPE_m has been developed by Akaike [51],

$$FPE_m = \frac{N + (m + 1)}{N - (m + 1)} \; P_m \qquad (2.53)$$

The order of the AR model or MAX is chosen as one that minimises the FPE. A major objection to Akaike's FPE criterion while using Burg's recursive procedure is that the AR model orders tend to be overestimated when the range of search is close to the length of the time series. However, it has been observed to give good results [39,54] if the range of search is limited to N/2 where N is the length of the time series.

Once MAX has been fixed, the autocovariance function R(k) for k > MAX can be extrapolated by

$$R(MAX + L) = - \sum_{k=1}^{MAX} \alpha_{MAX,k} \; R_{(MAX-k+L)} \quad ; \quad L = 1,2... \qquad (2.54)$$

The inverse of the autocovariance matrix can also be found very easily as shown by Burg [36]. Let A_N be the NxN complex

autocovariance matrix of the time series of length N,

$$A_N = \begin{bmatrix} R(0) & R^*(1) & R^*(2) & \cdots & R^*(N-1) \\ R(1) & R(0) & R^*(1) & \cdots & R^*(N-2) \\ \vdots & \vdots & \vdots & & \vdots \\ R(N-1) & R(N-2) & R(N-3) & \cdots & R(0) \end{bmatrix} \qquad (2.55)$$

and

$$R(p) = E[X(m)\ X^*(m-p)]$$

Let T_N be a NxN matrix whose columns are the prediction error coefficients obtained at each step of the recursion,

$$\begin{bmatrix} 1 & & & & 0 \\ \alpha_{MAX,1} & 1 & & & \\ \vdots & \alpha_{MAX,1} & \ddots & & \\ & \vdots & 1 & & \\ \alpha_{MAX,MAX} & & \alpha_{MAX-1,1} & \ddots & \\ & \ddots & \vdots & & 1 \\ 0 & & \alpha_{MAX,MAX} & \alpha_{MAX-1,MAX-1} \cdots & \alpha_{11}\ \ 1 \end{bmatrix} \qquad (2.56)$$

and let P_N be an NxN diagonal matrix whose elements are the prediction error powers

$$P_N = \begin{bmatrix} P_{MAX} & & & & & & 0 \\ & P_{MAX} & & & & & \\ & & \ddots & & & & \\ & & & P_{MAX} & & & \\ & & & & P_{MAX-1} & & \\ & & & & & P_{MAX-2} & \\ & & & & & & \ddots \\ 0 & & & & & & P_1 \\ & & & & & & & P_0 \end{bmatrix} \qquad (2.57)$$

then it can be shown that

$$T_N^{*T} A_N T_N = P_N \qquad (2.58)$$

$$\text{or} \quad A_N^{-1} = T_N P_N^{-1} T_N^{*T} \qquad (2.59)$$

Regarding the statistical properties of the MEM estimator, due to the nonlinear nature of estimation, the variance of the spectral estimate cannot be easily obtained. Kromer [55] and Berk [56] determined the asymptotic properties of the MEM spectral estimator. According to their findings, MEM spectral estimate is Gaussian and unbiased in an asymptotic manner. If $\tilde{S}(f)$ denotes the MEM estimate using a model of

order m and time series of length N, then,

$$\mathrm{Var}[\hat{S}(f)] = (2m/N)\, S^2(f)$$

where S(f) is the true spectral density.

Estimates for various moments of the MEM spectral estimator are difficult to obtain because of its nonlinear nature.

CHAPTER 3

OPTIMUM RECEIVER FORMULATION

In this chapter, the optimum receiver for the radar detection problem posed in Chapter 2, is obtained. We consider only Swerling 1 target models and the Neyman-Pearson criterion for optimisation. In Section 3.1, we derive the optimum receiver by solving an associated integral equation. In Section 3.2, we obtain an expression for the performance of such an optimum receiver.

3.1 Integral Equation Approach to the Optimum Receiver

Restating for convenience the radar detection problem posed in (2.30), we have for a Swerling 1 target,

$$\tilde{r}(t) = \sqrt{E_t} \sum_{m=0}^{M-1} \tilde{B}\, \tilde{f}(t-mT_p)\exp(j\omega_D t) + \sqrt{E_t} \sum_{m=0}^{M-1} \sum_{k=0}^{L} \tilde{b}_{mk}\, \tilde{f}(t-kT-mT_p) + \tilde{w}(t) \qquad :H_1$$

$$\tilde{r}(t) = \sqrt{E_t} \sum_{m=0}^{M-1} \sum_{k=0}^{L} \tilde{b}_{mk}\, \tilde{f}(t-kT-mT_p) + \tilde{w}(t) \qquad :H_0$$

$$T_i \le t \le T_f \qquad (3.1)$$

where $E[\tilde{B}] = 0$, $E[\tilde{w}(t)] = 0$, $E[\tilde{b}_{mk}] = 0$, $E[|\tilde{B}|^2] = 2\sigma_B^2$,

$E[\tilde{w}(t)\tilde{w}^*(u)] = N_o\delta(t-u)$, $E[\tilde{b}_{mk}\tilde{b}^*_{nj}] = \tilde{R}_{\tilde{b}_k}(m-n)\,\delta_{kj}$.

Equation (3.1) uses the notation of Section 2.4. For convenience, we denote $\tilde{R}_{b_k}(m-n)$ as $\tilde{R}_k(m-n)$.

This hypothesis testing problem of detecting a target in the zero'th range bin and with Doppler shift ω_D, is a case of detecting a signal with unknown parameters in coloured noise. The usual way [5] to solve such problems is to use the Karhunen-Loeve (KL) expansion $\tilde{r}(t) = \sum_k \tilde{r}_k \tilde{\varphi}_k(t)$ where the $\tilde{\varphi}_k(t)$'s form a complete orthonormal set. $\tilde{\varphi}_k(t)$'s are obtained by solving the integral equation,

$$\lambda_i \, \tilde{\varphi}_i(t) = \int_{T_i}^{T_f} \tilde{K}_{\tilde{n}}(t,u) \, \tilde{\varphi}_i(u) \, du \qquad (3.2)$$

where $\tilde{K}_{\tilde{n}}(t,u)$ is the covariance function of the coloured noise. The optimum receiver computes

$$\tilde{\ell} \triangleq \int_{T_i}^{T_f} \tilde{r}(t) \, \tilde{g}^*(t) \, dt \qquad (3.3)$$

and compares $|\tilde{\ell}|^2$ with a threshold. $\tilde{g}(t)$ is obtained by solving the integral equation,

$$\sum_{m=0}^{M-1} \tilde{f}(t-mT_p) \exp(j\omega_D t) = \int_{T_i}^{T_f} \tilde{K}_{\tilde{n}}(t,u) \, \tilde{g}(u) \, du \qquad (3.4)$$

$$T_i \leq t \leq T_f$$

We now proceed to solve the integral equation (3.4) and obtain $\tilde{g}(t)$. $\tilde{K}_{\tilde{n}}(t,u)$ is given by

$$\tilde{K}_{\tilde{n}}(t,u) = E[(\tilde{n}_c(t) + \tilde{w}(t)(\tilde{n}_c^*(u) + \tilde{w}^*(u))]$$

where (3.5)

$$\tilde{n}_c(t) = \sqrt{E}_t \sum_{m=0}^{M-1} \sum_{k=0}^{L} \tilde{b}_{mk}\, \tilde{f}(t-kT-mT_p)$$

As thermal noise and clutter are independent processes,

$$\tilde{K}_{\tilde{n}}(t,u) = E[\tilde{n}_c(t)\, \tilde{n}_c^*(u)] + E[\tilde{w}(t)\, \tilde{w}^*(u)]$$

$$= \tilde{K}_c(t,u) + N_o\delta(t-u) \qquad (3.6)$$

where $\tilde{K}_c(t,u)$ is given by,

$$\tilde{K}_c(t,u) = E[\tilde{n}_c(t)\tilde{n}_c^*(u)]$$

$$= E[E_t[\sum_{m=0}^{M-1} \sum_{k=0}^{L} \tilde{b}_{mk}^*\, \tilde{f}(t-kT-mT_p)] \times$$

$$[\sum_{n=0}^{M-1} \sum_{j=0}^{L} \tilde{b}_{nj}^*\, \tilde{f}^*(u-jT-nT_p)]] \qquad (3.7)$$

As $E[\tilde{b}_{mk}\, \tilde{b}_{nj}^*] = \tilde{R}_k(m-n)\, \delta_{jk}$ from (3.1), we have,

$$\tilde{K}_c(t,u) = E_t \sum_{m=0}^{M-1} \sum_{n=0}^{M-1} \sum_{k=0}^{L} \tilde{R}_k(m-n)\, \tilde{f}(t-kT-mT_p)\, \tilde{f}^*(u-kT-nT_p) \qquad (3.8)$$

From (3.4) we have

$$\tilde{g}(t) = -\frac{1}{N_o} \int_{T_i}^{T_f} \tilde{K}_c(t,u)\, \tilde{g}(u)\, du + \frac{1}{N_o} \sum_{m=0}^{M-1} \tilde{f}(t-mT_p)\exp(j\omega_D t)$$

$$T_i \le t \le T_f \qquad (3.9)$$

This is a Fredholm integral equation of the second kind with $\tilde{K}_c(t,u)$ given by (3.7) as its kernal. As $\tilde{K}_c(t,u)$ is Hermitian and non-negative definite (being a covariance function), it can be shown [57] that there exists a unique solution for $\tilde{g}(t)$.

Substituting (3.6) and (3.8) in (3.4) we get,

$$\sum_{m=o}^{M-1} \tilde{f}(t-mT_p)\exp(j\omega_D t)$$

$$= E_t \int_{T_i}^{T_f} \Big[\sum_{m=o}^{M-1} \sum_{n=o}^{M-1} \sum_{k=o}^{L} \tilde{R}_k(m-n)\tilde{f}(t-kT-mT_p)\tilde{f}^*(u-kT-nT_p)\Big]\tilde{g}(u)du + N_o\tilde{g}(t) \qquad (3.10a)$$

or

$$\sum_{m=o}^{M-1} \tilde{f}(t-mT_p)\exp(j\omega_D t)$$

$$= E_t \sum_{m=o}^{M-1} \sum_{k=o}^{L} (\tilde{f}(t-kT-mT_p))\Big[\sum_{n=o}^{m-1} \tilde{R}_k(m-n) \int_{T_i}^{T_f} \tilde{f}^*(u-kT-nT_p)\tilde{g}(u)du\Big] + N_o\tilde{g}(t) \qquad (3.10b)$$

Observing the term within the square brackets in (3.10b) we find $\tilde{g}(t)$ will be of the form

$$\tilde{g}(t) = \tilde{g}_{ds} \sum_{m=o}^{M-1} \tilde{f}(t-mT_p)\exp(j\omega_D t) + \sum_{m=o}^{M-1} \sum_{k=o}^{L} \tilde{g}_{mk}\, \tilde{f}(t-kT-mT_p) \qquad (3.11)$$

This gives the structure of the optimum receiver. We will now substitute this expression for $\tilde{g}(t)$ in the integral equation (3.10b) and solve for $\tilde{g}_{ds}$ and $\tilde{g}_{mk}$'s to determine the receiver completely. Define

$$\tilde{f}_I(t-kT) \triangleq \begin{bmatrix} \tilde{f}(t-kT) \\ \tilde{f}(t-kT-T_p) \\ \vdots \\ \tilde{f}(t-kT-(M-1)T_p) \end{bmatrix}_{Mx1}$$

$$\text{for } k = 0, \ldots, L \qquad (3.12a)$$

and

$$\tilde{\Lambda}_k = \begin{bmatrix} \tilde{R}_k(0) & \tilde{R}_k^*(1) & \cdots & \tilde{R}_k^*(M-1) \\ \tilde{R}_k(1) & \tilde{R}_k(0) & \cdots & \tilde{R}_k^*(M-2) \\ \vdots & \vdots & & \vdots \\ \tilde{R}_k(M-1) & \tilde{R}_k(M-2) & \cdots & \tilde{R}_k(0) \end{bmatrix}_{Mxm}$$

$$\text{for } k = 0, \ldots, L \qquad (3.12b)$$

Writing (3.8) in matrix notation we have,

$$\tilde{K}_c(t,u) = E_t \sum_{k=0}^{L} \tilde{f}_I^T(t-kT)\, \tilde{\Lambda}_k\, \tilde{f}_I^*(u-kT) \qquad (3.13)$$

Define,

$$\tilde{f}_S(t) \triangleq \begin{bmatrix} \tilde{f}(t)\exp(j\omega_D t) \\ \tilde{f}(t-T_p)\exp(j\omega_D t) \\ \vdots \\ \tilde{f}(t-(M-1)T_p)\exp(j\omega_D t) \end{bmatrix}_{Mx1}, \quad I_S \triangleq \begin{bmatrix} 1 \\ 1 \\ \vdots \\ 1 \end{bmatrix}_{Mx1} \tag{3.14}$$

and

$$\tilde{g}_k \triangleq \begin{bmatrix} \tilde{g}_{ok} \\ \tilde{g}_{1k} \\ \vdots \\ \tilde{g}_{(M-1)k} \end{bmatrix}_{Mx1} \quad \text{for } k = 0, 1, 2, \ldots, L \tag{3.15}$$

Writing (3.11) in matrix notation we have,

$$\tilde{g}(t) = \tilde{g}_{ds}\, \tilde{f}_S^T(t)\, I_S + \sum_{k=o}^{L} \tilde{f}_I^T(t-kT)\, \tilde{g}_k \tag{3.16}$$

Define

$$\tilde{\rho}_{kS} \triangleq \int_{T_i}^{T_f} \tilde{f}_I^*(t-kT)\, \tilde{f}_S^T(t)\, dt$$

$$= \int_{T_i}^{T_f} \begin{bmatrix} \tilde{f}^*(t-kT) \\ \tilde{f}^*(t-kT-T_p) \\ \vdots \\ \tilde{f}^*(t-kT-(M-1)T_p) \end{bmatrix} [\tilde{f}(t)\exp(j\omega_D t) \ \ldots \ \tilde{f}(t-(M-1)T_p)\times \exp(j\omega_D t)]\, dt$$

$$\text{for } k = 0,1,\ldots L \tag{3.17}$$

Now because of the conditions imposed on the waveform $\tilde{f}(t)$ in (2.29) $\tilde{\rho}_{kS}$ will be a diagonal matrix. $\tilde{\rho}_{kS}$ is given by

$$\tilde{\rho}_{kS} = \begin{bmatrix} \tilde{\rho}^{0}_{kS} & & & 0 \\ & \tilde{\rho}^{1}_{kS} & & \\ & & \ddots & \\ 0 & & & \tilde{\rho}^{M-1}_{kS} \end{bmatrix}$$

where (3.18)

$$\tilde{\rho}^{w}_{kS} = \int_{T_i}^{T_f} \tilde{f}^{*}(t-kT-wT_p)\tilde{f}(t-wT_p)\exp(j\omega_D t)\,dt$$

Define,

$$\tilde{\rho}_{kh} \triangleq \int_{T_i}^{T_f} \tilde{f}_I^{*}(t-kT)\,\tilde{f}_I^{T}(t-hT)dt \quad ; \quad k,h = 0,1,\ldots,L$$

$$= \int_{T_i}^{T_f} \begin{bmatrix} \tilde{f}^{*}(t-kT) \\ \tilde{f}^{*}(t-kT-T_p) \\ \vdots \\ \tilde{f}^{*}(t-kT-(M-1)T_p) \end{bmatrix} \times \left[\tilde{f}(t-hT) \ \ldots \ \tilde{f}(t-hT-(M-1)T_p)\right]dt$$

$$k,h = 0,1,\ldots,L \qquad (3.19)$$

Again because of the conditions imposed in (2.29), $\tilde{\rho}_{kh}$ will be a diagonal matrix. $\tilde{\rho}_{kh}$ is given by

$$\tilde{\rho}_{kh} = \tilde{\beta}_{k-h}\, I_D \qquad (3.20)$$

where I_D is an identity matrix and

$$\tilde{\beta}_{k-h} = \int_{T_i}^{T_f} \tilde{f}^*(t-kT)\, \tilde{f}(t-hT)dt.$$

We observe $\tilde{\beta}_o = 1$ and $\tilde{\beta}_{k-h} = \tilde{\beta}^*_{h-k}$.

Substituting (3.6), (3.13) and (3.16) in the integral equation (3.4) we get,

$$\tilde{f}_S^T(t)\, I_S = N_o[\tilde{g}_{ds}\tilde{f}_S^T(t)I_S + \sum_{k=o}^{L} \tilde{f}_I^T(t-kT)\tilde{g}_k]$$
$$+ E_t \int_{T_i}^{T_f} [\sum_{k=o}^{L} \tilde{f}_I^T(t-kT)\, \tilde{\Lambda}_k \tilde{f}_I^*(u-kT)]\times$$
$$[\tilde{g}_{ds}\, \tilde{f}_S^T(u)\, I_S + \sum_{q=o}^{L} f_I^T(u-qt)\tilde{g}_q]du \qquad (3.21)$$

or

$$\tilde{f}_S^T(t)\, I_S = N_o[\tilde{g}_{ds}\tilde{f}_S^T(t)\, I_S + \sum_{k=o}^{L} \tilde{f}_I^T(t-kT)\tilde{g}_k]$$
$$+ E_t\, \tilde{g}_{ds} \sum_{k=o}^{L} \tilde{f}_I^T(t-kT)\, \tilde{\Lambda}_k\, \tilde{\rho}_{kS}\, I_S$$
$$+ E_t \sum_{q=o}^{L} \sum_{k=o}^{L} \tilde{f}_I^T(t-kT)\, \tilde{\Lambda}_k\, \tilde{\rho}_{kq}\, \tilde{g}_q \qquad (3.22)$$

Define

$$\tilde{C}_{kS} \triangleq \tilde{\rho}_{kS}\, I_S \qquad \text{for} \quad k = 0,1,2,\ldots,L \qquad (3.23)$$

From (3.22) we have

$$\tilde{f}_S^T(t)\ I_S = N_o\ \tilde{g}_{ds}\ \tilde{f}_S^T(t)\ I_S + N_o \sum_{k=o}^{L} \tilde{f}_I^T(t-kT)\ \tilde{g}_k$$

$$+ E_t\ \tilde{g}_{ds} \sum_{k=o}^{L} \tilde{f}_I^T(t-kT)\ \tilde{\Lambda}_k\ \tilde{C}_{kS}$$

$$+ E_t \sum_{q=o}^{L} \sum_{k=o}^{L} \tilde{f}_I^T(t-kT)\ \tilde{\Lambda}_k\ \tilde{\beta}_{k-q}\ \tilde{g}_q \qquad (3.24)$$

Observing (3.11) we see that $\tilde{g}_{ds}$ is just a scale factor and by choosing a particular value for $\tilde{g}_{ds}$, the $\tilde{g}_{mk}$'s and $\tilde{g}(t)$ will be suitably scaled. In conformity with (3.10) we choose $\tilde{g}_{ds} = 1/N_o$. Substituting the value of $\tilde{g}_{ds} = 1/N_o$ in (3.24) we get

$$0 = N_o \sum_{k=o}^{L} \tilde{f}_I^T(t-kT)\tilde{g}_k + \frac{E_t}{N_o} \sum_{k=o}^{L} \tilde{f}_I^T(t-kT)\ \tilde{\Lambda}_k\ \tilde{C}_{kS}$$

$$+ E_t \sum_{q=o}^{L} \sum_{k=o}^{L} \tilde{f}_I^T(t-kT)\ \tilde{\Lambda}_k\ \tilde{\beta}_{k-q}\ \tilde{g}_q \qquad (3.25)$$

Expanding (3.25) we get

$$\tilde{f}_I^T(t)\,[E_t\tilde{\Lambda}_o + N_o I_D]\tilde{g}_o + E_t\tilde{\beta}_1\tilde{f}_I^T(t-T)\ \tilde{\Lambda}_1\tilde{g}_o + \ldots E_t\tilde{\beta}_L\tilde{f}_I^T(t-LT)\ \tilde{\Lambda}_L\tilde{g}_o$$

$$+E_t\,\tilde{\beta}_1\ \tilde{f}_I^T(t)\ \tilde{\Lambda}_o\ \tilde{g}_1 \quad + \tilde{f}_I^T(t-T)\,[E_t\ \tilde{\Lambda}_1 + N_o I_D]\tilde{g}_1 + \ldots E_t\,\tilde{\beta}_{L-1}\tilde{f}_I^T(t-LT)\,\tilde{\Lambda}_L\tilde{g}_1$$

$$+ \quad . \qquad . \qquad .$$

$$+E_t\,\tilde{\beta}_L^*\tilde{f}_I^T(t)\ \tilde{\Lambda}_o\tilde{g}_L \quad + \ldots\ldots\ldots + \tilde{f}_I^T(t-LT)\,[E_t\,\tilde{\Lambda}_L + N_o I_D]\tilde{g}_L$$

$$= -\frac{E_t}{N_o}\,[\tilde{f}_I^T(t)\ \tilde{\Lambda}_o\ \tilde{C}_{oS} + \ldots\ \tilde{f}_I^T(t-LT)\,\tilde{\Lambda}_L\ \tilde{C}_{LS}] \qquad (3.26)$$

Now multiplying (3.25) or (3.26) by $\tilde{f}_I^*(t-iT)$ for i=0,1,2...L and integrating with respect to t from T_i to T_f we obtain the following set of matrix equations,

$$N_o \sum_{k=o}^{L} \tilde{\beta}_{i-k}\,\tilde{g}_k + E_t \sum_{q=o}^{L}\sum_{k=o}^{L} \tilde{\beta}_{i-k}\,\tilde{\beta}_{k-q}\,\tilde{\Lambda}_k\,\tilde{g}_q$$

$$= -\frac{E_t}{N_o} \sum_{k=o}^{L} \tilde{\beta}_{i-k}\,\tilde{\Lambda}_k\,\tilde{C}_{kS} \qquad \text{for } i=0,1,2,\ldots L \qquad (3.27)$$

or rearranging terms,

$$E_t \sum_{q=o}^{L}\sum_{\substack{k=o\\k\neq q}}^{L} \tilde{\beta}_{i-k}\,\tilde{\beta}_{k-q}\,\tilde{\Lambda}_k\,\tilde{g}_q + \sum_{k=o}^{L} \tilde{\beta}_{i-k}(N_o\,I_D + E_t\,\tilde{\Lambda}_k)\tilde{g}_k$$

$$= -\frac{E_t}{N_o} \sum_{k=o}^{L} \tilde{\beta}_{i-k}\,\tilde{\Lambda}_k\,\tilde{C}_{kS} \qquad \text{for } i=0,1,2\ldots L \qquad (3.28)$$

Again rearranging terms and expanding,

$$[\tilde{\beta}_i(N_oI_D + E_t\,\tilde{\Lambda}_o) + \sum_{\substack{k=o\\k\neq o}}^{L} E_t\tilde{\beta}_{i-k}\tilde{\beta}_{k-o}\,\tilde{\Lambda}_k]\tilde{g}_o$$

$$+ [\tilde{\beta}_{i-1}(N_oI_D + E_t\,\tilde{\Lambda}_1) + \sum_{\substack{k=o\\k\neq 1}}^{L} E_t\tilde{\beta}_{i-k}\tilde{\beta}_{k-1}\,\tilde{\Lambda}_k]\tilde{g}_1 + \cdots$$

$$+ [\tilde{\beta}_{i-L}(N_oI_D + E_t\,\tilde{\Lambda}_L) + \sum_{\substack{k=o\\k\neq L}}^{L} E_t\tilde{\beta}_{i-k}\tilde{\beta}_{k-L}\,\tilde{\Lambda}_k]\tilde{g}_L$$

$$= -\frac{E_t}{N_o} \sum_{k=o}^{L} \tilde{\beta}_{i-k}\,\tilde{\Lambda}_k\,\tilde{C}_{kS}$$

$$\text{for } i = 0,1,2\ldots L \qquad (3.29)$$

Equations (3.28) or (3.29) are a set of (L+1) simultaneous matrix equations in (L+1) unknowns $\tilde{g}_k$'s for k = 0,1,2,...L. The $\tilde{g}_k$'s are obtained as solution to this set of equations. We observe that $\tilde{C}_{kS}$ is the only term that will change if the hypothesis testing problem is changed to detect targets at other range bins.

In an actual situation, the number of matrix equations to be solved depends on the $\tilde{C}_{kS}$, $\tilde{\Lambda}_k$ and $\tilde{\beta}_k$ terms for k=0,1....L. From (3.18), (3.20) and (3.23) we observe that $\tilde{\beta}_k$ and $\tilde{C}_{kS}$ terms depends on the ambiguity function

$$\left| \int_{T_i}^{T_f} \tilde{f}\left(t - \frac{\tau'}{2}\right) \tilde{f}^*\left(t + \frac{\tau'}{2}\right) \exp(j\,\omega' t)\, dt \right|^2$$

of the waveform $\tilde{f}(t)$. The optimum receiver structure is shown in Fig. 3.1.

3.2 Performance of the Optimum Receiver

From Section 3.1, the optimum receiver computes $\tilde{\ell} = \int_{T_i}^{T_f} \tilde{r}(t)\, \tilde{g}^*(t)\, dt$ and then compares $|\tilde{\ell}|^2$ with a threshold,

$$|\tilde{\ell}|^2 = \left| \int_{T_i}^{T_f} \tilde{r}(t)\, \tilde{g}^*(t)\, dt \right|^2 \underset{H_o}{\overset{H_1}{\gtrless}} \eta_T \qquad (3.30)$$

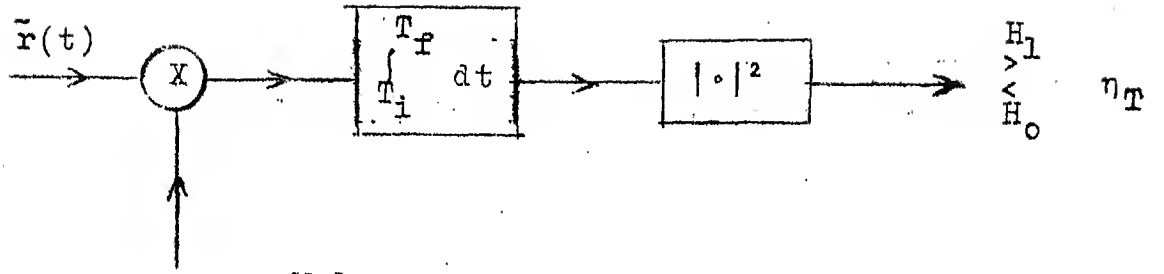

$$\tilde{g}^*(t) = \frac{1}{N_o} \sum_{m=o}^{M-1} f^*(t-mT_p)\exp(-j\omega_D t)$$

$$+ \sum_{m=o}^{M-1} \sum_{k=o}^{L} \tilde{g}^*_{mk}\, \tilde{f}^*(t-kT-mT_p)$$

Fig. 3.1 Optimum Receiver for Swerling 1 Target Models (Complex Operations).

The sufficient statistic $\tilde{\ell}$ is a complex Gaussian random variable. $|\tilde{\ell}|^2$ will have an exponential probability density function. In such a case, it can be shown [28] that

$$P_F = (P_D)^{1+\Delta} \tag{3.31}$$

where P_F denotes the probability of false alarm, and

P_D denotes the probability of detection, and

$$\Delta = \frac{E[\,|\tilde{\ell}|^2 / H_1] - E[\,|\tilde{\ell}|^2 / H_o]}{E[\,|\tilde{\ell}|^2 / H_o]} \tag{3.32}$$

Now

$$E[\,|\tilde{\ell}|^2 / H_o] = E\Big[\int_{T_i}^{T_f}\int_{T_i}^{T_f} \tilde{r}(t)\tilde{r}^*(u)\,\tilde{g}^*(t)\,g(u)\,dt\,du\Big]$$

$$= \int_{T_i}^{T_f}\int_{T_i}^{T_f} \tilde{K}_{\tilde{n}}(t,u)\,\tilde{g}^*(t)\,\tilde{g}(u)\,dt\,du \tag{3.33}$$

Using (3.4) in (3.33) we get,

$$E[\,|\tilde{\ell}|^2 / H_o] = \int_{T_i}^{T_f}\Big[\sum_{m=o}^{M-1} \tilde{f}(t-mT_p)\exp(j\omega_D t)\Big]\tilde{g}^*(t)dt$$

$$= \int_{T_i}^{T_f}\Big[\sum_{m=o}^{M-1} f(t-mT_p)\exp(j\omega_D t)\Big]^*\,\tilde{g}(t)dt \tag{3.34}$$

Also,

$$E[\,|\tilde{\ell}|^2\,/H_1] = E_t E[\,|\tilde{B}|^2] \int_{T_i}^{T_f}\int_{T_i}^{T_f}\Big[\sum_{m=o}^{M-1}\tilde{f}(t-mT_p)\exp(j\omega_D t)\Big]\tilde{g}^*(t)\times$$

$$\Big[\sum_{n=o}^{M-1}\tilde{f}^*(u-nT_p)\exp(-j\omega_D u)\Big]\tilde{g}(u)\,du\,dt$$

$$+\,E[|\tilde{\ell}|^2\,/H_o] \qquad (3.35)$$

From (3.32), (3.34) and (3.35) we get

$$\Delta = 2\sigma_B^2 E_t \int_{T_i}^{T_f}\Big[\sum_{m=o}^{M-1}\tilde{f}(t-mT_p)\exp(j\omega_D t)\Big]\tilde{g}^*(t)\,dt \qquad (3.36)$$

Substituting for $\tilde{g}(t)$ from (3.11) (with $\tilde{g}_{ds} = 1/N_o$) we have,

$$\Delta = 2\sigma_B^2 E_t \int_{T_i}^{T_f}\Big[\sum_{m=o}^{M-1}\tilde{f}(t-mT_p)\exp(j\omega_D t)\Big]\times$$

$$\Big[-\frac{1}{N_o}\sum_{n=o}^{M-1}\tilde{f}^*(t-nT_p)\exp(-j\omega_D t) + \sum_{p=o}^{M-1}\sum_{k=o}^{L}\tilde{g}^*_{pk}\tilde{f}^*(t-kT-pT_p)\Big]$$

(3.37)

Simplifying,

$$\Delta = 2\sigma_B^2 E_t\Big[-\frac{M}{N_o} + \sum_{m=o}^{M-1}\sum_{k=o}^{L}\tilde{g}^*_{mk}\,\rho^m_{kS}\Big] \qquad (3.38)$$

where $\rho^m_{kS} = \int_{T_i}^{T_f}\tilde{f}^*(t-kT-mT_p)f(t-mT_p)\exp(j\omega_D t)\,dt$

or

$$\Delta = \frac{2\sigma_B^2 E_t}{N_o}\Big[M + N_o\sum_{m=o}^{M-1}\sum_{k=o}^{L}\tilde{g}^*_{mk}\,\rho^m_{kS}\Big] \qquad (3.39)$$

The degradation in performance when clutter is present is due to the $\tilde{g}^{*}_{mk}\ \tilde{\rho}^{m}_{kS}$ terms. Of course, $\tilde{g}_{mk}$ also depends on the $\tilde{\rho}^{m}_{kS}$ terms as can be seen from (3.29). As is evident from (3.29) and (3.39), the optimum receivef performance depends on the statistics of clutter and thermal noise as well as on the ambiguity function of the waveform $\tilde{f}(t)$. This performance of the optimum receiver could be improved by waveform or signal design. Of course, this calls for joint optimisation of the transmitter and receiver for a particular clutter environment.

As in general, the statistics of clutter are time varying, the coefficients ($\tilde{g}_k$'s) of the optimum receiver have to be continually updated to meet this changing clutter environment. This makes implementation of the optimum receiver unwieldy and complicated. If there are 16 hits/scan (M=16), a set of (L+1)16 simultaneous equations with complex coefficients have to be solved each time the receiver coefficients ($\tilde{g}_k$'s) are to be updated. Also in practical situations, where the statistics of clutter are a priori not known, optimum receivers which continually estimate the required clutter statistics and then update their coefficients ($\tilde{g}_k$'s) are difficult to implement with present day technology. In view of this, in Chapters 4 and 5, we propose and evaluate suboptimum

66003

receivers and study how the Maximum Entropy Method (MEM) can be used to adaptively determine the parameters of these receivers.

CHAPTER 4

STRUCTURED OPTIMUM RECEIVER FORMULATION

In Chapter 3, we found that the optimum receiver implementation in a changing clutter environment is extremely complicated. Global adaptive optimum receivers which continually estimate the required clutter statistics are difficult to implement with present day technology. In this chapter, we impose a structure on the receiver and within the constraints imposed by that structure, derive an optimum receiver for Swerling 1 target models. This receiver is termed Structured Optimum Receiver. In addition, we see how the scalar complex form of the maximum entropy method (MEM) can be successfully applied to continually estimate the required statistics of clutter therby enabling the parameters of the structured optimum receiver to be determined adaptively. In Section 4.1, we discuss the structure that is imposed on the receiver. In Section 4.2 we obtain a structured optimum receiver for Swerling 1 target models and compare the method followed to those of Delong and Hofstetter [18], Spafford [17] and Rummler [16]. In Section 4.3, we obtain an expression for the performance of such a receiver. In Section 4.4, we evaluate the performance of such a receiver for the cases when the required clutter statistics are a priori known and

when MEM is used to estimate the required clutter statistics. The performance of the structured optimum receiver in both these cases is compared with that of a conventional matched filter receiver. A large number of receiver operating characteristic (ROC) graphs indicating the performance of such a receiver, under varying conditions of the target, clutter and thermal noise are included in this section. These ROC's have been obtained by computer simulation and numerical computation.

4.1 Matched Filter Structure Imposition

Restating for convenience the radar detection problem posed in (2.30), we have

$$\tilde{r}(t) = \sqrt{E_t} \sum_{m=0}^{M-1} \tilde{B}_m \tilde{f}(t-mT_p) \exp(j\omega_D t)$$

$$+ \sqrt{E_t} \sum_{m=0}^{M-1} \sum_{k=0}^{L} \tilde{b}_{mk} \tilde{f}(t-kT-mT_p) + \tilde{w}(t) \qquad : H_1$$

$$\tilde{r}(t) = \sqrt{E_t} \sum_{m=0}^{M-1} \sum_{k=0}^{L} \tilde{b}_{mk} \tilde{f}(t-kT-mT_p) + \tilde{w}(t) \qquad : H_0$$

$$T_i \leq t \leq T_f \qquad (4.1)$$

where $E[\tilde{B}] = 0$, $E[\tilde{w}(t)] = 0$, $E[\tilde{b}_{mk}] = 0$, $E[|\tilde{B}|^2] = 2\sigma_B^2$,

$E[\tilde{w}(t)\,\tilde{w}^*(u)] = N_o\,\delta(t-u)$, $E[\tilde{b}_{mk}\,\tilde{b}^*_{nj}] = \tilde{R}_{\tilde{b}_k}(m-n)\,\delta_{kj}$.

Equation (4.1) uses the notation of Section 2.4. For

convenience, we denote $\tilde{R}_{b_k}(m-n)$ as $\tilde{R}_k(m-n)$.

The received signal $\tilde{r}(t)$ is passed through a matched filter (matched to a single pulse return) and sampled appropriately for returns corresponding to a single range bin (zero'th range bin in this case) during the entire scan. This is shown in Fig. 4.1. A matched filter structure is chosen, as intuitively it appears to be the best structure to impose and relatively easy to implement. Also a matched filter is the optimum receiver in the absence of clutter. It turns out that in the case of a Swerling 1 target model, imposing this structure implies choosing a class of transmit/receive waveforms.

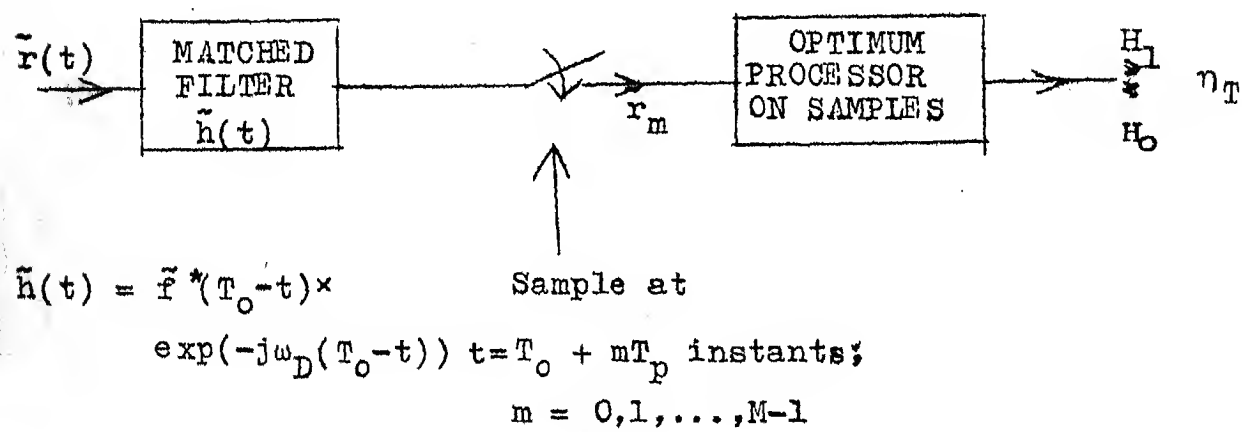

Fig. 4.1 Matched Filter Structured Optimum Receiver (Complex Operations).

The impulse response $\tilde{h}(t)$ of the matched filter is given by

$$\tilde{h}(t) = \tilde{f}^{*}(T_o - t)\, \exp(-j\omega_D(T_o - t)) \tag{4.2}$$

The output of the matched filter $\tilde{r}_m$ at time $t = T_o + mT_p$ on hypothesis H_1 is given by

$$\begin{aligned}
\tilde{r}_m = & \int_{T_i}^{T_f} \left[\sqrt{E_t} \sum_{m=o}^{M-1} \tilde{B}_m \tilde{f}(u - mT_p)\, \exp(j\omega_D u)\right] \times \\
& \left[\tilde{f}^{*}(T_o - t + u) \exp(-j\omega_D(T_o - t + u))\right] du \Big|_{t = T_o + mT_p} \\
& + \int_{T_i}^{T_f} \left[\sqrt{E_t} \sum_{m=o}^{M-1} \sum_{k=o}^{L} \tilde{b}_{mk}\, \tilde{f}(u - kT - mT_p)\right] \times \\
& \left[\tilde{f}^{*}(T_o - t + u)\, \exp(-j\omega_D(T_o - t + u))\right] du \Big|_{t = T_o + mT_p} \\
& + \int_{T_i}^{T_f} \tilde{w}(u) \tilde{f}^{*}(T_o - t + u)\, \exp(-j\omega_D(T_o - t + u)) du \Big|_{t = T_o + mT_p}
\end{aligned} \tag{4.3}$$

Using the conditions stated in (2.29) and simplifying we have,

$$\begin{aligned}
\tilde{r}_m = & \sqrt{E_t}\, \tilde{B}_m \exp(j\omega_D m T_p) \\
& + \sqrt{E_t} \sum_{k=o}^{L} \tilde{b}_{mk} \int_{T_i}^{T_f} \tilde{f}(u - kT - mT_p) \tilde{f}^{*}(u - mT_p) \exp(-j\omega_D(u - mT_p)) du \\
& + \tilde{w}_m
\end{aligned} \tag{4.4}$$

or

$$\tilde{r}_m = \sqrt{E_t}\,\tilde{B}_m \exp(j\omega_D T_p m) + \sqrt{E_t} \sum_{k=o}^{L} \tilde{b}_{mk} \int_{T_i}^{T_f} \tilde{f}(u-kT)\tilde{f}^*(u) \exp(-j\omega_D u)\, du + \tilde{w}_m \qquad (4.5)$$

where

$$\tilde{w}_m = \int_{T_i}^{T_f} \tilde{w}(t)\, \tilde{f}^*(t-mT_p) \exp(-j\omega_D(t-mT_p))dt \qquad (4.6)$$

Define

$$\tilde{\alpha}_{k,\omega_D} \triangleq \int_{T_i}^{T_f} \tilde{f}(t-kT)\tilde{f}^*(t) \exp(-j\omega_D t)\, dt \qquad (4.7)$$

and

$$\tilde{d}_m = \sum_{k=o}^{L} \tilde{b}_{mk}\, \tilde{\alpha}_{k,\omega_D} \qquad (4.8)$$

It is observed that $\tilde{\alpha}_{k,\omega_D}$ depends on the ambiguity function of the waveform $\tilde{f}(t)$.

From (4.5), (4.7) and (4.8) the hypothesis testing problem can now be stated as

$$\tilde{r}_m = \sqrt{E_t}\tilde{B}_m \exp(j\omega_D m T_p) + \sqrt{E_t}\,\tilde{d}_m + \tilde{w}_m \quad : H_1$$

$$\tilde{r}_m = \sqrt{E_t}\,\tilde{d}_m + \tilde{w}_m \quad : H_o$$

$$m = 0,1,\ldots,M-1 \qquad (4.9)$$

where $E[\tilde{B}_m] = 0$, $E[\tilde{d}_m] = 0$, $E[\tilde{w}_m] = 0$, $E[|\tilde{B}_m|^2] = 2\sigma_B^2$,

$$E[\tilde{d}_m \tilde{d}_n^*] = [\sum_{k=0}^{L} \tilde{R}_k(m-n) \mid \tilde{\alpha}_{k,\omega_D} \mid^2], \quad E[\tilde{w}_m \tilde{w}_n^*] = N_o \delta_{mn}.$$

The above hypothesis testing problem is now solved to obtain the structured optimum receiver. The Neyman-Pearson criterion is used for optimum processing of the samples. The receiver structure so obtained will be a structured optimum one as $\tilde{r}(t)$ is first passed through a matched filter before solving the hypothesis testing problem.

4.2 Structured Optimum Receiver for Swerling 1 Target Models

From (4.9) for a Swerling 1 target model we have,

$$\tilde{r}_m = \sqrt{E_t}\, \tilde{B} \exp(j\omega_D m T_p) + \sqrt{E_t}\, \tilde{d}_m + \tilde{w}_m \quad : H_1$$

$$\tilde{r}_m = \sqrt{E_t}\, \tilde{d}_m + \tilde{w}_m \quad : H_o$$

$$m = 0,1,2,\ldots,M-1 \qquad (4.10)$$

The $\tilde{d}_m$'s are jointly complex Gaussian random variables as they have been obtained from a complex Gaussian random process. Let

$$I_m = \sqrt{E_t}\, \tilde{d}_m + \tilde{w}_m \qquad (4.11)$$

Using (4.11) in (4.10) we have,

$$\tilde{r}_m = \sqrt{E_t}\, \tilde{B} \exp(j\omega_D m T_p) + \tilde{I}_m \quad : H_1$$

$$\tilde{r}_m = \tilde{I}_m \quad : H_o$$

$$m = 0,1,\ldots,M-1 \qquad (4.12)$$

$\tilde{I}_m$'s are also jointly complex Gaussian random variables. Define

$$\tilde{I} \triangleq \begin{bmatrix} \tilde{I}_0 \\ \tilde{I}_1 \\ \vdots \\ \tilde{I}_{M-1} \end{bmatrix}, \quad \tilde{d} \triangleq \begin{bmatrix} \tilde{d}_0 \\ \tilde{d}_1 \\ \vdots \\ \tilde{d}_{M-1} \end{bmatrix}, \quad \tilde{w} \triangleq \begin{bmatrix} \tilde{w}_0 \\ \tilde{w}_1 \\ \vdots \\ \tilde{w}_{M-1} \end{bmatrix}$$

$$\tilde{u} \triangleq \begin{bmatrix} \tilde{u}_0 \\ \tilde{u}_1 \\ \vdots \\ \tilde{u}_{M-1} \end{bmatrix} = \begin{bmatrix} 1 \\ \exp(j\omega_D T_p) \\ \vdots \\ \exp(j\omega_D (M-1) T_p) \end{bmatrix}, \quad \tilde{r} \triangleq \begin{bmatrix} \tilde{r}_0 \\ \tilde{r}_1 \\ \vdots \\ \tilde{r}_{M-1} \end{bmatrix} \tag{4.13}$$

Now

$$E[\tilde{d}] = 0, \quad E[\tilde{I}] = 0, \quad E[\tilde{r}] = 0, \quad E[\tilde{B}] = 0, \quad E[\tilde{w}] = 0 \tag{4.14}$$

Let

$$E[\tilde{d}\ \tilde{d}^{*T}] = 2h^2\ \tilde{A}_d \tag{4.15}$$

where the term $2h^2$ is used to make the diagonal elements of $\tilde{A}_d$ equal to unity. $2h^2$ represents the expected value of the clutter power in each sample when $E_t = 1$.

Now

$$\tilde{I} = \sqrt{E_t}\ \tilde{d} + \tilde{w} \tag{4.16}$$

and

$$E[\tilde{I}\ \tilde{I}^{*T}] = E_t\ E[\tilde{d}\ \tilde{d}^{*T}] + E[\tilde{w}\ \tilde{w}^{*T}] = E_t\ 2h^2\ \tilde{A}_d + N_o\ I_D \tag{4.17}$$

where I_D is an identity matrix.

Let

$$E[\tilde{I}\ \tilde{I}^{*T}] = 2\beta^2\ \tilde{A}_I \tag{4.18}$$

where $2\beta^2 = 2h^2 E_t + N_o$ and the diagonal elements of $\tilde{A}_I$ are equal to unity. $2\beta^2$ represents the expected value of the total clutter and thermal noise power in each sample. $\tilde{A}_I$ is a positive definite matrix.

Using (4.12), (4.13), (4.15), (4.16) and (4.18), the hypothesis testing problem can now be stated as

$$\begin{aligned} \tilde{r} &= \sqrt{E_t}\ \tilde{B}\ \tilde{u} + \tilde{I} \quad : H_1 \\ \tilde{r} &= \tilde{I} \quad : H_o \end{aligned} \tag{4.19}$$

where the probability density function of $\tilde{I}$ is given by

$$\tilde{p}_{\tilde{I}}(\tilde{I}) = \frac{1}{(2\pi\beta^2)^M\ \mathrm{Det}(\tilde{A}_I)} \exp\left[-\frac{1}{2\beta^2}\ (\tilde{I}^{*T}\ \tilde{A}_I^{-1}\ \tilde{I})\right] \tag{4.20}$$

This hypothesis testing problem will be solved using the Neyman-Pearson criterion for optimisation. As stated in Chapter 2, this criterion leads to the likelihood ratio test,

$$\Lambda(\tilde{r}) = \frac{p_{\tilde{r}/H_1}(\tilde{r}/H_1)}{p_{\tilde{r}/H_o}(\tilde{r}/H_o)} \underset{H_o}{\overset{H_1}{\gtrless}} \eta_T \tag{4.21}$$

where $p_{\tilde{r}/H_1}(\tilde{r}/H_1)$ and $p_{\tilde{r}/H_o}(\tilde{r}/H_o)$ are the joint probability density functions of the observations given that H_1 and H_o are

true respectively. $\Lambda(\tilde{r})$ is the likelihood ratio. We first obtain the likelihood ratio given $\tilde{B}$ $(\Lambda(\tilde{r}/\tilde{B}))$. Now,

$$\Lambda(\tilde{r}/\tilde{B}) = \frac{p_{\tilde{r}/\tilde{B},H_1}(\tilde{r}/\tilde{B},H_1)}{p_{\tilde{r}/H_o}(\tilde{r}/H_o)} \tag{4.22}$$

where

$$p_{\tilde{r}/\tilde{B},H_1}(\tilde{r}/\tilde{B},H_1) = \frac{1}{(2\pi\beta^2)^m \, \mathrm{Det}(\tilde{A}_I)}$$

$$\exp[-\frac{1}{2\beta^2}(\tilde{r}-\sqrt{E_t}\,\tilde{B}\,\tilde{u})^{*T}\,\tilde{A}_I^{-1}(\tilde{r}-\sqrt{E_t}\,\tilde{B}\,\tilde{u})] \tag{4.23}$$

and

$$p_{\tilde{r}/H_o}(\tilde{r}/H_o) = \frac{1}{(2\pi\beta^2)^M \, \mathrm{Det}(\tilde{A}_I)} \exp[-\frac{1}{2\beta^2}(\tilde{r}^{*T}\,\tilde{A}_I^{-1}\,\tilde{r})] \tag{4.24}$$

Substituting the values of $p_{\tilde{r}/\tilde{B},H_1}(\tilde{r}/\tilde{B},H_1)$ and $p_{\tilde{r}/H_o}(\tilde{r}/H_o)$ in (4.22) we get,

$$\Lambda(\tilde{r}/\tilde{B}) = \exp[\frac{1}{2\beta^2}(\sqrt{E_t}\,\tilde{B}^*\tilde{u}^{*T}\,\tilde{A}_I^{-1}\,\tilde{r}$$

$$+ \sqrt{E_t}\,\tilde{B}\,\tilde{r}^{*T}\,\tilde{A}_I^{-1}\,\tilde{u} - E_t|\tilde{B}|^2\,\tilde{u}^{*T}\,\tilde{A}_I^{-1}\,\tilde{u})] \tag{4.25}$$

As $\tilde{A}_I^{-1}$ is Hermitian, the quadratic form $\tilde{u}^{*T}\,\tilde{A}_I^{-1}\,\tilde{u}$ will be a real number. Let

$$Y = \tilde{u}^{*T}\,\tilde{A}_I^{-1}\,\tilde{u} \tag{4.26}$$

As $\tilde{r}^{*T}\,\tilde{A}_I^{-1}\,\tilde{u}$ and $\tilde{u}^{*T}\,\tilde{A}_I^{-1}\,\tilde{r}$ are scalars,

$$\tilde{u}^{*T}\,\tilde{A}_I^{-1}\,\tilde{r} = (\tilde{u}^{*T}\,\tilde{A}_I^{-1}\,\tilde{r})^T = (\tilde{r}^{*T}\,\tilde{A}_I^{-1}\,\tilde{u})^* \qquad (4.27)$$

From (4.25)

$$\Lambda(\tilde{r}/\tilde{B}) = \exp\left[\frac{1}{2\beta^2}\left(\sqrt{E_t}\,B(\tilde{r}^{*T}\,\tilde{A}_I^{-1}\,\tilde{u}) + \sqrt{E_t}\,\tilde{B}^*(\tilde{r}^{*T}\,\tilde{A}_I^{-1}\,\tilde{u})^* - E_t\,|\tilde{B}|^2\,Y\right)\right] \qquad (4.28)$$

Let

$$\tilde{B} = |\tilde{B}|\,\exp(j\theta) \qquad (4.29)$$

As $\tilde{B}$ is a zero mean complex Gaussian random variable, $|\tilde{B}|$ has a Rayleigh probability density given by

$$p_{|\tilde{B}|}(|\tilde{B}|) = \begin{cases} \dfrac{|\tilde{B}|}{\sigma_B^2}\exp\left[-\dfrac{|\tilde{B}|^2}{2\sigma_B^2}\right) & ; \quad |\tilde{B}| \geq 0 \\ 0 & ; \quad |\tilde{B}| < 0 \end{cases} \qquad (4.30)$$

θ is uniformly distributed between 0 and 2π and is independent of $|\tilde{B}|$. Let

$$\tilde{r}^{*T}\,\tilde{A}_I^{-1}\,\tilde{u} = |\,\tilde{r}^{*T}\,\tilde{A}_I^{-1}\,\tilde{u}\,|\exp(-j\alpha) \qquad (4.31)$$

Then

$$\Lambda(\tilde{r}/\tilde{B}) = \Lambda(\tilde{r}/|\tilde{B}|,\theta)$$

$$= \exp\left[\frac{1}{2\beta^2}\left(\sqrt{E_t}|\tilde{B}|\exp(j\theta)\,|\,\tilde{r}^{*T}\,\tilde{A}_I^{-1}\,\tilde{u}|\exp(-j\alpha) + \sqrt{E_t}|\tilde{B}|\exp(-j\theta)\,|\,\tilde{r}^{*T}\,\tilde{A}_I^{-1}\,\tilde{u}|\exp(j\alpha) - E_t|\tilde{B}|^2 Y\right)\right] \qquad (4.32)$$

or

$$\Lambda(\tilde{r}/\tilde{B}) = \exp\Big[\frac{1}{2\beta^2}\big(2\sqrt{E_t}|\tilde{B}|\,|\tilde{r}^{*T}\tilde{A}_I^{-1}\tilde{u}|\cos(\theta-\alpha) - E_t|\tilde{B}|^2 Y\big)\Big] \tag{4.33}$$

Now

$$\Lambda(\tilde{r}/|\tilde{B}|) = \frac{1}{2\pi}\int_0^{2\pi}\Lambda(\tilde{r}/|\tilde{B}|,\theta)\,d\theta \tag{4.34}$$

or

$$\Lambda(\tilde{r}/|\tilde{B}|) = \frac{1}{2\pi}\int_0^{2\pi}\exp\Big[-\frac{|\tilde{B}|^2 E_t Y}{2\beta^2}\Big]\exp\Big[\frac{\sqrt{E_t}|\tilde{B}||\tilde{r}^{*T}\tilde{A}_I^{-1}\tilde{u}|\cos(\theta-\alpha)}{\beta^2}\Big]$$

$$= \exp\Big[-\frac{|\tilde{B}|^2 E_t Y}{2\beta^2}\Big] I_o\Big(\frac{\sqrt{E_t}|\tilde{B}||\tilde{r}^{*T}\tilde{A}_I^{-1}u|}{\beta^2}\Big) \tag{4.35}$$

where $I_o(.)$ is the modified Bessel function of zero order.

Now

$$\Lambda(\tilde{r}) = \int_0^{\infty}(\tilde{r}/|\tilde{B}|)\,p_{|\tilde{B}|}(|\tilde{B}|)\,d|\tilde{B}| \tag{4.36}$$

Substituting for $p_{|\tilde{B}|}(|\tilde{B}|)$ from (4.30) we get,

$$\Lambda(r) = \int_0^{\infty}\exp\Big[-\frac{E_t Y|\tilde{B}|^2}{2\beta^2}\Big] I_o\Big(\frac{\sqrt{E_t}|\tilde{B}|\,|r^{*T}\tilde{A}_I^{-1}\tilde{u}|}{\beta^2}\Big)\frac{|\tilde{B}|}{\sigma_B^2}\times$$

$$\exp\Big(-\frac{|\tilde{B}|^2}{2\sigma_B^2}\Big)\,d|\tilde{B}| \tag{4.37}$$

This is a special case of the integral,

$$\int_0^{\infty} t^{\mu-1} I_v(\alpha t)\exp(-p^2t^2)\,dt$$

$$= \frac{\Gamma(\frac{\mu+v}{2})(\frac{\alpha}{2p})^v}{2p^{\mu}\Gamma(v+1)}\exp\Big[\frac{\alpha^2}{4p^2}\Big]{}_1F_1\Big(\frac{v-\mu}{2}+1;\ v+1;\ \frac{-\alpha^2}{4p^2}\Big) \tag{4.38}$$

where $\Gamma(.)$ is the gamma function and ${}_1F_1(a; c; z)$ is the confluent hypergeometric function.

Simplifying (4.37) using (4.38), and taking the log likelihood ratio, we obtain the optimum decision rule as

$$|\tilde{r}^{*T} \tilde{A}_I^{-1} \tilde{u}|^2 \underset{H_o}{\overset{H_1}{\gtrless}} \eta_T \tag{4.40}$$

Let

$$\tilde{v} \triangleq [\tilde{v}_o, \tilde{v}_1, \ldots, \tilde{v}_{M-1}]^T = \tilde{A}_I^{-1} \tilde{u} \tag{4.41}$$

The optimum decision rule can then be written as

$$|\tilde{r}^{*T} \tilde{v}|^2 \underset{H_o}{\overset{H_1}{\gtrless}} \eta_T \tag{4.42}$$

or

$$|\tilde{v}^{*T} \tilde{r}|^2 \underset{H_o}{\overset{H_1}{\gtrless}} \eta_T \tag{4.43}$$

Equation (4.43) can also be written as

$$\left|\sum_{m=o}^{M-1} \tilde{r}_m \tilde{v}_m^*\right|^2 \underset{H_o}{\overset{H_1}{\gtrless}} \eta_T \tag{4.44}$$

The structured optimum receiver corresponding to (4.44) is shown in Fig. 4.2.

We observe from (4.3) that $\tilde{r}_m$ could also be obtained by correlating $\tilde{r}(t)$ with $\tilde{f}^*(t-mT_p) \exp(-j\omega_D(t-mT_p))$,

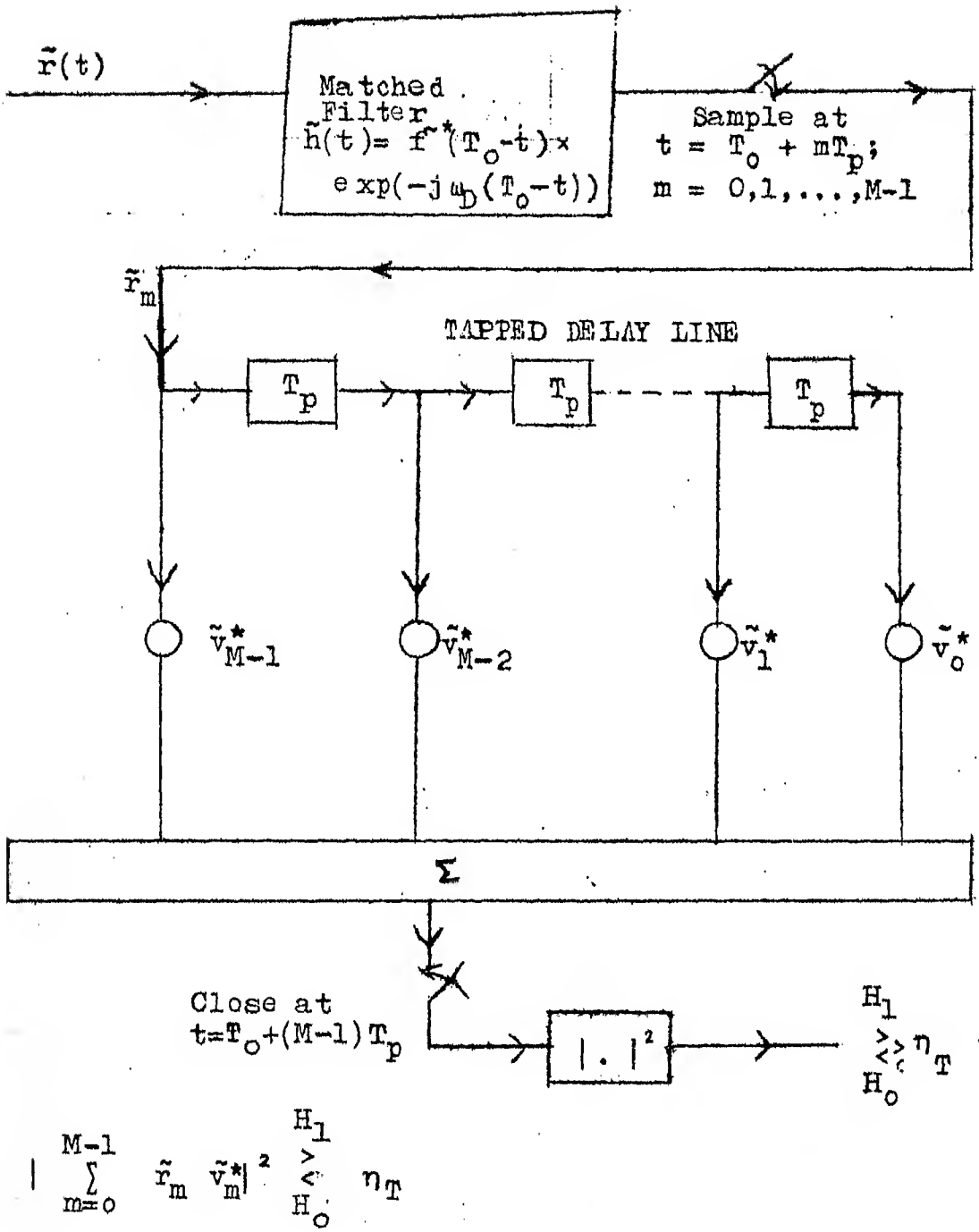

Fig.4.2 Structured Optimum Receiver for Swerling 1 Target Models (Complex Operations).

or

$$\tilde{r}_m = \int_{T_i}^{T_f} \tilde{r}(t)\, \tilde{f}^*(t-mT_p)\, \exp(-j\omega_D(t-mT_p))\, dt \qquad (4.45)$$

Using (4.45) in (4.44), the optimum test is given by

$$\left| \int_{T_i}^{T_f} \tilde{r}(t)\left[\sum_{m=0}^{M-1} \tilde{v}_m \exp(j\omega_D mT_p)\, \tilde{f}^*(t-mT_p) \times \exp(-j\omega_D t)\right]dt \right|^2 \underset{H_0}{\overset{H_1}{\gtrless}} \eta_T \qquad (4.46)$$

An alternate realisation of the receiver can be obtained by correlating the received waveform $\tilde{r}(t)$ with

$$\sum_{m=0}^{M-1} \tilde{v}_m \exp(j\omega_D mT_p)\, \tilde{f}^*(t-mT_p) \exp(-j\omega_D t)$$

and taking the modulus square to get the sufficient statistic. Fig. 4.3 shows an alternate realisation of the structured optimum receiver based on (4.46).

From (4.46) we observe that imposing a matched filter structure on the receiver is equivalent to choosing a class of transmit/receive waveforms. In this particular case, the transmit waveform (by transmit waveform, we mean the reflected signal from the target only) is given by

$$\sum_{m=0}^{M-1} \exp(j\omega_D mT_p)\, \tilde{f}(t-mT_p) \exp(j\omega_D(t-mT_p)) \qquad (4.47)$$

and the receive waveform is given by

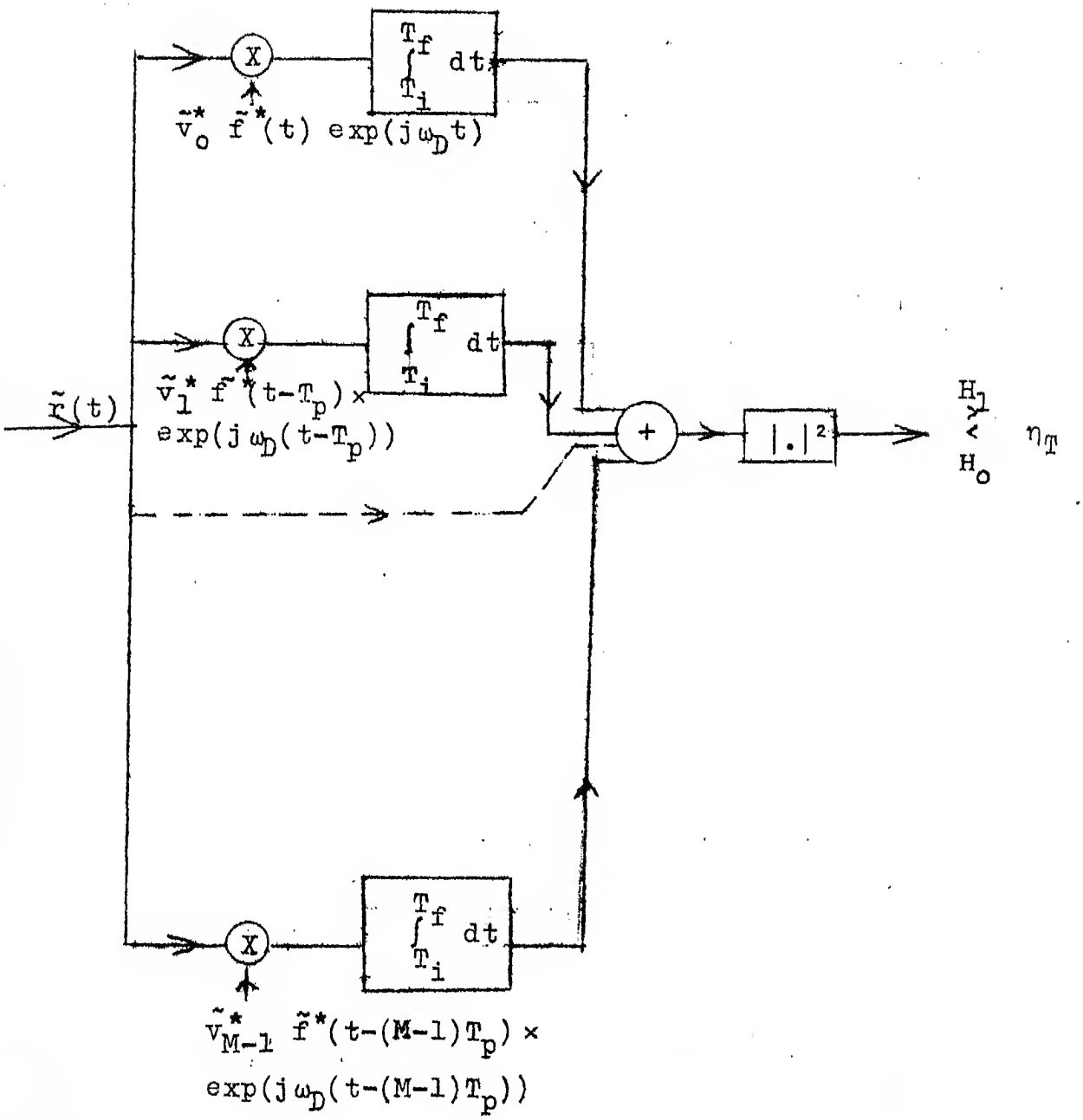

Fig.4.3 Alternate Realisation of the Structured Optimum Receiver (Complex Operations).

$$\sum_{m=0}^{M-1} \tilde{v}_m \, \tilde{f}(t-mT_p) \exp(j\omega_D(t-mT_p)) \qquad (4.48)$$

Also it need be mentioned here that Delong and Hofstetter [18], Spafford [17], and Rummler [16] have obtained the same receiver structure for a slowly fluctuating point target under a different criterion. They have assumed a class of transmit/receive waveforms similar to the ones in (4.47) and (4.48) and maximised the signal to interference ratio(SIR). Each has followed a different method of maximising the SIR, which is their criterion, and the results obtained by them are identical to the one obtained here. It can be easily shown that when the return signal $\tilde{r}(t)$ is a complex Gaussian process, maximising the SIR is equivalent to maximising the probability of detection (P_D) for a given probability of false alarm (P_F). Delong et.al[18]and Spafford [17] have also proposed steps for joint optimisation of the transmitted signal and receiver for a class of transmit/receive waveform for a given clutter scattering function.

A knowledge of $\tilde{v}$ or $\tilde{\Lambda}_I^{-1}$ is required to implement the receiver shown in Fig. 4.2. The inverse covariance matrix $\tilde{\Lambda}_I^{-1}$ may be estimated from $\tilde{r}_m$'s, using the complex form of the maximum entropy method (MEM), during those scans, when no target is present in that range bin, or a decision to that effect has been taken. It was shown in Chapter 2, that $\tilde{\Lambda}_I^{-1}$ could be obtained directly without the need to obtain $\tilde{\Lambda}_I$

and then compute its inverse. This estimate of $\tilde{A}_I^{-1}$ could be averaged over several such scans. In a recent paper [43], Kesler and Haykin report using recorded radar clutter data to carry out MEM analysis to obtain the clutter spectrum. It was found that 16 samples (or equivalently 16 hits/scan) were adequate to get a 'very good' spectrum. The difference in the spectrum, when 256 samples and 16 samples were used respectively, was negligible. Even 8 samples gave a reasonably good spectrum. Thus a good estimate of $\tilde{A}_I^{-1}$ may be obtained from real radar data by using MEM. As $\tilde{A}_I^{-1}$ is being calculated during those scans when no target is present or a decision to that effect has been taken, the quasi time invariant nature of the statistics of clutter are also taken into account. Thus the structured optimum receiver for Swerling 1 target models can be implemented even when the clutter statistics are a priori not known.

4.3 Performance of Structured Optimum Receiver for Swerling 1 Target Models

From (4.44) the optimum decision rule is given by

$$z \triangleq |\tilde{\ell}|^2 = \left| \sum_{m=0}^{M-1} r_m v_m^* \right|^2 \underset{H_0}{\overset{H_1}{\gtrless}} \eta_T \qquad (4.49)$$

where $\tilde{\ell}$ is a sufficient statistic.

Now $\tilde{r}_m$'s are jointly complex Gaussian random variables as $\tilde{I}_m$'s are jointly complex Gaussian and $\tilde{I}_m$'s and $\tilde{B}$ are

independent. $\tilde{\ell}$ is a linear combination of $\tilde{r}_m$'s and is also a complex Gaussian random variable.

The probability of false alarm P_F is given by

$$P_F = \int_{\eta_T}^{\infty} p_{z/H_o}(z/H_o)dz \tag{4.50}$$

and the probability of detection P_D is given by

$$P_D = \int_{\eta_T}^{\infty} p_{z/H_1}(z/H_1)dz \tag{4.51}$$

The probability density function of z will be exponential. Then from (3.31) and (3.32) we have,

$$P_F = (P_D)^{1+\Delta} \tag{4.52}$$

where

$$\Delta = \frac{E[\,|\tilde{\ell}|^2\,/H_1] - E[\,|\tilde{\ell}|^2\,/H_o]}{E[\,|\tilde{\ell}|^2\,/H_o]} \tag{4.53}$$

Δ is called the signal to interference ratio (SIR). It may be observed from (4.52) that maximising P_D for a particular value of P_F is equivalent to maximising Δ.

In the case of the structured optimum receiver,

$$\tilde{\ell} = \sum_{m=o}^{M-1} \tilde{r}_m \tilde{v}_m^* \tag{4.54}$$

$$|\tilde{\ell}|^2 = [\sum_{m=o}^{M-1} \tilde{r}_m \tilde{v}_m^*][\sum_{k=o}^{M-1} \tilde{r}_k^* \tilde{v}_k] = \tilde{v}^{*T}\, \tilde{r}\, \tilde{r}^{*T}\, v \tag{4.55}$$

$$E[\,|\tilde{\ell}|^2\,/H_o] = E[(\tilde{v}^{*T}\,\tilde{r}\,\tilde{r}^{*T}\tilde{v})/H_o] = \tilde{v}^{*T}\,E[\tilde{I}\,\tilde{I}^{*T}]\tilde{v}$$

$$= 2\beta^2\,\tilde{v}^{*T}\,\tilde{A}_I\,\tilde{v} \qquad (4.56)$$

$$E[\,|\tilde{\ell}|^2\,/H_1] = E[(\tilde{v}^{*T}\,\tilde{r}\,\tilde{r}^{*T}\,\tilde{v})/H_1] = \tilde{v}^{*T}\,E[(\tilde{r}\,\tilde{r}^{T})/H_1]\tilde{v} \qquad (4.57)$$

Now

$$E[\tilde{r}\tilde{r}^{*T}/H_1] = E_t\,E[\,|\tilde{B}\,|^2]\,\tilde{u}\,\tilde{u}^{*T} + 2\beta^2\tilde{A}_I \qquad (4.58)$$

Let

$$A_T \triangleq \tilde{u}\,\tilde{u}^{*T} \qquad (4.59)$$

Then

$$[E[\,|\tilde{\ell}|^2/H_1] = 2\sigma_B^2\,E_t\,\tilde{v}^{*T}\,\tilde{A}_T\,\tilde{v} + 2\beta^2\,\tilde{v}^{*T}\,\tilde{A}_I\,\tilde{v} \qquad (4.60)$$

and

$$\Delta = \frac{2\sigma_B^2\,E_t\,\tilde{v}^{*T}\tilde{A}_T\,\tilde{v}}{2\beta^2\,\tilde{v}^{*T}\,\tilde{A}_I\,\tilde{v}} = \frac{2\sigma_B^2\,E_t\,\tilde{v}^{*T}\,\tilde{A}_T\,\tilde{v}}{(2h^2E_t+N_o)\tilde{v}^{*T}\tilde{A}_I\tilde{v}} \qquad (4.61)$$

$2\sigma_B^2\,E_t$ and $2\beta^2$ are the expected value of the target and interference power in each sample respectively.

4.4 Performance Evaluation of the Structured Optimum Receiver by Simulation and Numerical Computation

The performance of the structured optimum receiver, for both the cases when the required clutter statistics are a priori known, and when the maximum entropy method is used to estimate the required clutter statistics, is evaluated by

means of computer simulation and numerical computation. The performance of the structured optimum receiver in both these cases is compared with the performance of a conventional matched filter receiver. Performance evaluation is done for varying conditions of target power, target velocity, clutter power, clutter spectral width, thermal noise power etc. As is commonly done in most performance evaluations, the clutter returns are assumed to have a Gaussian shaped power spectral density. A Gaussian shaped power spectral density corresponds to an infinite step autoregressive model.

The entire simulation scheme is discussed in Appendix A. Briefly, zero-mean complex Gaussian clutter samples $\tilde{d}_k$'s, with Gaussian shaped power spectral density, are generated on the computer. Zero-mean complex white Gaussian samples $\tilde{w}_k$'s are also generated on the computer and these are added to $\tilde{d}_k$'s to obtain interference samples $\tilde{I}_k$'s. These $\tilde{I}_k$'s correspond to the output of the matched filter in Fig. 4.2 when no target is present. Then the complex form of the maximum entropy method is used to estimate the inverse of the total interference covariance matrix. Performance evaluation for various cases is now done using variations of (4.61). Details of this are given below.

Number of hits/scan (M) = 16

Pulse repetition frequency ($1/T_p$) = 540 Hz

This means each sample is spaced 1/540 seconds apart.

We use the following notation:

$\tilde{A}_I$ denotes the actual interference covariance matrix.

$\tilde{A}^{-1}_{MEM}$ denotes the MEM estimate of the inverse of the interference covariance matrix.

P_c denotes the expected value of the clutter power/sample.

$P_c = 2h^2 E_t$.

P_T denotes the expected value of the target power/sample.

$P_T = 2\sigma_B^2 E_t$.

N_o denotes the expected value of the thermal noise power/sample.

f_3 denotes the two-sided half-power width (in Hz) of the clutter power spectral density.

f_o denotes the centre frequency (in Hz) of the clutter power spectral density.

f_D denotes the Doppler frequency shift (in Hz) due to the target motion.

$\tilde{A}_T$ and $\tilde{u}$ are as defined in (4.13) and (4.59) respectively.

The performance of the structured optimum receiver, when the required clutter statistics are a priori known, is evaluated by calculating Δ_{th} where

$$\Delta_{th} = \frac{2\sigma_B^2 E_t \tilde{v}^{*T} \tilde{A}_T \tilde{v}}{(2h^2E_t+N_o)\tilde{v}^{*T}\tilde{A}_I\tilde{v}} = \frac{P_T \tilde{v}^{*T} \tilde{A}_T \tilde{v}}{(P_c+N_o)\tilde{v}^{*T} \tilde{A}_I \tilde{v}} \qquad (4.62)$$

where $\tilde{v} = \tilde{A}_I^{-1} \tilde{u}$

$$P_F = (P_D)^{1+\Delta_{th}} \tag{4.63}$$

For any given clutter statistics, this performance is the maximum attainable by the structured optimum receiver. This receiver is denoted as structured optimum receiver S1.

The performance of the structured optimum receiver, when the required clutter statistics are estimated using the complex form of the MEM is evaluated by calculating Δ_{sto} where

$$\Delta_{sto} = \frac{2\sigma_B^2 E_t \tilde{v}^{*T} \tilde{A}_T \tilde{v}}{(2h^2E_t+N_o)\tilde{v}^{*T} \tilde{A}_I \tilde{v}} = \frac{P_T \tilde{v}^{*T} \tilde{A}_T \tilde{v}}{(P_c+N_o) \tilde{v}^{*T} \tilde{A}_I \tilde{v}} \tag{4.64}$$

where $\tilde{v} = \tilde{A}_{MEM}^{-1} \tilde{u}$

$$P_F = (P_D)^{1+\Delta_{sto}} \tag{4.65}$$

This receiver is denoted as structured optimum receiver S2. The performance of the conventional matched filter receiver is evaluated by calculating

$$\Delta_{mf} = \frac{2\sigma_B^2 E_t \tilde{u}^{*T} \tilde{A}_T \tilde{u}}{(2h^2E_t+N_o)\tilde{u}^{*T} \tilde{A}_I \tilde{u}} = \frac{P_T u^{*T} \tilde{A}_T \tilde{u}}{(P_c + N_o)\tilde{u}^{*T} \tilde{A}_I \tilde{u}} \tag{4.66}$$

$$F = (P_D)^{1+\Delta_{mf}} \tag{4.67}$$

performance of the conventional matched filter receiver no clutter is present is evaluated by calculating

$$\Delta_{ideal} = \frac{2\sigma_B^2 E_t \tilde{u}^{*T} \tilde{A}_T \tilde{u}}{N_o \tilde{u}^{*T} \tilde{u}} = \frac{P_T \tilde{u}^{*T} \tilde{A}_T \tilde{u}}{N_o \tilde{u}^{*T} \tilde{u}} \qquad (4.68)$$

$$P_F = (P_D)^{1+\Delta_{ideal}} \qquad (4.69)$$

Δ_{th}, Δ_{sto}, Δ_{mf} and Δ_{ideal} were calculated for a large number of cases by varying P_T, P_c, N_o, f_D and f_3. These are presented in Table 1. The receiver operating characteristic (ROC) graphs for some of these cases are given in Figs.4.4 to 4.16.

The following observations are made on the overall performance of the structured optimum receiver, for both the cases when the clutter statistics are apriori known, and when they are estimated using the MEM:

(a) In the fairly wide range of situations considered the performance of the structured optimum receiver when clutter statistics are a priori known or when they are estimated by MEM, is far superior to that of the conventional matched filter receiver whose design ignores the presence of clutter in the received signal.

(b) In a large number of cases, the difference between Δ_{sto} and Δ_{th} is under 15 percent. This percentage difference decreases with increase in the target velocity. MEM appears to be able to estimate the required clutter statistics 'reasonably well' with only 16 samples.

(c) The performance of the three receivers is greatly dependent on the target velocity or Doppler shift. Δ_{ideal} in Table 1 gives the maximum attainable performance when no clutter is present, everything else remaining the same. At very low target doppler shifts (20 Hz and below), the performance of all the three receivers is poor. However, even here the structured optimum receivers perform better than the conventional matched filter receiver. At target Doppler shifts of 100 Hz or more and for f_3 equal to 10 Hz or less, the performance of the structured optimum receivers approach the maximum attainable performance (when no clutter is present) to within about 20 percent (in terms of Δ) even when the clutter is as high as 50 dB above the thermal noise power level. However, the conventional matched filter performance is very poor.

(d) The performance of the structured optimum receivers improve as the clutter spectral width decreases. This improvement in performance (in terms of Δ) is very noticeable at target Doppler shifts of 40 Hz and below. At a target Doppler shift of 40 Hz and f_3 equal to 1 Hz, the difference in performance of the structured optimum receivers and the maximum attainable performance (when no clutter is present) is less than 20 percent even when the clutter is as high as 30 dB above the thermal noise power.

(e) At a target doppler shift of 100 Hz and f_3 equal to 10 Hz, the variation in performance (in terms of Δ) of the structured optimum receivers, as the clutter power increases from 0 dB to 50 dB above the thermal noise power, is less than 20 percent. This variation in performance decreases as the clutter spectral width decreases.

Pulse repetition frequency $(1/T_p)$ = 540 Hz

Number of hits/scan = 16

Centre frequency of the clutter spectra (f_o) = 0 Hz

$P_F = (P_D)^{1+\Delta}$

where Δ = Signal to interference ratio

S.No.	f_3 Hz	CLUTTER POWER/ SAMPLE P_c	THERMAL WHITE NOISE POWER/ SAMPLE N_o	TARGET POWER/ SAMPLE P_T	TARGET DOPPLER SHIFT F_D Hz	Δ_{ideal}	Δ_{mf}	Δ_{sto}	Δ_{th}	COMMENTS
1	2	3	4	5	6	7	8	9	10	11
1	0.0	0.0	1.0	10.0	100.0	160.0	160.0	159.97	160.0	No Clutter
2	10.0	1.0	1.0	10.0	100.0	160.0	155.17	155.25	157.41	Clutter power being varied for f_3 = 10Hz
3	10.0	100.0	1.0	10.0	100.0	160.0	38.94	144.15	153.74	
4	10.0	1000.0	1.0	10.0	100.0	160.0	4.99	141.50	151.94	
5	10.0	10000.0	1.0	10.0	100.0	160.0	0.51	128.36	145.55	
6	10.0	100000.0	1.0	10.0	100.0	160.0	0.051	121.88	139.70	
7	10.0	1000.0	1.0	10.0	0.0	160.0	0.010	0.010	0.015	Target velocity being varied for f_3 = 10 Hz
8	10.0	1000.0	1.0	10.0	10.0	160.0	0.014	0.08	0.17	
9	10.0	1000.0	1.0	10.0	20.0	160.0	0.035	1.40	3.5	
10	10.0	1000.0	1.0	10.0	30.0	160.0	0.25	12.38	21.38	
11	10.0	1000.0	1.0	10.0	40.0	160.0	0.434	49.77	62.8	
12	10.0	1000.0	1.0	10.0	200.0	160.0	11.41	150.05	157.12	
13	10.0	1000.0	1.0	10.0	270.0	160.0	17.10	152.17	157.60	

Continued...

1	2	3	4	5	6	7	8	9	10	11
14	10.0	100.0	1.0	1000.0	5.0	16000.0	11.24	21.51	25.0	Very large targets at low velocity
15	10.0	10.0	1.0	100.0	100.0	1600.0	1220.53	1508.76	1546.67	Large targets weak clutter
16	20.0	1.0	1.0	10.0	100.0	160.0	148.47	153.74	156.31	Clutter power
17	20.0	100.0	1.0	10.0	100.0	160.0	18.25	139.62	148.45	being varied for
18	20.0	1000.0	1.0	10.0	100.0	160.0	2.03	127.50	139.85	f_3 = 20 Hz
19	20.0	1000.0	1.0	10.0	10.0	160.0	0.015	0.02	0.035	Target velocity
20	20.0	1000.0	1.0	10.0	20.0	160.0	0.03	0.15	0.25	being varied
21	20.0	1000.0	1.0	10.0	40.0	160.0	0.29	8.3	14.23	for f_3 = 20 Hz
22	1.0	1.0	1.0	10.0	100.0	160.0	159.50	155.78	159.92	Clutter power
23	1.0	100.0	1.0	10.0	100.0	160.0	121.98	152.73	157.13	being varied
24	1.0	1000.0	1.0	10.0	100.0	160.0	38 .87	151.19	154.37	for f_3 = 1.0 Hz
25	1.0	1000.0	1.0	10.0	5.0	160.0	0.01	1.25	1.36	Target velocity
26	1.0	1000.0	1.0	10.0	10.0	160.0	0.013	5.45	6.55	being varied
27	1.0	1000.0	1.0	10.0	40.0	160.0	0.45	129.6	141.3	for
28	1.0	1000.0	1.0	10.0	270.0	160.0	145.84	156.41	158.30	f_3 = 1.0 Hz

(continued...)

(Table 1 continued)

1	2	3	4	5	6	7	8	9	10	11
29	10.0	10000.0	0.1	10.0	50.0	1600.0	0.024	253.1	494.4	Very high clutter to thermal noise and high target to thermal noise ratios.
30	10.0	10000.0	0.1	10.0	100.0	1600.0	0.51	1220.7	1400.7	
31	10.0	10000.0	0.1	10.0	270.0	1600.0	1.91	1454.1	1538.8	
32	10.0	100000.0	0.1	10.0	50.0	1600.0	0.0024	137.3	271.8	
33	10.0	100000.0	0.1	10.0	100.0	1600.0	0.051	1027.1	1340.5	
34	10.0	100000.0	0.1	10.0	270.0	1600.0	0.19	1408.4	1553.0	

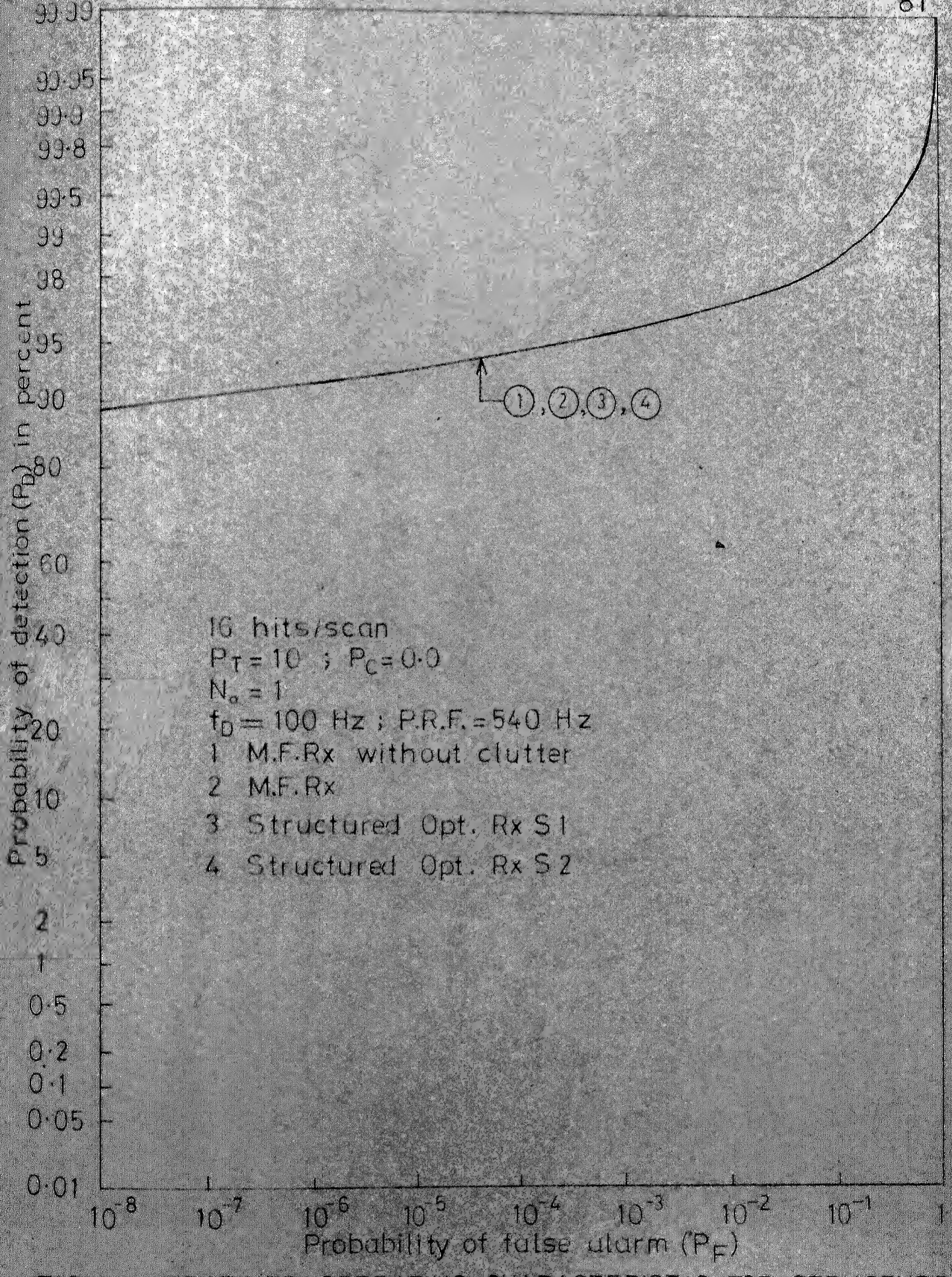

FIG. 4.4 RECEIVER OPERATING CHARACTERISTIC FOR STRUCTURED OPTIMUM AND MATCHED FILTER RECEIVERS

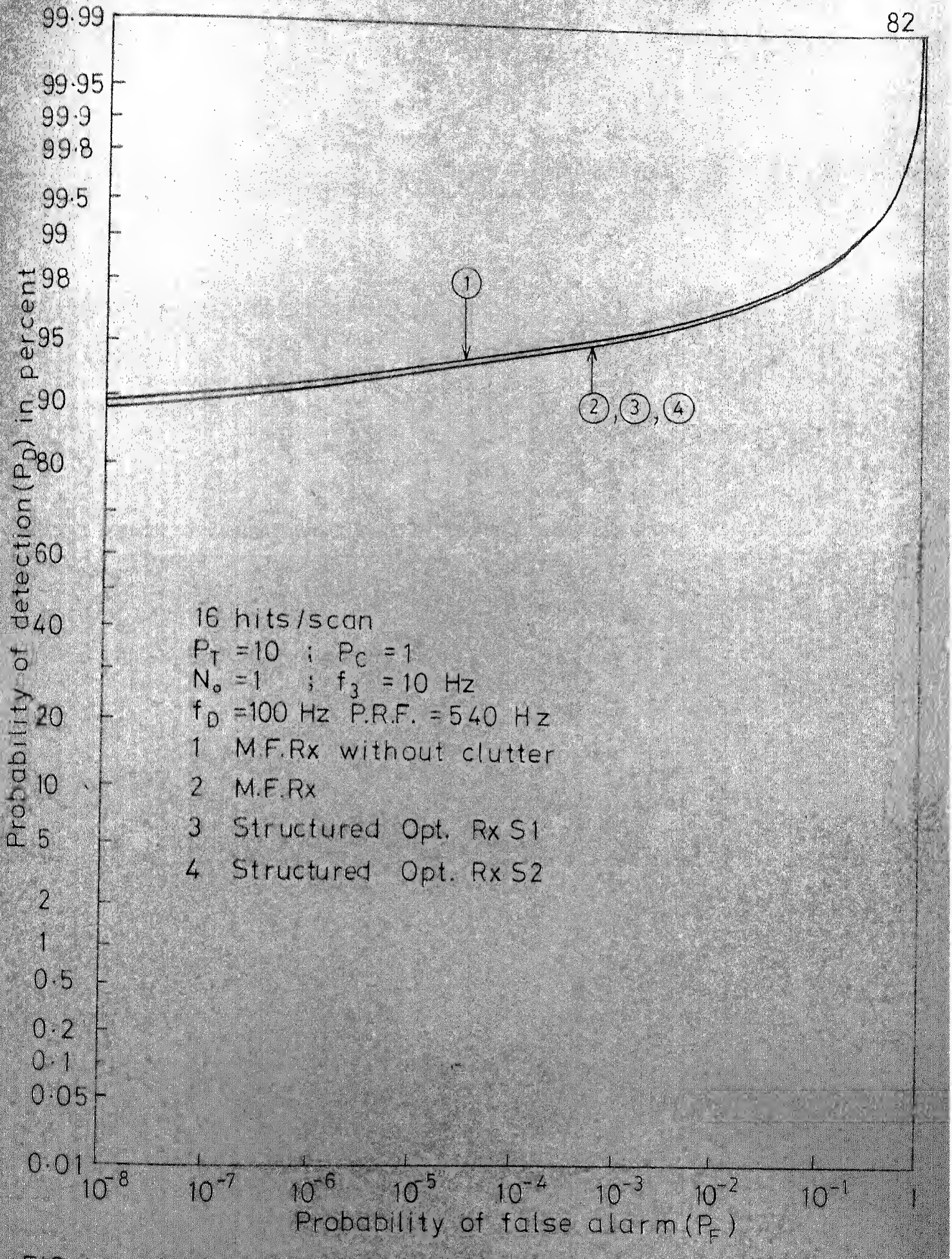

FIG.4·5 RECEIVER OPERATING CHARACTERISTIC FOR STRUCTURED OPTIMUM AND MATCHED FILTER RECEIVERS

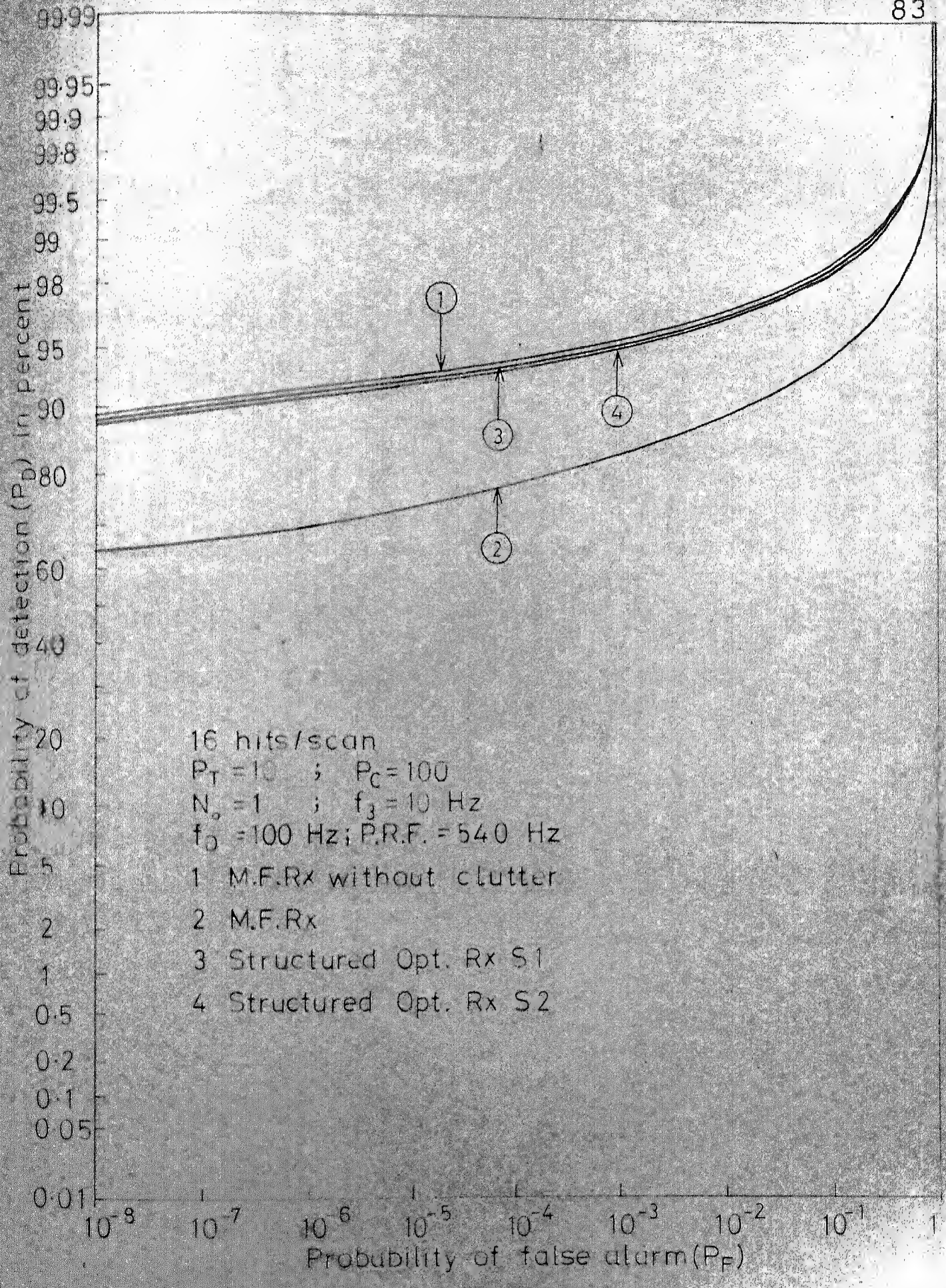

FIG. 4·6 RECEIVER OPERATING CHARACTERISTIC FOR STRUCTURED OPTIMUM AND MATCHED FILTER RECEIVERS

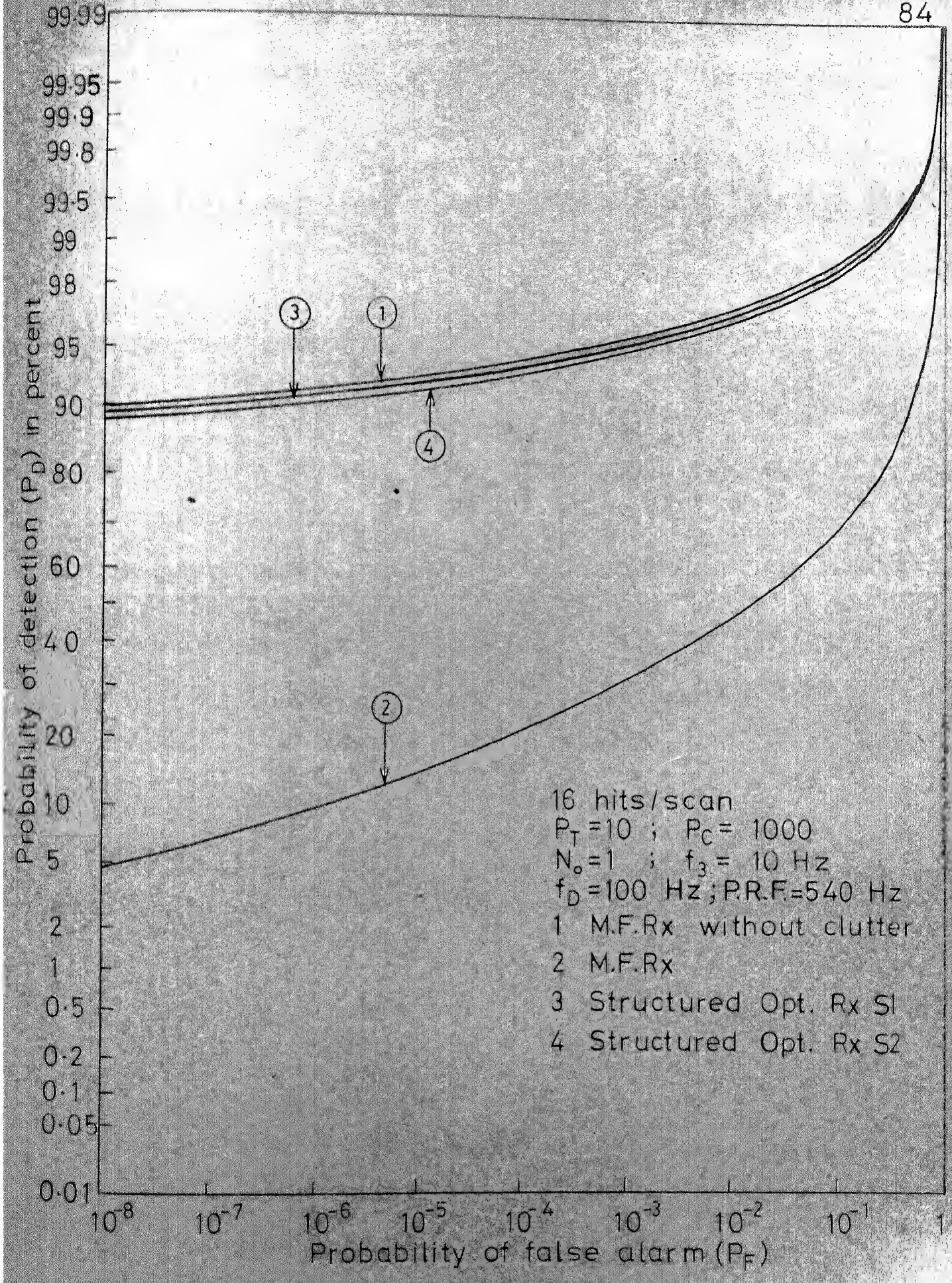

FIG.4·7 RECEIVER OPERATING CHARACTERISTIC FOR STRUCTURED OPTIMUM AND MATCHED FILTER RECEIVERS

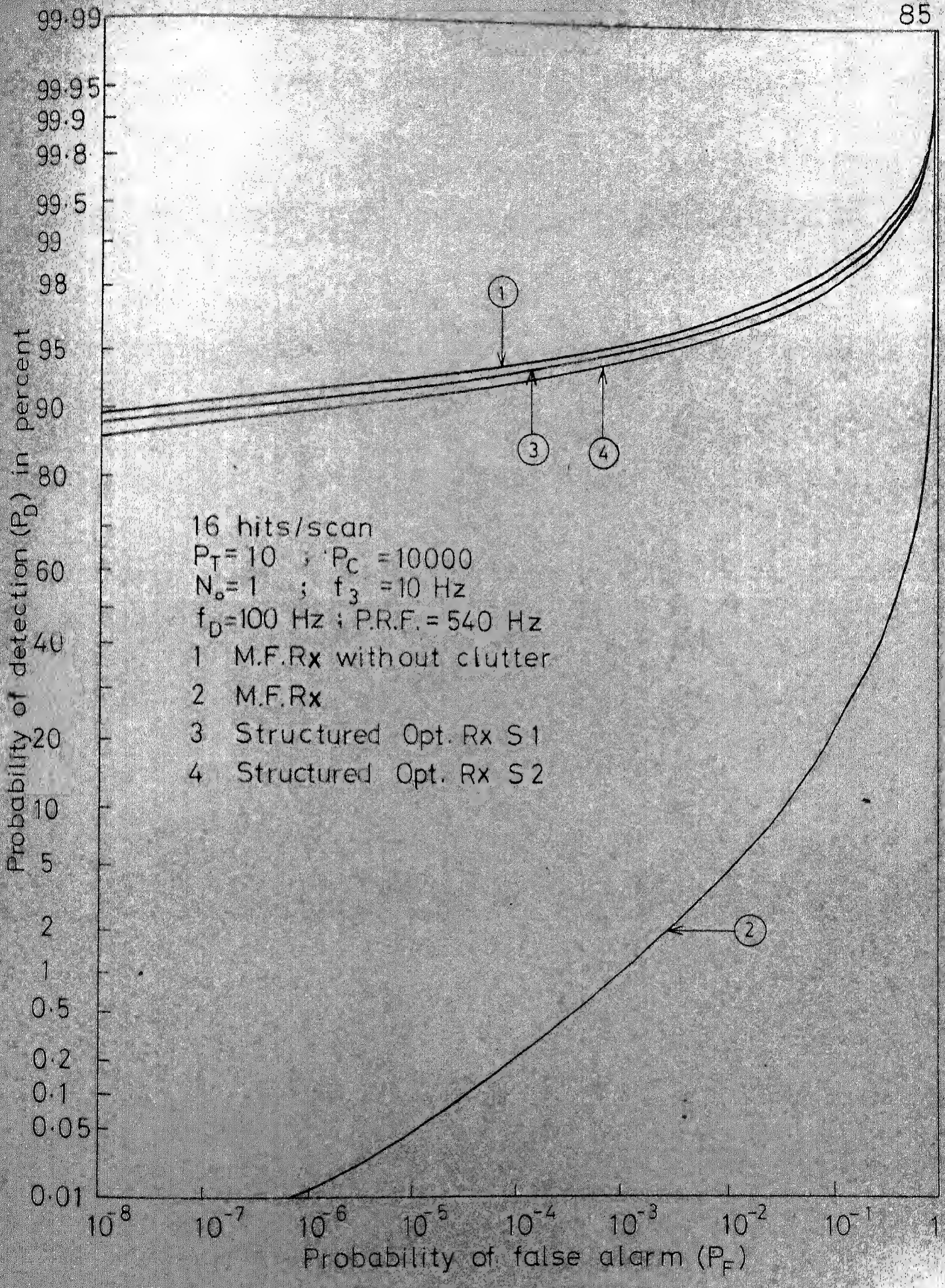

FIG. 4·8 RECEIVER OPERATING CHARACTERISTIC FOR STRUCTURED OPTIMUM AND MATCHED FILTER RECEIVERS

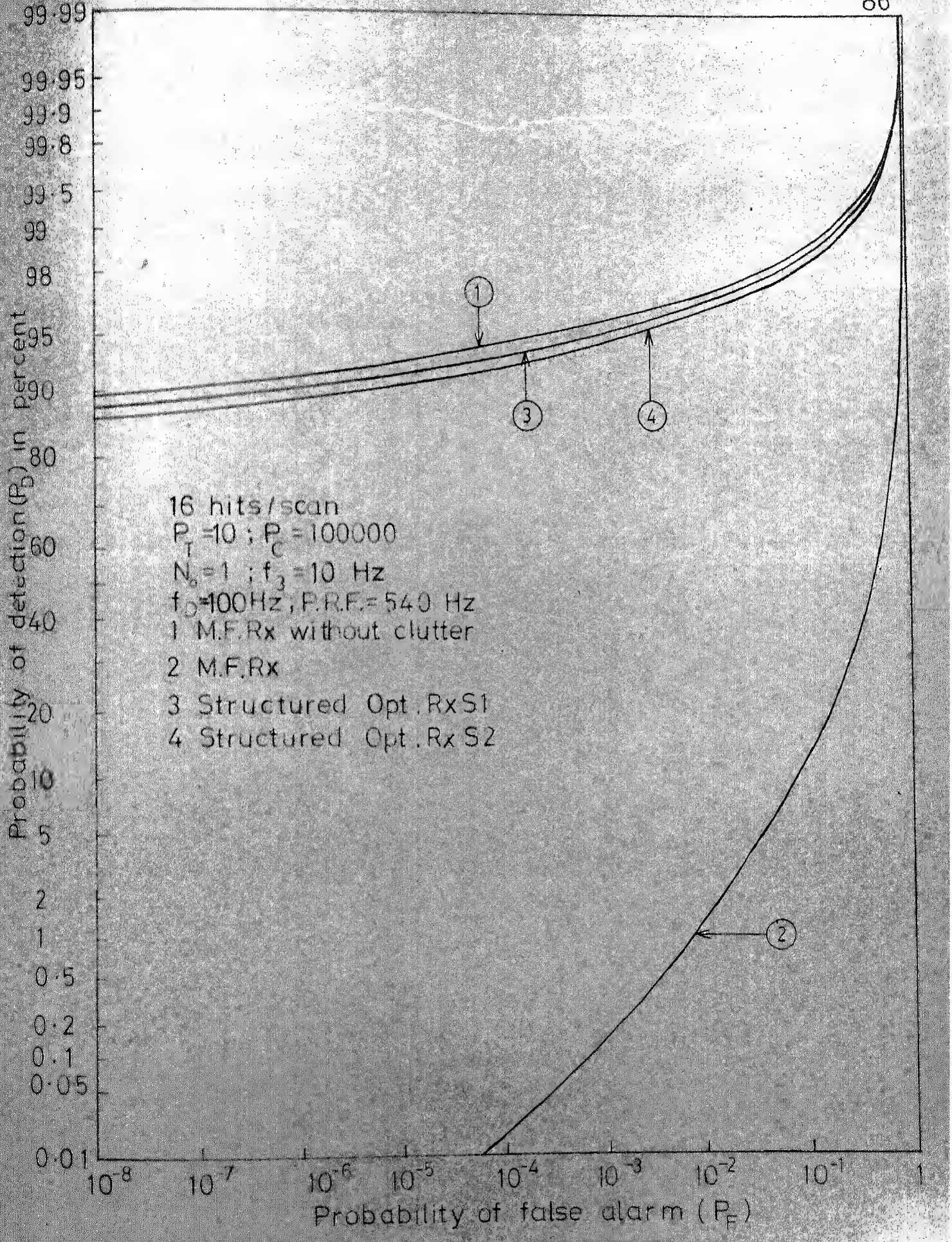

FIG.4·9 RECEIVER OPERATING CHARACTERISTIC FOR STRUCTURED OPTIMUM AND MATCHED FILTER RECEIVERS

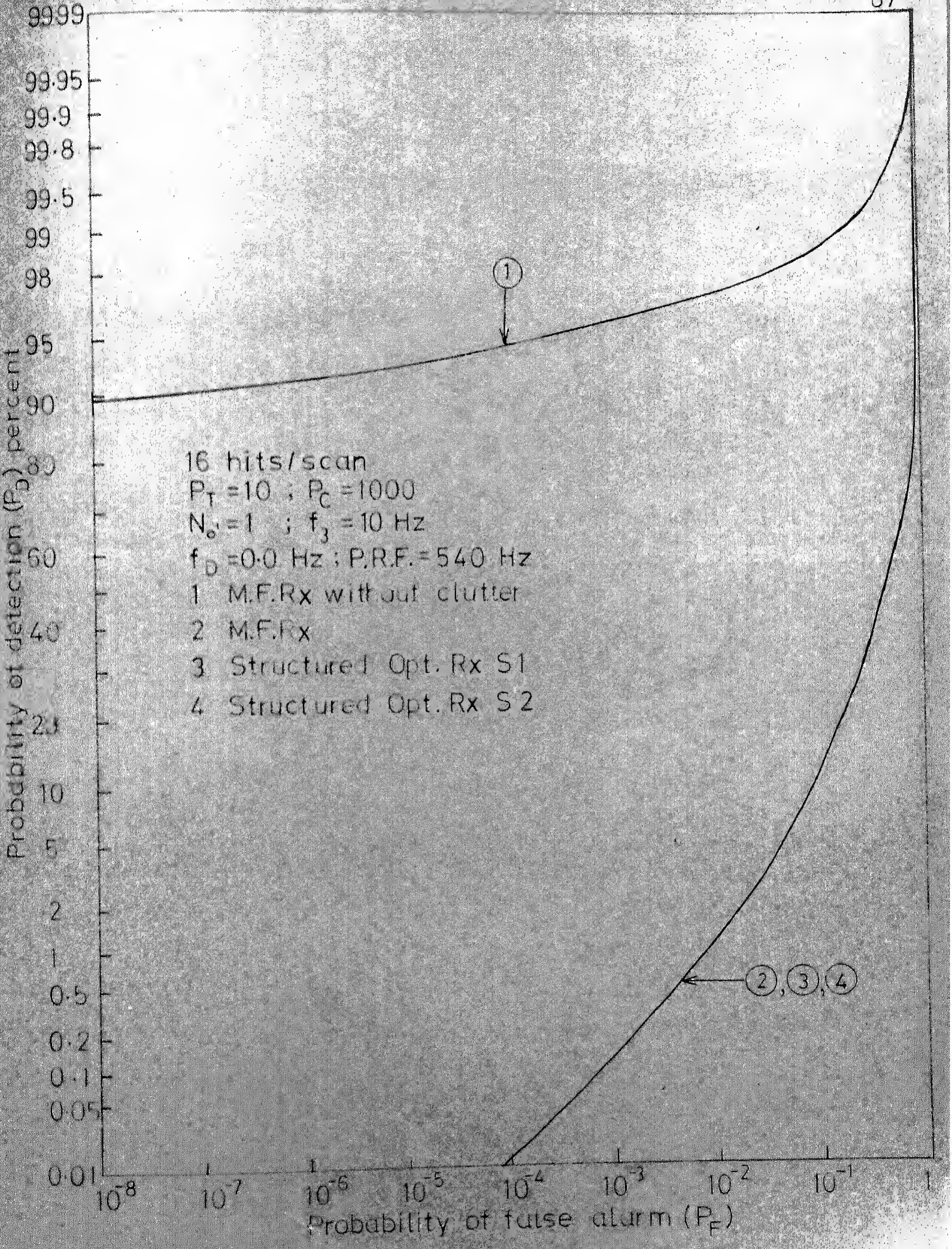

FIG.4·10 RECEIVER OPERATING CHARACTERISTIC FOR STRUCTURED OPTIMUM AND MATCHED FILTER RECEIVERS

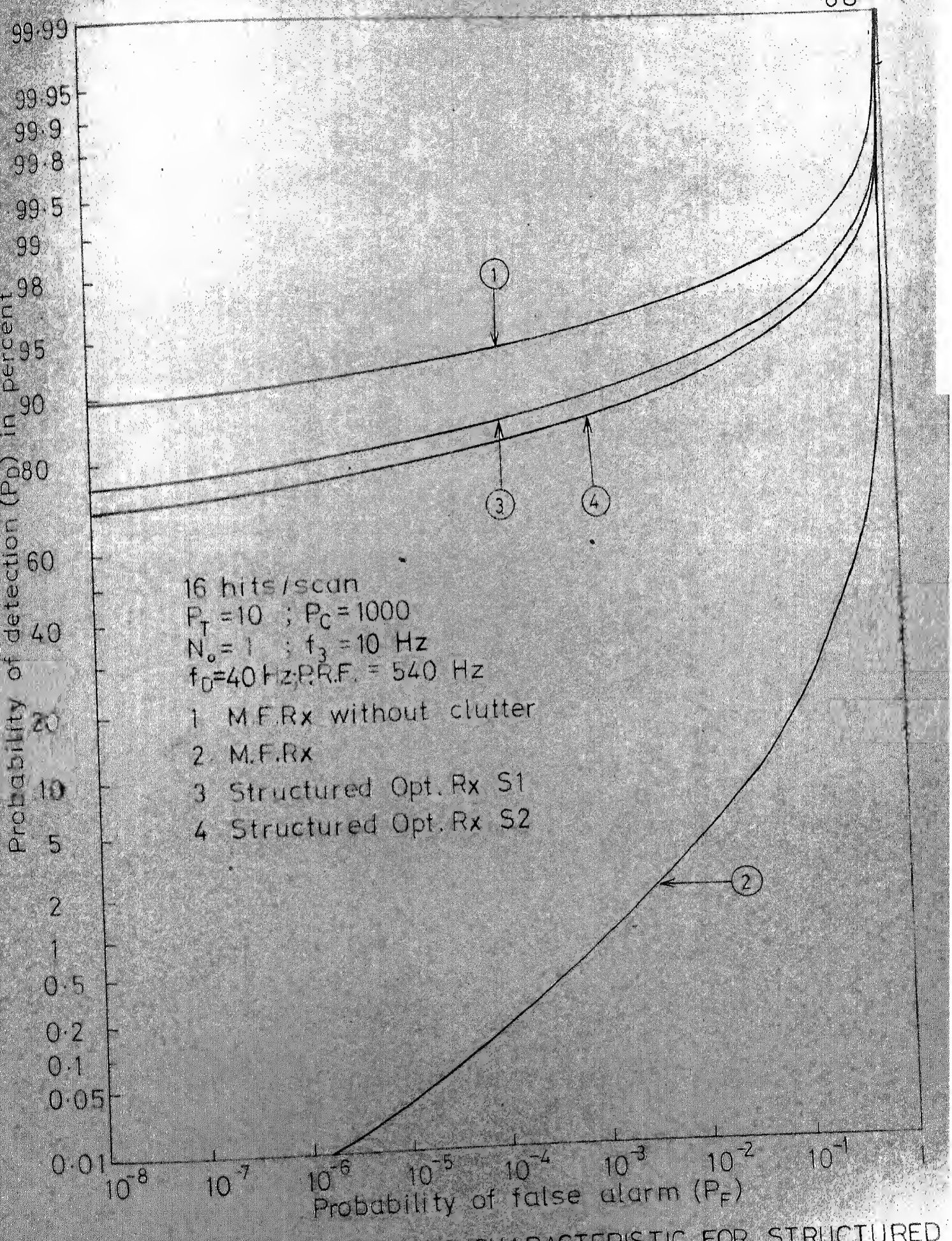

FIG. 4·11 RECEIVER OPERATING CHARACTERISTIC FOR STRUCTURED OPTIMUM AND MATCHED FILTER RECEIVERS

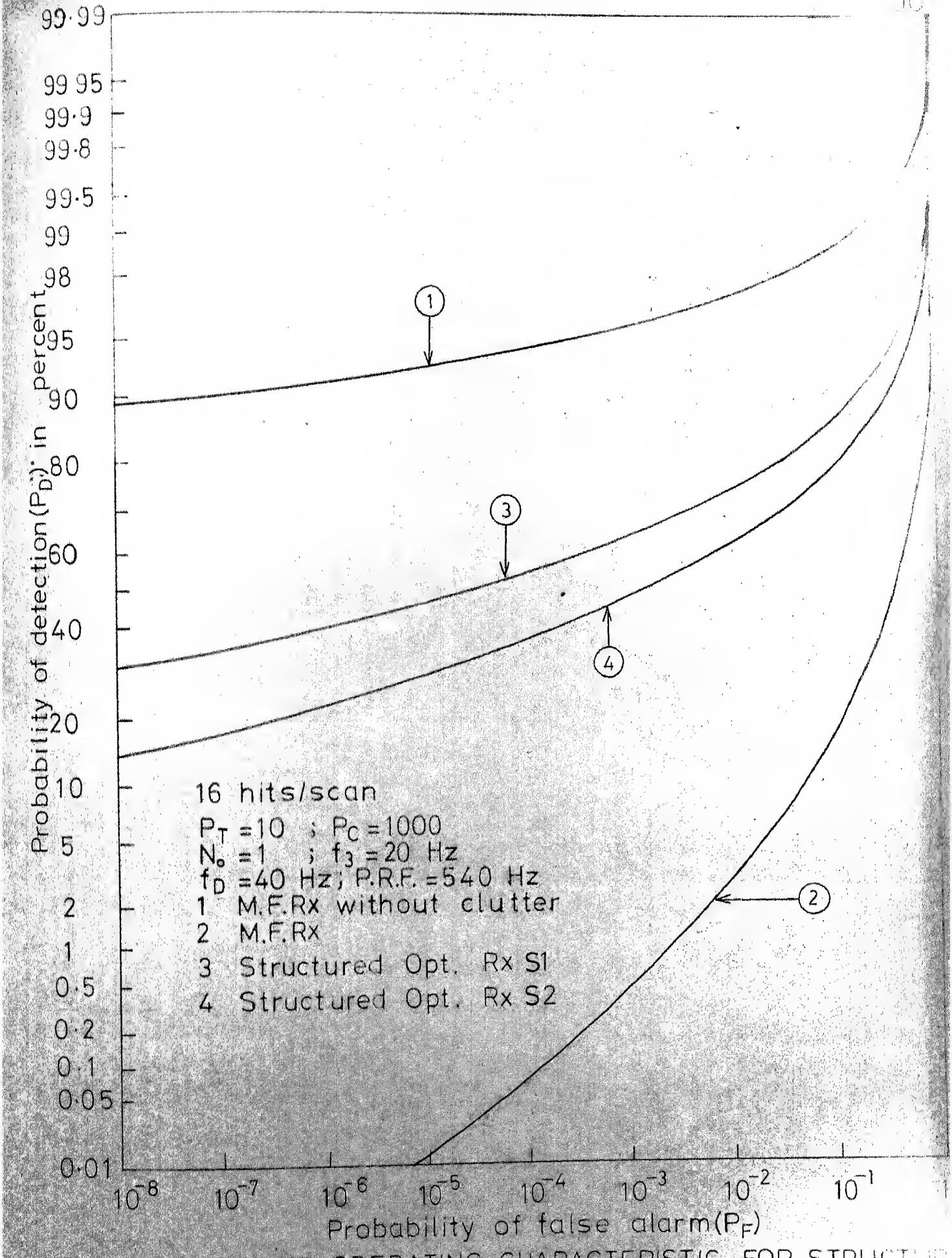

FIG.4·13 RECEIVER OPERATING CHARACTERISTIC FOR STRUCTURED OPTIMUM AND MATCHED FILTER RECEIVERS

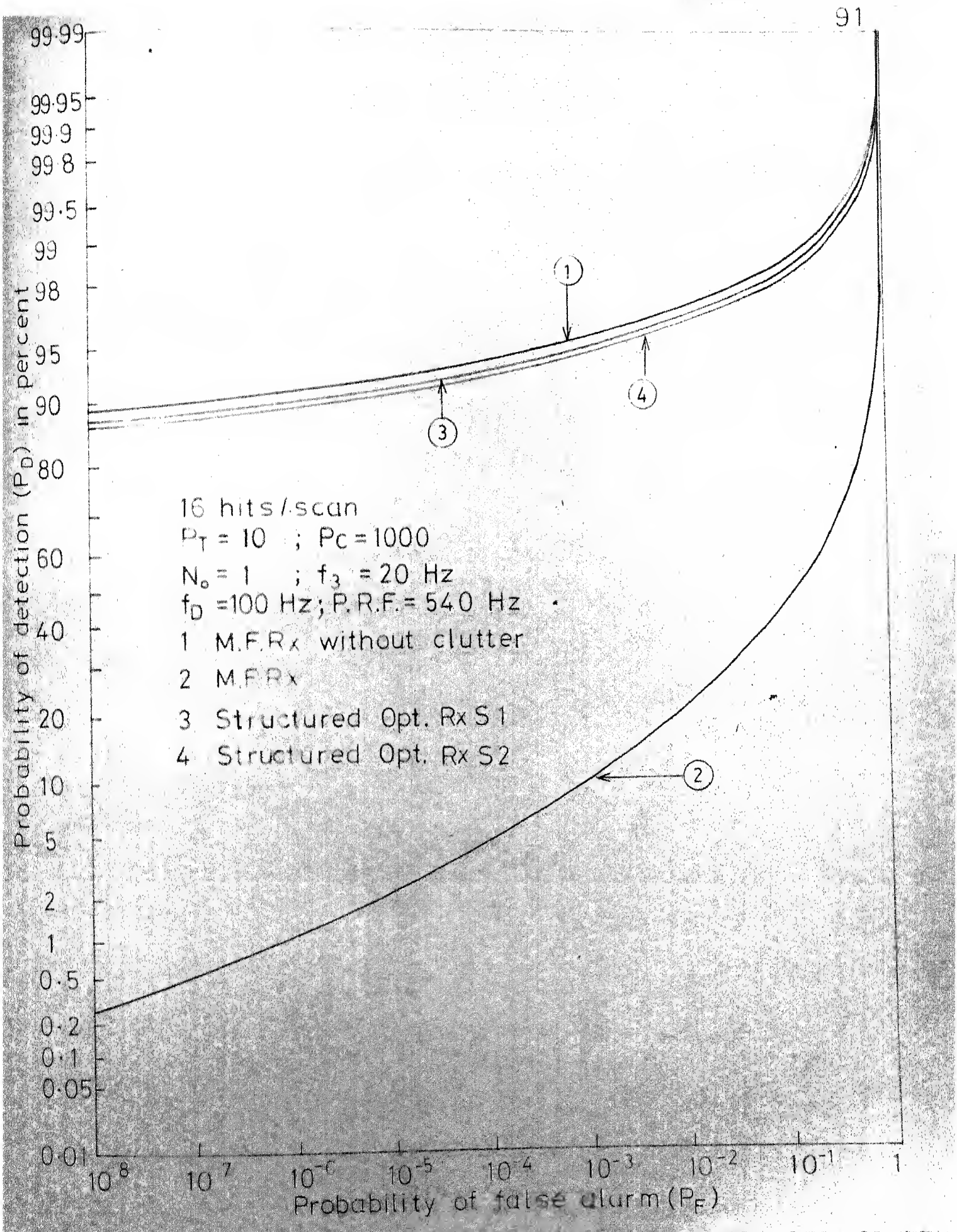

FIG. 4·14 RECEIVER OPERATING CHARACTERISTIC FOR STRUCTURED OPTIMUM AND MATCHED FILTER RECEIVRS

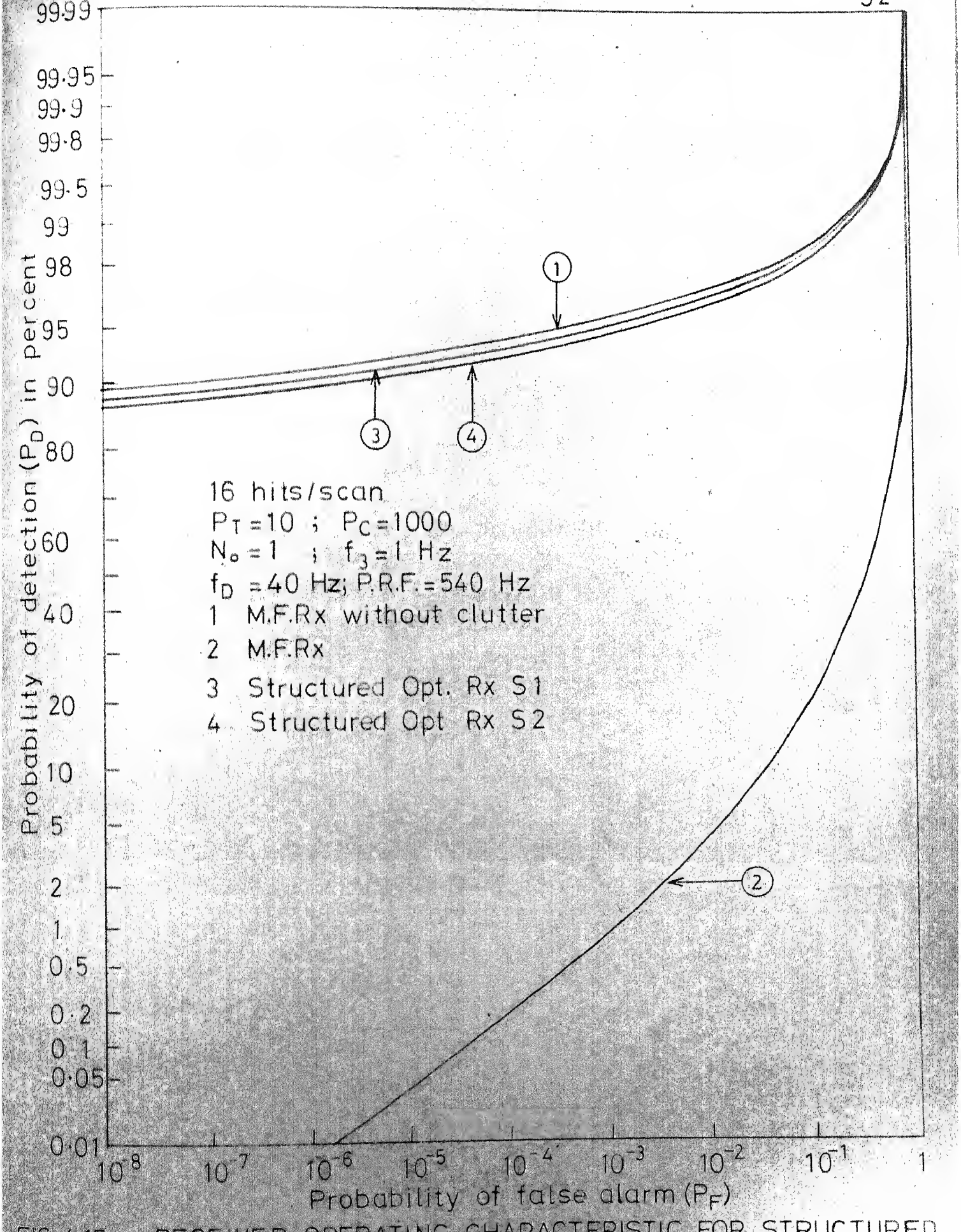

FIG.4.15 RECEIVER OPERATING CHARACTERISTIC FOR STRUCTURED OPTIMUM AND MATCHED FILTER RECEIVERS

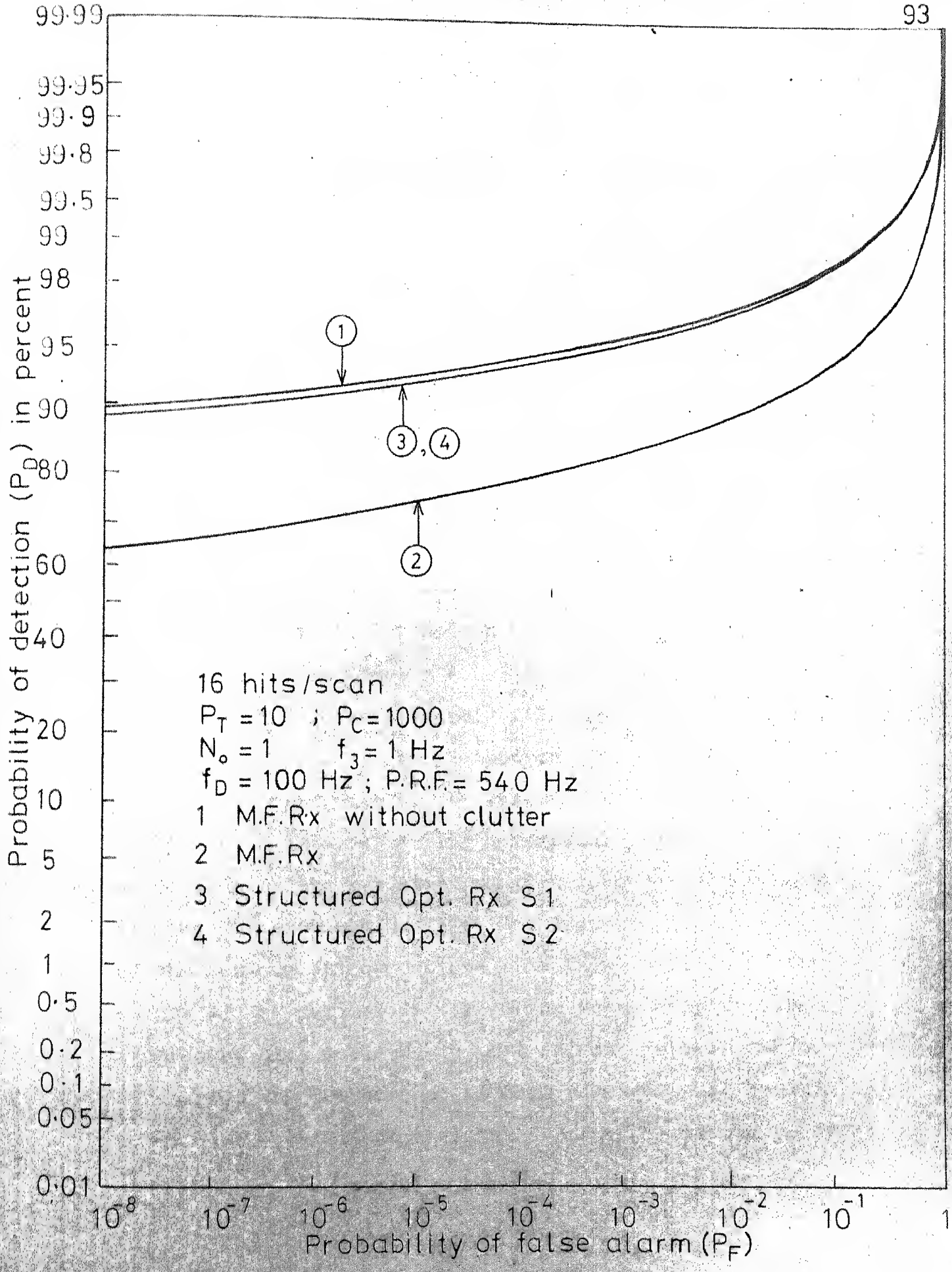

FIG. 4·16 RECEIVER OPERATING CHARACTERISTIC FOR STRUCTURED OPTIMUM AND MATCHED FILTER RECEIVERS

CHAPTER 5

STRUCTURED RECEIVER FORMULATION

In this chapter, we propose a structured receiver, that in many instances is simpler to implement than the structured optimum receiver of Chapter 4. This structured receiver is based on interpreting the maximum entropy method as an attempt to determine the structure of a whitening filter for a time series. Again a matched filter structure is imposed on the receiver for the reasons stated in Chapter 4. The received signal is passed through this matched filter (matched to a single pulse return) and the output of the matched filter is sampled appropriately for returns corresponding to the range bin of interest during a particular scan. Further processing on the resulting samples is done by a whitening filter. This whitening filter is adaptively estimated by the maximum entropy method from these samples at the output of the matched filter during scans when no target is present or a decision to that effect has been taken. Of course, the performance of this receiver will be inferior or at most equal to that of the structured optimum receiver.

In Section 5.1, we propose a structured receiver based on the above whitening filter concept and discuss how this structured receiver can be used for both coherent and noncoherent detection. In Section 5.2 we obtain an expression for the performance of the proposed structured receiver with coherent detection, for Swerling 1 target models. In Section 5.3, we present a generalised procedure and derive formulae to obtain the probability of detection (P_D) and probability of false alarm (P_F) for receivers where correlated complex Gaussian samples are modulus squared and added. This procedure also takes into account the effect of a whitening filter or a moving target indicator (MTI) filter prior to modulus squaring operation. Using this procedure, the P_D and P_F of the proposed structured receiver with noncoherent detection may be calculated. In Section 5.4, we evaluate the performance of such receivers, for both coherent and noncoherent detection, for Swerling 1 target models. Their performance is compared with that of a double line canceller MTI receiver. This is considered appropriate as the structured receivers using noncoherent detection turn out to be similar to an adaptive MTI receiver. Again a large number of receiver operating characteristic (ROC) graphs indicating the performance of such a receiver, under varying conditions of the target, clutter and thermal noise are included in this Section. These ROC's have been obtained by computer simulation and numerical computation.

5.1 Structured Receiver Based on the Whitening Filter Concept of MEM

The received signal $\tilde{r}(t)$ in (2.30) or (4.1) is passed through a matched filter (matched to a single pulse return) and the output of the matched filter is sampled appropriately for returns corresponding to a single range bin (zero'th range bin in this case) during a particular scan. From (4.12) the resulting hypothesis testing problem for a Swerling 1 target model can be written as

$$\begin{aligned} \tilde{r}_m &= \sqrt{E_t}\,\tilde{B}\exp(j\omega_D m T_p) + \tilde{I}_m \quad : H_1 \\ \tilde{r}_m &= \tilde{I}_m \quad : H_o \end{aligned}$$

$$m = 0,1,\ldots,M-1 \qquad (5.1)$$

The $\tilde{I}_m$'s constitute a coloured noise time series. As seen in Chapter 2, the maximum entropy method can be viewed as an attempt to determine a filter structure that whitens the observed time series. It can also be interpreted as an attempt to determine a prediction error filter for a given time series. From (2.43), the transfer function $\tilde{H}(f)$ of such a whitening or prediction error filter is given by (in complex envelope notation)

$$\tilde{H}(f) = \sum_{i=0}^{MAX} \tilde{\alpha}_i \exp(-j2\pi f i T_p) \qquad (5.2)$$

where $\tilde{\alpha}_o = 1$. $\tilde{\alpha}_i$'s for $i = 1,2,\ldots,$MAX and MAX are determined by solving (2.44) recursively. In the hypothesis testing

problem of (5.1), $\tilde{\alpha}_i$'s and MAX are determined from $\tilde{r}_m$'s during those scans when there is no target or a decision to that effet has been taken. This is illustrated in Fig. 5.1 where $\tilde{\varepsilon}_m$ is the whitened output of the filter when

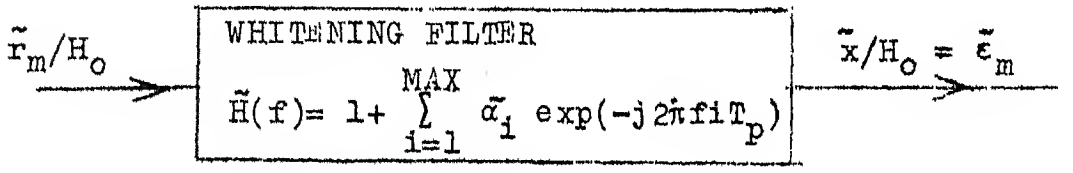

Fig.5.1 Interference Whitening Filter Obtained by MEM (Complex Operations).

the input consists of clutter and thermal noise. Now whether the $\tilde{\varepsilon}_m$'s are actually white noise samples or not depends on the statistics of $\tilde{I}_m$'s and how adequately an autoregressive (AR) model of a finite order can be used to describe the observed time series. In the rest of the discussion throughout this section, $\tilde{\varepsilon}_m$'s are assumed to be white noise samples in the context of the MEM whitening filter. The normalised covariance matrix of $\tilde{\varepsilon}_m$'s is therefore assumed to be an identity matrix. However, in Sections 5.2 - 5.4, when we evaluate the performance of structured receivers, the whitening filter is taken to be just a linear filter following the matched filter. In the current scan, when hypothesis H_1 or H_o is being tested, the $\tilde{r}_m$'s are sent through this whitening filter. Let $\tilde{x}_m$ denote

the output of the whitening filter. During the initialisation phase, to obtain $\tilde{x}_m$'s for m = 0, 1, ... (MAX-1), the past values of $\tilde{r}_m$'s for m = -1, -2, ... -(MAX), are required. As these are not known, two variations of the hypothesis testing problem follow. The first variation is to assume the past values of $\tilde{r}_m$'s for m = -1,-2,...-(MAX) to be equal to their mean or expected value $E[\tilde{r}_m]$. This is equal to zero as the samples are zero mean random variables. Then the hypothesis testing problem becomes,

$$\tilde{x}_m = \sqrt{E_t} \sum_{\substack{i=0 \\ i \leq m}}^{MAX} \tilde{\alpha}_i \tilde{B} \exp(j \omega_D (m-i) T_p) + \tilde{\varepsilon}_m \quad : H_1$$

$$\tilde{x}_m = \tilde{\varepsilon}_m \quad : H_o$$

$$\text{where } \tilde{\alpha}_o = 1 \text{ and } m = 0,1,\ldots,M-1 \qquad (5.3)$$

This hypothesis testing problem will be denoted as hypothesis testing problem A.

The second variation is to ignore the first (MAX-1) samples at the output of the whitening filter and test for hypothesis H_1 or H_o only from m = MAX, MAX+1,..., M-1. This calls for no assumption, but the entire available data containing target information is not being utilised. This hypothesis testing problem can be stated as

$$\tilde{x}_m = \sqrt{E_t} \sum_{i=o}^{MAX} \tilde{\alpha}_i \tilde{B} \exp(j \omega_D (m-i) T_p) + \tilde{\epsilon}_m \quad : H_1$$

$$\tilde{x}_m = \tilde{\epsilon}_m \quad : H_o$$

where $\tilde{\alpha}_o = 1$ and $m = MAX, MAX+1, \ldots, M-1$ (5.4)

This hypothesis testing problem will be denoted as hypothesis testing problem B. The difference in performance of structured receivers based on hypotheses testing problems A and B respectively, is brought out clearly in Section 5.4.

The hypotheses testing problems of (5.3) and (5.4) can now be easily solved. We will consider the structured receiver for the following cases:

(a) Hypothesis testing problem A with coherent detection. Hypothesis testing problem A is solved using the Neyman-Pearson criterion for optimisation. A similar hypothesis testing problem has been solved in Section 4.2. Using the same procedure the decision rule can be stated as

$$\left| \sum_{m=o}^{M-1} \tilde{x}_m \tilde{s}_m^* \right|^2 \underset{H_o}{\overset{H_1}{\gtrless}} \eta_T \qquad (5.5)$$

where $\tilde{s}_m = \sum_{\substack{i=o \\ i \le m}}^{MAX} \tilde{\alpha}_i \exp(j \omega_D (m-i) T_p)$.

The structured receiver corresponding to (5.5) is denoted as structured receiver A1 and is shown in Fig. 5.2.

(b) Hypothesis testing problem A with noncoherent (square law) detection. In this case the decision rule is stated as

$$\sum_{m=o}^{M-1} |\tilde{x}_m|^2 \underset{H_o}{\overset{H_1}{\gtrless}} \eta_T \qquad (5.6)$$

This decision rule is simpler to implement than (5.5). The structured receiver corresponding to (5.6) is denoted as structured receiver A2 and is shown in Fig. 5.3.

(c) Hypothesis testing problem B with coherent detection. This hypothesis testing problem is solved using the Neyman-Pearson criterion for optimisation. A similar hypothesis testing problem has been solved in Section 4.2. Using the same procedure, the decision rule can be stated as

$$\left| \sum_{m=MAX}^{M-1} \tilde{x}_m \, \tilde{s}_m^* \right|^2 \underset{H_o}{\overset{H_1}{\gtrless}} \eta_T \qquad (5.7)$$

where $\tilde{s}_m = \sum_{i=o}^{MAX} \tilde{\alpha}_i \exp(j\omega_D(m-i)T_p)$; $m \geq MAX$

The structured receiver corresponding to (5.7) is denoted as structured receiver B1 and is shown in Fig. 5.4.

(d) Hypothesis testing problem B with noncoherent detection. In this case the decision rule is stated as

$$\sum_{m=MAX}^{M-1} |\tilde{x}_m|^2 \underset{H_o}{\overset{H_1}{\gtrless}} \eta_T \qquad (5.8)$$

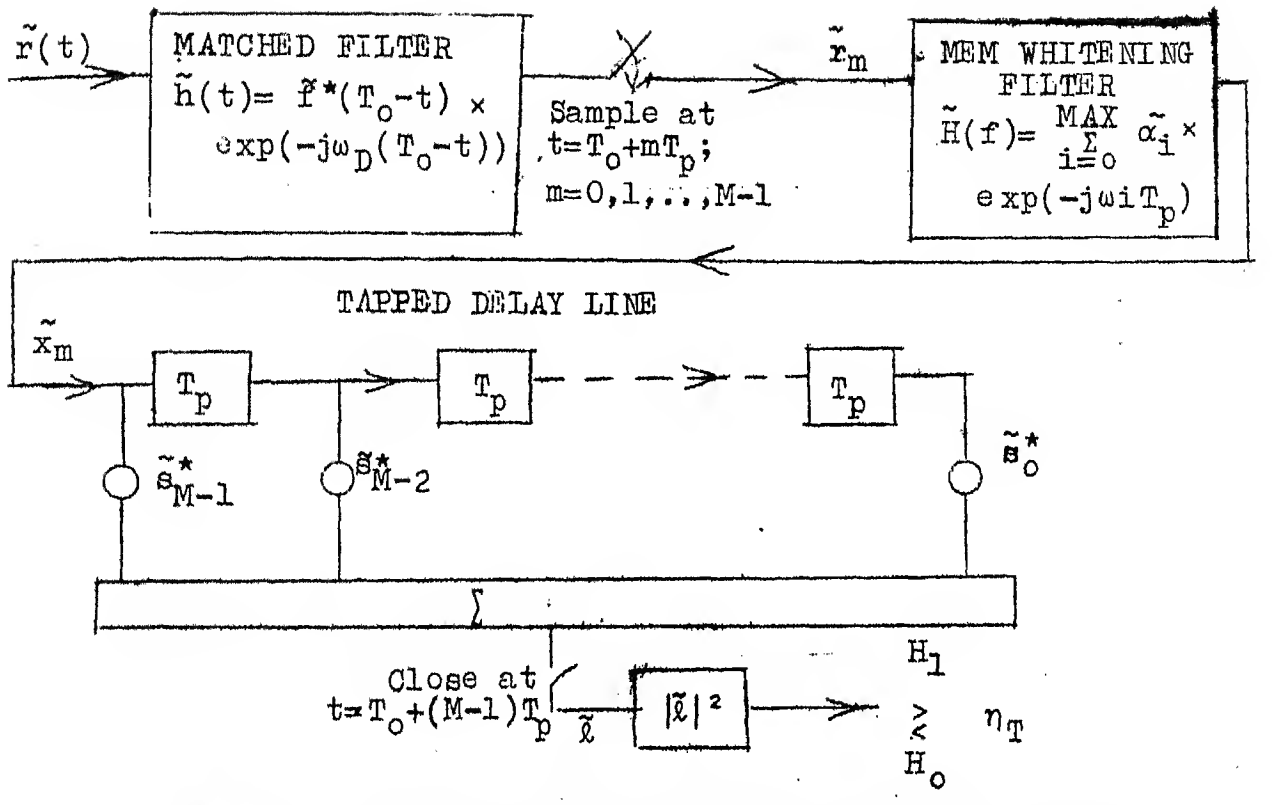

Fig.5.2 Structured Receiver A1 (Complex Operations).

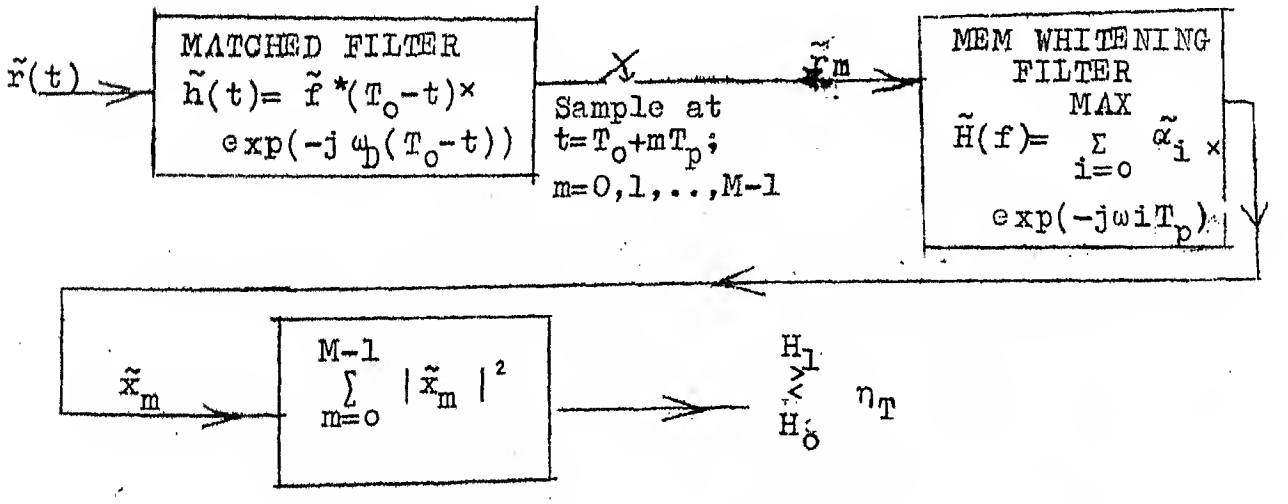

Fig. 5.3 Structured Receiver A2 (Complex Operations).

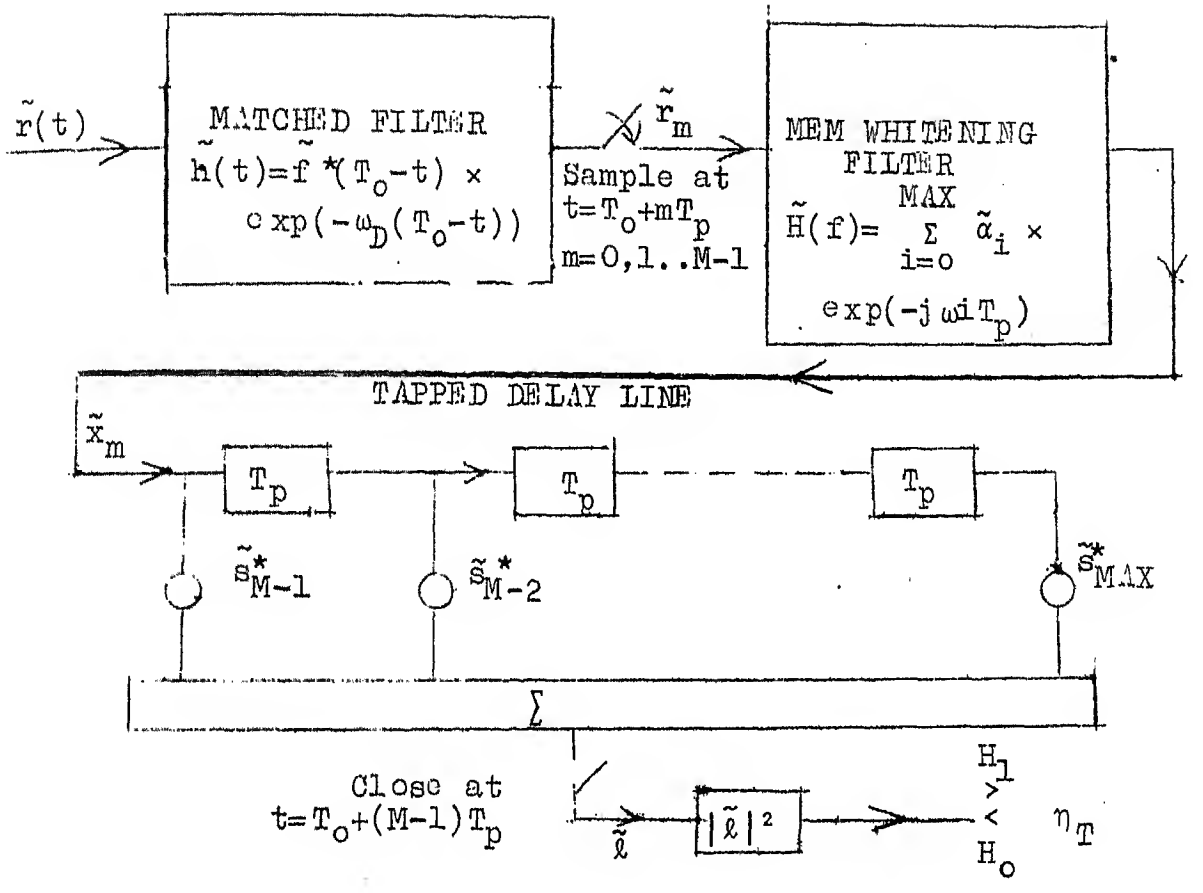

Fig.5.4 Structured Receiver B1(Complex Operations).

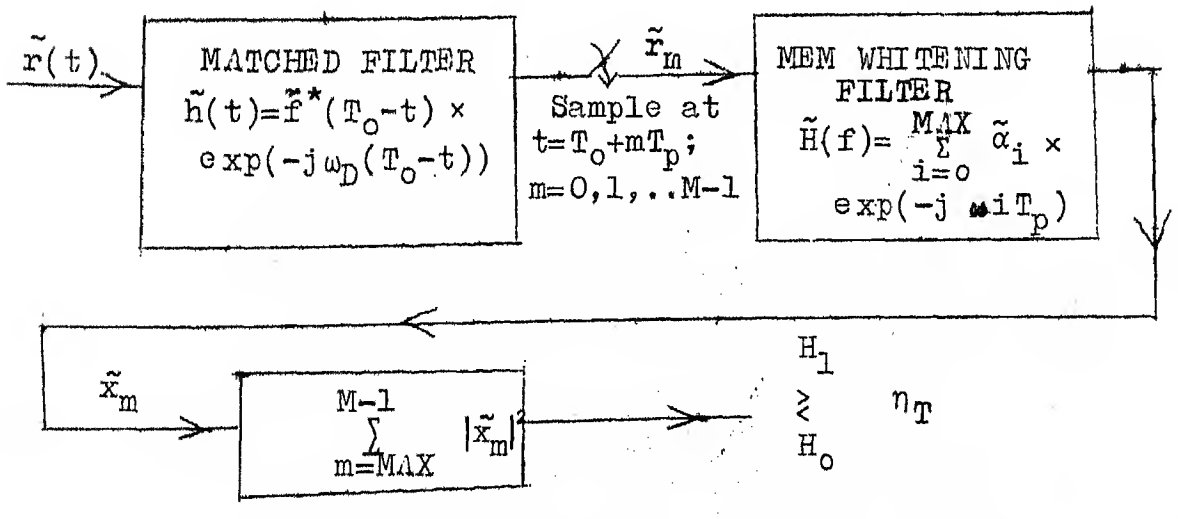

Fig.5.5 Structured Receiver B2 (Complex Operations).

Again this decision rule is simpler to implement than (5.7). The structured receiver corresponding to (5.8) is denoted as structured receiver B2 and is shown in Fig. 5.5.

5.2 Performance of the Structured Receiver with Coherent Detection

In calculating the performance of the structured receiver, the whitening filter is taken to be just a linear filter with transfer function given by (5.2).

From (5.5) and (5.7), the decision rule is given by

$$|\tilde{\ell}|^2 = \left| \sum_{m=o}^{M-1} \tilde{x}_m \tilde{s}_m^* \right|^2 \underset{H_o}{\overset{H_1}{\gtrless}} \eta_T \quad \text{for structured receiver A1}$$

where $$\tilde{s}_m = \sum_{\substack{i=o \\ i \le m}}^{MAX} \tilde{\alpha}_i \exp(j\omega_D(m-i)T_p)$$

and

$$|\tilde{\ell}|^2 = \left| \sum_{m=MAX}^{M-1} \tilde{x}_m \tilde{s}_m^* \right|^2 \underset{H_o}{\overset{H_1}{\gtrless}} \eta_T \quad \text{for structured receiver B1}$$

where $$\tilde{s}_m = \sum_{i=o}^{MAX} \tilde{\alpha}_i \exp(j\omega_D(m-i)T_p) \quad ; \quad m \ge MAX$$

$\tilde{\ell}$ is a sufficient statistic and is a complex Gaussian random variable. In such a case from Section 4.3, we have

$$P_F = (P_D)^{1+\Delta} \quad \text{where} \quad \Delta = \frac{E[\,|\tilde{\ell}|^2/H_1] - E[\,|\tilde{\ell}|^2/H_o]}{E[\,|\tilde{\ell}|^2/H_o]} \qquad (5.9)$$

Define

$$\tilde{x} = \begin{bmatrix} \tilde{x}_0 \\ \tilde{x}_1 \\ \vdots \\ \tilde{x}_{M-1} \end{bmatrix}, \quad \tilde{x}_{TR} = \begin{bmatrix} \tilde{x}_{MAX} \\ \tilde{x}_{MAX+1} \\ \vdots \\ \tilde{x}_{M-1} \end{bmatrix}, \quad \tilde{s} = \begin{bmatrix} \tilde{s}_0 \\ \tilde{s}_1 \\ \vdots \\ \tilde{s}_{M-1} \end{bmatrix}, \quad \tilde{s}_{TR} = \begin{bmatrix} \tilde{s}_{MAX} \\ \tilde{s}_{MAX+1} \\ \vdots \\ \tilde{s}_{M-1} \end{bmatrix} \tag{5.10}$$

$\tilde{r}$ is as defined in (4.13).

From (5.3) we observe that

$$\tilde{x} = \tilde{F}\,\tilde{r} \tag{5.11a}$$

where

$$\tilde{F} \triangleq \begin{bmatrix} \tilde{\alpha}_0 & & & & \\ \tilde{\alpha}_1 & \tilde{\alpha}_0 & & & \\ \tilde{\alpha}_2 & \tilde{\alpha}_1 & \tilde{\alpha}_0 & & 0 \\ \cdot & & & & \\ \cdot & & & & \\ \cdot & & & & \\ \tilde{\alpha}_{MAX} & \tilde{\alpha}_{MAX-1} & \cdots & \tilde{\alpha}_0 & \\ & \ddots & & \ddots & \\ 0 & & \tilde{\alpha}_{MAX} & \cdots & \tilde{\alpha}_0 \end{bmatrix} \tag{5.11b}$$

$$E[\tilde{x}\ \tilde{x}^{*T}] = E[\tilde{F}\ \tilde{r}\ \tilde{r}^{*T}\ \tilde{F}^{*T}] = \tilde{F}\ E[\tilde{r}\ \tilde{r}^{*T}]\tilde{F}^{*T} \tag{5.12}$$

From (5.4) we again observe that

$$\tilde{x}_{TR} = \tilde{F}_{TR}\ \tilde{r}$$

where

$$\tilde{F}_{TR} = \begin{bmatrix} \tilde{\alpha}_{MAX} & \cdots & \tilde{\alpha}_o & & 0 \\ & \ddots & & \ddots & \\ 0 & & \tilde{\alpha}_{MAX} & \cdots & \tilde{\alpha}_o \end{bmatrix}_{(M-MAX)xM} \tag{5.13b}$$

$$E[\tilde{x}_{TR}\ \tilde{x}_{TR}^{*T}] = \tilde{F}_{TR}\ E[\tilde{r}\ \tilde{r}^{*T}]\tilde{F}_{TR}^{*T} \tag{5.14}$$

Proceeding along the same lines as in Section 4.3 and using the same notation for the target and interference covariance matrix, we have

For structured receiver A1,

$$E[\ |\tilde{\ell}|^2/H_o] = 2\beta^2\ \tilde{s}^{*T}\ \tilde{F}\ \tilde{\Lambda}_I\ \tilde{F}^{*T}\ \tilde{s} \tag{5.15}$$

and

$$E[\ |\tilde{\ell}|^2/H_1] = 2\sigma_B^2\ E_t\ \tilde{s}^{*T}\ \tilde{F}\ \tilde{\Lambda}_T\ \tilde{F}^{*T}\ \tilde{s} + 2\beta^2\ \tilde{s}^{*T}\ \tilde{F}\ \tilde{\Lambda}_I\ F^{*T}\ \tilde{s} \tag{5.16}$$

and

$$\Delta_{A1} = \frac{2\sigma_B^2 E_t \tilde{s}^{*T} \tilde{F} \tilde{\Lambda}_T \tilde{F}^{*T} \tilde{s}}{2\beta^2 \tilde{s}^{*T} \tilde{\Lambda}_I \tilde{F}^{*T} \tilde{s}} = \frac{2\sigma_B^2 E_t \tilde{s}^{*T} \tilde{F} \tilde{\Lambda}_T \tilde{F}^{*T} \tilde{s}}{(2h^2E_t+N_o)\tilde{s}^{*T} \tilde{F} \tilde{\Lambda}_I \tilde{F}^{*T} \tilde{s}} \tag{5.17}$$

For structured receiver B1,

$$[E[\,|\tilde{\ell}|^2/H_o] = 2\beta^2 \tilde{s}_{TR}^{*T} \tilde{F}_{TR} \tilde{\Lambda}_I \tilde{F}_{TR}^{*T} \tilde{s}_{TR} \tag{5.18}$$

and

$$E[|\tilde{\ell}|^2/H_1] = 2\sigma_B^2 E_t \tilde{s}_{TR}^{*T} \tilde{F}_{TR} \tilde{\Lambda}_T \tilde{F}_{TR}^{*T} \tilde{s}_{TR} + 2\beta^2 \tilde{s}_{TR}^{*T} \tilde{F}_{TR} \tilde{\Lambda}_I \tilde{F}_{TR}^{*T} \tilde{s}_{TR} \tag{5.19}$$

and

$$\Delta_{B1} = \frac{2\sigma_B^2 E_t \tilde{s}_{TR}^{*T} \tilde{F}_{TR} \tilde{\Lambda}_T \tilde{F}_{TR}^{*T} \tilde{s}_{TR}}{2\beta^2 \tilde{s}_{TR}^{*T} \tilde{F}_{TR} \tilde{\Lambda}_I \tilde{F}_{TR}^{*T} \tilde{s}_{TR}} = \frac{2\sigma_B^2 E_t \tilde{s}_{TR}^{*T} \tilde{F}_{TR} \tilde{\Lambda}_T \tilde{F}_{TR}^{*T} \tilde{s}_{TR}}{(2h^2E_t+N_o)\tilde{s}_{TR}^{*T} \tilde{F}_{TR} \tilde{\Lambda}_I \tilde{F}_{TR}^{*T} \tilde{s}_{TR}} \tag{5.20}$$

Again $2\sigma_B^2E_t$ and $2\beta^2$ are the expected values of the target and interference power in each sample respectively.

5.3 A Generalised Procedure to Calculate P_D and P_F for Receivers where the Sufficient Statistic is obtained by a Summation of Modulus Squared Correlated Jointly Complex Gaussian Random Variables.

In this section, the expressions for P_D and P_F for receivers with the general configuration shown in Fig. 5.6 are derived. $\tilde{r}(t)$ is a complex Gaussian random process under both hypotheses H_1 and H_o respectively and y is a sufficient statistic.

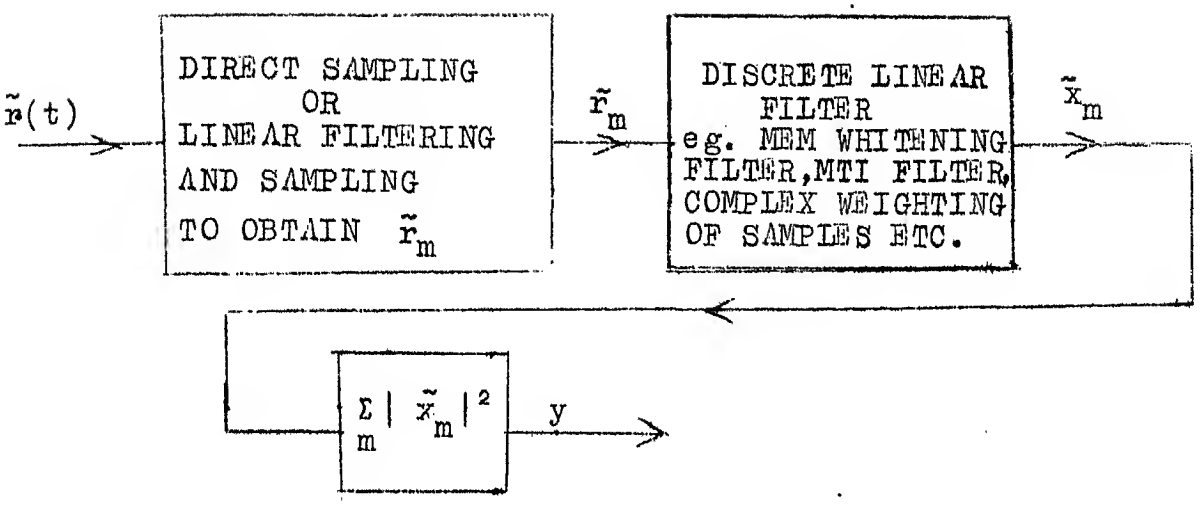

Fig.5.6 General Configuration of the Receiver (Complex Operations) for which P_D and P_F Expressions are obtained.

We follow the same notation as in Section 5.2, and proceed with the derivation using the statistics of $\tilde{r}_m$'s. Under hypothesis H_o, let

$$\tilde{r}_m = \tilde{f}_m , \quad m = 0,1,\ldots,M-1 \tag{5.21}$$

and under hypothesis H_1, let

$$\tilde{r}_m = \sqrt{E_t}\,\tilde{B}\,\tilde{u}_m + \tilde{I}_m , \quad m = 0,1,\ldots,M-1 \tag{5.22}$$

where $\tilde{f}_m$'s are jointly complex Gaussian random variables and constitute the correlated interference samples and $\tilde{B}$ is a complex Gaussian random variable and $\sqrt{E_t}\,\tilde{B}\,\tilde{u}_m$ constitutes the signal samples. $\tilde{B}$ and $\tilde{I}_m$'s are independent. Therefore,

$\tilde{r}_m$'s under both hypotheses H_o and H_1 are jointly complex Gaussian random variables. Again following the same notation as in Section 5.2, let

$$\tilde{I} = [\tilde{I}_o \cdots \tilde{I}_{M-1}]^T, \quad \tilde{u} = [\tilde{u}_o \cdots \tilde{u}_{M-1}]^T, \quad \tilde{r} = [\tilde{r}_o \cdots \tilde{r}_{M-1}]^T$$

and

$$E[\tilde{I}] = 0, \quad E[\tilde{B}] = 0, \quad E[|\tilde{B}|^2] = 2\sigma_B^2, \quad E[\tilde{I}\,\tilde{I}^{*T}] = 2\beta^2\,\tilde{\Lambda}_I \tag{5.23}$$

Equations (5.21) and (5.22) can be written as

$$\begin{aligned} \tilde{r} &= \sqrt{E_t}\,\tilde{B}\,\tilde{u} + \tilde{I} \quad &: H_1 \\ \tilde{r} &= \tilde{I} \quad &: H_o \end{aligned} \tag{5.24}$$

where $E[(\tilde{r}\,\tilde{r}^{*T})/H_o] = 2\beta^2\,\tilde{\Lambda}_I$

and $E[(\tilde{r}\,\tilde{r}^{*T})/H_1] = 2\sigma_B^2\,E_t\,\tilde{u}\,\tilde{u}^{*T} + 2\beta^2\,\tilde{\Lambda}_I = 2\gamma^2\Lambda_R$

$2\beta^2$ represents the expected value of the interference power in each sample. $2\gamma^2$ represents the expected value of the combined signal and interference power in each sample when the signal is present.

We now have the following joint density functions,

$$p_{\tilde{r}/H_o}(\tilde{r}/H_o) = \frac{1}{(2\pi\beta^2)^M\,\mathrm{Det}(\tilde{\Lambda}_I)}\exp\left[-\frac{1}{2\beta^2}(\tilde{r}^{*T}\,\tilde{\Lambda}_I^{-1}\,\tilde{r})\right] \tag{5.25}$$

and

$$p_{\tilde{r}/H_1}(\tilde{r}/H_1) = \frac{1}{(2\pi\gamma^2)^M\,\mathrm{Det}(\tilde{\Lambda}_R)}\exp\left[-\frac{1}{2\gamma^2}(\tilde{r}^{*T}\,\tilde{\Lambda}_R^{-1}\,\tilde{r})\right] \tag{5.26}$$

When no output samples are ignored, the discrete linear filter (Whitening, MTI etc.) output may be described by means of an MxM transfer matrix F such that

$$\tilde{x} = \tilde{F}\,\tilde{r} \qquad \text{where} \quad \tilde{x} = [\tilde{x}_0, \ldots, \tilde{x}_{M-1}]^T \tag{5.27}$$

When the first M-p output samples are ignored, the required filter output may be described by means of a pxM transfer matrix $\tilde{F}_{TR}$ such that

$$\tilde{x}_{TR} = \tilde{F}_{TR}\,\tilde{r} \qquad \text{where} \quad \tilde{x}_{TR} = [\tilde{x}_{M-p}, \ldots, \tilde{x}_{M-1}]^T \tag{5.28}$$

For structured receivers A2 and B2 of Section 5.1, F and F_{TR} are as defined in (5.11) and (5.13) respectively. When no filter is used, $\tilde{F}$ and $\tilde{F}_{TR}$ are identity matrices. In the case of complex weighting of the samples, $\tilde{F}$ and $\tilde{F}_{TR}$ are diagonal matrices with different weights on the diagonal.

Without loss of generality, we proceed to calculate, P_D and P_F for the case represented by (5.27).

Then, the joint density function of $\tilde{x}_m$'s is given by

$$p_{\tilde{x}/H_0}(\tilde{x}/H_0) = \frac{1}{(2\pi\beta^2)^M \, \mathrm{Det}(\tilde{D}_I)} \exp\left[-\frac{1}{2\beta^2}(\tilde{x}^{*T}\,\tilde{D}_I^{-1}\,\tilde{x})\right] \tag{5.29}$$

and

$$p_{\tilde{x}/H_1}(\tilde{x}/H_1) = \frac{1}{(2\pi\gamma^2)^M \, \mathrm{Det}(\tilde{D}_R)} \exp\left[-\frac{1}{2\gamma^2}(\tilde{x}^{*T}\,\tilde{D}_R^{-1}\,\tilde{x})\right] \tag{5.30}$$

where

$$\tilde{D}_I = \tilde{F}\ \tilde{A}_I\ \tilde{F}^{*T} \qquad \text{and} \qquad \tilde{D}_R = \tilde{F}\ \tilde{A}_R\ \tilde{F}^{*T} \tag{5.31}$$

The output of the summer/integrator is given by

$$y = \sum_{m=0}^{M-1} |\tilde{x}_m|^2 = \tilde{x}^{*T}\ \tilde{x} \tag{5.32}$$

$\tilde{D}_R$ and $\tilde{D}_I$ are Hermitian matrices and both are positive definite. They may be diagonalised by solving the eigenvalue problems

$$\tilde{D}_I\ \tilde{L}_I^{(k)} = \lambda_k\ \tilde{L}_I^{(k)} \quad ; \quad k = 0,1,\ldots,M-1 \tag{5.33}$$

and

$$\tilde{D}_R\ \tilde{L}_R^{(k)} = \mu_k\ \tilde{L}_R^{(k)} \quad ; \quad k = 0,1,\ldots,M-1 \tag{5.34}$$

The eigenvalues λ_k's and μ_k's will be real and positive. $\tilde{L}_I^{(k)}$'s and $\tilde{L}_R^{(k)}$'s are their corresponding eigenvectors. In (5.33), if all the eigenvalues are distinct, the eigenvectors are orthogonal and can be made orthonormal. If there are repeated eigenvalues, the corresponding eigenvectors will not be orthogonal, but as $\tilde{D}_I$ is Hermitian, these eigenvectors will be linearly independent. These eigenvectors can then be transformed into orthonormal vectors using the Gram-Schmidt orthonormalisation procedure. Therefore, in general we assume that $\tilde{L}_I^{(k)}$'s are orthonormal for $k = 0,1,\ldots,M-1$. The same argument holds true for the eigenvalues and eigenvectors of (5.34).

Let

$$\tilde{L}_I = \begin{bmatrix} \vdots & & \vdots \\ \tilde{L}_I^{(0)} & \cdots & \tilde{L}_I^{(M-1)} \\ \vdots & & \vdots \end{bmatrix}$$

and

$$\tilde{L}_R = \begin{bmatrix} \vdots & & \vdots \\ \tilde{L}_R^{(0)} & \cdots & \tilde{L}_R^{(M-1)} \\ \vdots & & \vdots \end{bmatrix} \qquad (5.35)$$

Then from elementary matrix theory,

$$\tilde{L}_I^{*T} \tilde{D}_I \tilde{L}_I = \begin{bmatrix} \lambda_0 & & & \\ & \lambda_1 & & 0 \\ & & \ddots & \\ & 0 & & \lambda_{M-1} \end{bmatrix}$$

and

$$\tilde{L}_R^{*T} \tilde{D}_R \tilde{L}_R = \begin{bmatrix} \mu_0 & & & \\ & \mu_1 & & 0 \\ & & \ddots & \\ & 0 & & \mu_{M-1} \end{bmatrix} \qquad (5.36)$$

We make the following transformations in (5.32):

$$\tilde{z} = \tilde{L}_I^{*T}\,\tilde{x} \qquad \text{when } H_o \text{ is true} \tag{5.37}$$

and

$$\tilde{z} = \tilde{L}_R^{*T}\,\tilde{x} \qquad \text{when } H_1 \text{ is true} \tag{5.38}$$

where $\tilde{z} = [\tilde{z}_o, \tilde{z}_1, \ldots, \tilde{z}_{M-1}]^T$

The summer output in the both cases can be represented by

$$y = \tilde{x}^{*T}\,\tilde{x} = \tilde{z}^{*T}\,\tilde{z} = \sum_{k=o}^{M-1} |\tilde{z}_k|^2 \tag{5.39}$$

However, the joint density function of $\tilde{z}$ when H_o is true ($p_{\tilde{z}/H_o}(\tilde{z}/H_o)$) is given by

$$p_{\tilde{z}/H_o}(\tilde{z}/H_o) = \frac{1}{(2\pi\beta^2)^M \prod_{k=o}^{M-1} \lambda_k} \exp\left(-\frac{1}{2\beta^2} \sum_{k=o}^{M-1} \frac{|\tilde{z}_k|^2}{\lambda_k}\right) \tag{5.40}$$

and the joint density function of $\tilde{z}$ when H_1 is true ($p_{\tilde{z}/H_1}(\tilde{z}/H_1)$) is given by

$$p_{\tilde{z}/H_1}(\tilde{z}/H_1) = \frac{1}{(2\pi\gamma^2)^M \prod_{k=o}^{M-1} \mu_k} \exp\left(-\frac{1}{2\gamma^2} \sum_{k=o}^{M-1} \frac{|\tilde{z}_k|^2}{\mu_k}\right) \tag{5.41}$$

The complex Gaussian vector $\tilde{z}$ consists of M independent complex Gaussian random variables $\tilde{z}_k$'s. When H_o is true, the variance of each random variable $\tilde{z}_k$ is given by $2\beta^2\,\lambda_k$. Let

$$n_k = |\tilde{z}_k|^2 \tag{5.42}$$

When H_o is true, n_k will have an exponential density function ($p_{n_k/H_o}(n_k/H_o)$) given by

$$p_{n_k/H_o}(n_k/H_o) = \begin{cases} \frac{1}{2\beta^2 \lambda_k} \exp(-\frac{n_k}{2\beta^2 \lambda_k}) ; & n_k \geq 0 \\ 0 ; & n_k < 0 \end{cases} \tag{5.43}$$

Also

$$E[\exp(-s\, n_k)/H_o] = \int_0^\infty [\exp(-s\, n_k)] p_{n_k/H_o}(n_k/H_o)\, dn_k$$

$$= \frac{1}{(1 + 2\beta^2 \lambda_k s)} \tag{5.44}$$

It may be observed from (5.39) that

$$\begin{bmatrix} p_{y/H_o}(y/H_o) \\ p_{y/H_1}(y/H_1) \end{bmatrix} = 0 \quad \text{for } y < 0 \tag{5.45}$$

where $p_{y/H_o}(y/H_o)$ and $p_{y/H_1}(y/H_1)$ are the density functions of y given H_o is true and given H_1 is true respectively.

As y/H_o(y given H_o is true) is obtained by a summation of M independent random variables n_k's, the Laplace transform (one sided) of $p_{y/H_o}(y/H_o)$ is the product of the Laplace

transform of the density functions of n_k's. Or

$$\mathcal{L}_{y/H_o}(s) \triangleq \int_o^\infty \exp(-sy)\, p_{y/H_o}(y/H_o)dy = \prod_{k=o}^{M-1} \mathcal{L}_{n_k/H_o}(s) \tag{5.46}$$

Using (5.44)

$$\mathcal{L}_{y/H_o}(s) = \prod_{k=o}^{M-1} \frac{1}{(1 + 2\beta^2 \lambda_k s)} \tag{5.47}$$

Similarly we can show that

$$\mathcal{L}_{y/H_1}(s) = \prod_{k=o}^{M-1} \frac{1}{(1 + 2\gamma^2 \mu_k s)} \tag{5.48}$$

We then have

$$p_{y/H_o}(y/H_o) = \frac{1}{2\pi j} \int_{c-j\infty}^{c+j\infty} \frac{\exp(sy)\, ds}{\prod_{k=o}^{M-1} (1+2\beta^2 \lambda_k s)}$$

$$= \frac{1}{2\pi j} \int_{c-j\infty}^{c+j\infty} \frac{\exp(\frac{s}{2\beta^2} y)\, d(s/2\beta^2)}{\prod_{k=o}^{M-1} (1 + \lambda_k s)} \tag{5.49}$$

and

$$p_{y/H_1}(y/H_1) = \frac{1}{2\pi j} \int_{c-j\infty}^{c+j\infty} \frac{\exp(sy)\, ds}{\prod_{k=o}^{M-1} (1+2\gamma^2 \mu_k s)}$$

$$= \frac{1}{2\pi j} \int_{c-j\infty}^{c+j\infty} \frac{\exp(\frac{s}{2\gamma^2} y)\, d(s/2\gamma^2)}{\prod_{k=o}^{M-1} (1 + \mu_k s)} \tag{5.50}$$

The expressions to obtain $p_{y/H_o}(y/H_o)$ and $p_{y/H_1}(y/H_1)$ in (5.49) and (5.50) respectively are similar. To simplify (5.49) or (5.50), we have to consider the following three cases:

(a) All eigenvalues are distinct.

(b) All eigenvalues are identical.

(c) A combination of distinct and repeated eigenvalues.

Case (a) : All eigenvalues are distinct.

We can express

$$\frac{1}{\prod_{k=o}^{M-1}(1+\lambda_k s)} = \frac{A_o}{(1+\lambda_o s)} + \frac{A_1}{(1+\lambda_1 s)} + \cdots \frac{A_{M-1}}{(1+\lambda_{M-1} s)} \qquad (5.51)$$

and obtain $A_o \cdots A_{M-1}$ by the partial fraction method etc.

Then simplifying and taking the inverse Laplace transform in (5.49), we obtain

$$p_{y/H_o}(y/H_o) = \sum_{m=o}^{M-1} \left[\prod_{\substack{k=o \\ k\neq m}}^{M-1} \left(1 - \frac{\lambda_k}{\lambda_m}\right) \right]^{-1} \frac{\exp(-y/2\beta^2\lambda_m)}{2\beta^2 \lambda_m}$$

$$\text{for } y \geq 0 \qquad (5.52)$$

Similarly we can obtain

$$p_{y/H_1}(y/H_1) = \sum_{m=o}^{M-1} \left[\prod_{\substack{k=o \\ k\neq m}}^{M-1} \left(1 - \frac{\mu_k}{\mu_m}\right) \right]^{-1} \frac{\exp(-y/2\gamma^2 \mu_m)}{2\gamma^2 \mu_m}$$

$$\text{for } y \geq 0 \qquad (5.53)$$

The probability of false alarm and the probability of detection are given by

$$P_F = \int_{\eta_T}^{\infty} p_{y/H_o}(y/H_o)dy = \sum_{m=o}^{M-1}\Big[\prod_{\substack{k=o\\k\neq m}}^{M-1}(1-\frac{\lambda_k}{\lambda_m})\Big]^{-1} \exp(\eta_T/2\beta^2\lambda_m) \tag{5.54}$$

and

$$P_D = \int_{\eta_T}^{\infty} p_{y/H_1}(y/H_1)dy = \sum_{m=o}^{M-1}\Big[\prod_{\substack{k=o\\k\neq m}}^{M-1}(1-\frac{\mu_k}{\mu_m})\Big]^{-1} \exp(-\eta_T/2\gamma^2\mu_m) \tag{5.55}$$

Case (b): All eigenvalues are identical.

Then

$$\lambda_k = \lambda \quad \text{for} \quad k = 0,1,\ldots,M-1 \tag{5.56}$$

and

$$\mu_k = \mu \quad \text{for} \quad k = 0,1,\ldots,M-1 \tag{5.57}$$

Now from (5.49) we have,

$$p_{y/H_o}(y/H_o) = \frac{1}{2\pi j}\int_{c-j\infty}^{c+j\infty}\frac{1}{(2\beta^2\lambda)^M}\,\frac{\exp(sy)\,ds}{(s+\frac{1}{2\beta^2})^M} \quad \text{for} \quad y \geq 0 \tag{5.58}$$

Simplifying we have,

$$p_{y/H_o}(y/H_o) = \frac{1}{(2\beta^2\lambda)^M}\,\frac{y^{M-1}\exp(-y/2\beta^2)}{(M-1)!} \quad \text{for} \quad y \geq 0 \tag{5.59}$$

Now

$$P_F = \int_{\eta_T}^{\infty} p_{y/H_o}(y/H_o)dy = \frac{1}{(2\beta^2\lambda)^M}\int_{\eta_T}^{\infty}\frac{y^{M-1}\exp(-y/2\beta^2)}{(M-1)!}\,dy$$

or

$$P_F = 1 - \int_0^{\eta_T} \frac{1}{(2\beta^2\lambda)^M} \frac{y^{M-1} \exp(-y/2\beta^2)}{(M-1)!} dy \qquad (5.60)$$

Substituting $t = y/2\beta^2$ and simplifying we get,

$$P_F = 1 - \int_0^{\eta_T/2\beta^2} \frac{t^{M-1} \exp(-t)}{(M-1)!} dt \qquad (5.61)$$

Now the integral $\int_0^{u\sqrt{(1+s)}} \frac{\exp(-v)v^s}{s!} dv$ is Pearson's form of the incomplete gamma function and has been defined by Pearson [58] as,

$$I(u,s) = \int_0^{u\sqrt{(1+s)}} \frac{\exp(-v)\, v^s}{s!} dv \qquad (5.62)$$

Pearson [58] has also tabulated it upto the seventh decimal place for $s \leq 50$. Therefore, from (5.61) and (5.62)

$$P_F = 1 - I\left(\frac{\eta_T/2\beta^2\lambda}{\sqrt{M}}, M-1\right) \qquad (5.63)$$

Following the same procedure, we can obtain

$$P_D = 1 - I\left(\frac{\eta_T/2\gamma^2\mu}{\sqrt{M}}, M-1\right) \qquad (5.64)$$

Case (c): A Combination of distinct and repeated eigenvalues.

In this case $1/[\prod_{k=0}^{M-1}(1+\lambda_k s)]$ or $1/[\prod_{k=0}^{M-1}(1+\mu_k s)]$ is to be expressed as a sum of partial fractions such that the methods of Case (a) and Case (b) can be applied to obtain P_D and P_F.

Using this procedure, P_D and P_F for structured receivers A2 and B2 may be evaluated. This procedure can also be to evaluate P_D and P_F for receivers using envelope square detection followed by post-detection integration. Here it must be mentioned that Marcum [7] and Swerling [8] have derived formulae to calculate P_D and P_F for such receivers when they are used to detect nonfluctuating and fluctuating (Swerling 1 - 4) targets in white noise. Kanter [59] has generalised Swerling's procedure to include the effects of clutter for Swerling 1 and Swerling 3 targets. Kantor has assumed the power spectral density of clutter to be symmetric. The procedure developed here makes no such assumptions about the clutter or interference spectrum and can be used in the case of both Swerling 1 and Swerling 2 targets. Also this procedure is easier to use than Kanter's procedure which calls for calculating the roots of an Mth degree polynomial, M being the number of hits/scan.

5.4 Performance Evaluation of the Structured Receiver by Simulation and Numerical Computation

The performance of the structured receivers A1, A2, B1 and B2 is evaluated by means of computer simulation and numerical computation. The performance of the structured receiver in all these cases is compared with the performance of a moving target indicator (MTI) using a double delay line canceller after the matched filter. This MTI configuration is shown in Fig. 5.7.

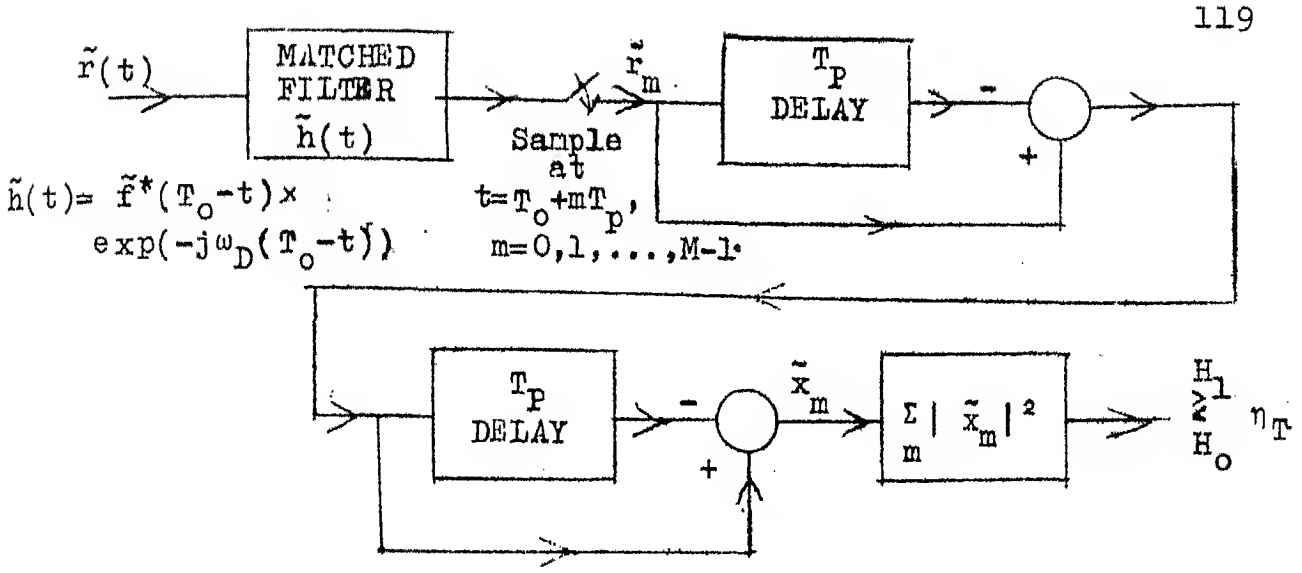

Fig. 5.7 MTI Using a Double Line Canceller (Complex Operations).

We have considered it appropriate to compare the performance of the structured receiver with that of an MTI receiver for two reasons. First, the delay line canceller MTI receiver is very widely used in operational radar systems to distinguish moving targets in clutter. The MTI receiver configuration shown in Fig. 5.7 is generally not used and the received signal is directly sampled and sent through the canceller loops, though radars using pulse compression techniques do have some sort of a matched filter front end. However, we use a matched filter front end for the MTI receiver (whose performance is evaluated here) in conformity with the structured receivers of Section 5.1. The second reason is that the structured receivers A2 and B2 turn out to be similar to an adaptive MTI receiver where the tap coefficients ($\tilde{\alpha}_i$'s) and the number of canceller loops (MAX)

are estimated adaptively from the received interference samples. As the tap coefficients are estimated on the basis of combined thermal noise and clutter, it is conjectured that the performance of the structured receiver will be superior to that of an adaptive MTI receiver where the canceller loops are designed to combat clutter alone.

The performance of the MTI receiver is evaluated for the following cases using the procedure discussed in Section 5.3.

(a) When all the M pulses at the output of the canceller are taken into account. This receiver is denoted as MTI receiver A.

(b) When the initial two pulses at the output of the canceller are ignored. Here the summation in Fig. 5.6 is from m = 3 to M-1. This receiver is denoted as MTI receiver B.

As in Chapter 4, the performance evaluation is done for varying conditions of target power, target velocity, clutter power, clutter spectral width, thermal noise power etc. Again, the clutter returns are assumed to have a Gaussian shaped power spectral density.

The entire simulation scheme is discussed in Appendix A. As in Chapter 4, zero-mean complex Gaussian clutter samples with Gaussian shaped power spectral density,

are generated on the computer. Zero-mean complex Gaussian white noise samples are also generated on the computer and these are added to the clutter samples to obtain interference samples $\tilde{I}_k$'s. These $\tilde{I}_k$'s correspond to the output of the matched filter in Figs. 5.2 - 5.7 when no target is present. Then, the complex form of the maximum entropy method is used to determine the tap coefficients ($\tilde{\alpha}_k$'s) and order (MAX) of the whitening filter. The performance evaluation of the structured receivers A1, A2, B1 and B2 and MTI receivers A and B is done using the expressions and formulae obtained in Sections 5.2 and 5.3. This evaluation is carried out for a large number of cases by varying P_T, P_c, N_o, f_D and f_3 where these terms are as denoted in Chapter 4. The receiver operating characteristics (ROC) for these cases are given in Figs. 5.8 - 5.20.

The following observations on the overall performance of the structured receivers A1, A2, B1 and B2, and on their comparative performance versus the MTI receivers A and B, are made:

(a) In the situations considered, the performance of the structured receivers (with either coherent or noncoherent detection) based on hypothesis testing problem B is far superior to that of MTI receiver B. Likewise, the performance of the structured receivers (again with either coherent or noncoherent detection) based on hypothesis testing problem A is superior or at least equal to that of MTI receiver A.

(b) When there is no clutter, the performance of the structured receivers based on hypothesis testing problem A is slightly better than the performance of the structured receivers based on hypothesis testing problem B. However, the performance of the structured receivers based on hypothesis testing problem B is far superior to that of the structured receivers based on hypothesis testing problem A even when the clutter power (P_c) is only 20 dB above the white noise power (N_o) and 10 dB above the target power (P_T). This superiority in performance increases with an increase in clutter power. Likewise, under similar clutter conditions, the MTI receiver B performs better than the MTI receiver A. At a target Doppler shift of 100 Hz and P_T equal to 10, the performance of the structured receiver A2 and the MTI receiver A approach the $P_D \simeq P_F$ limit when the clutter power is 30 dB above the white noise power.

(c) As expected, the structured receivers with coherent detection perform better than the structured receivers with noncoherent detection.

(d) In general, the performance of the structured receivers improve as the clutter spectral width decreases.

(e) The performance of both the structured and the MTI receivers is dependent on the target Doppler shift. For $P_c = 1000$ and $f_3 = 1$ Hz, the performance of the MTI receiver B deteriorates sharply when the target Doppler shift decreases from 100 Hz to 40 Hz. However, the performance deterioration

is much less in the case of the structured receivers B1 and B2 for the same change in target Doppler shift. In the case of the structured receivers B1 and B2, this performance deterioration, with a decrease in target Doppler shift, is more rapid as the clutter spectral width increases.

(f) It is observed that when f_3 is equal to 10 Hz, the performance of the MTI receiver B is thermal noise limited upto clutter power levels of 40 dB above the thermal noise power. This is obviously not so in the case of the structured receivers.

The performance of these structured receivers is inferior to the performance of the structured optimum receivers of Chapter 4. However, the implementation of the structured receivers (particularly with noncoherent detection) is easier than the implementation of the structured optimum receivers.

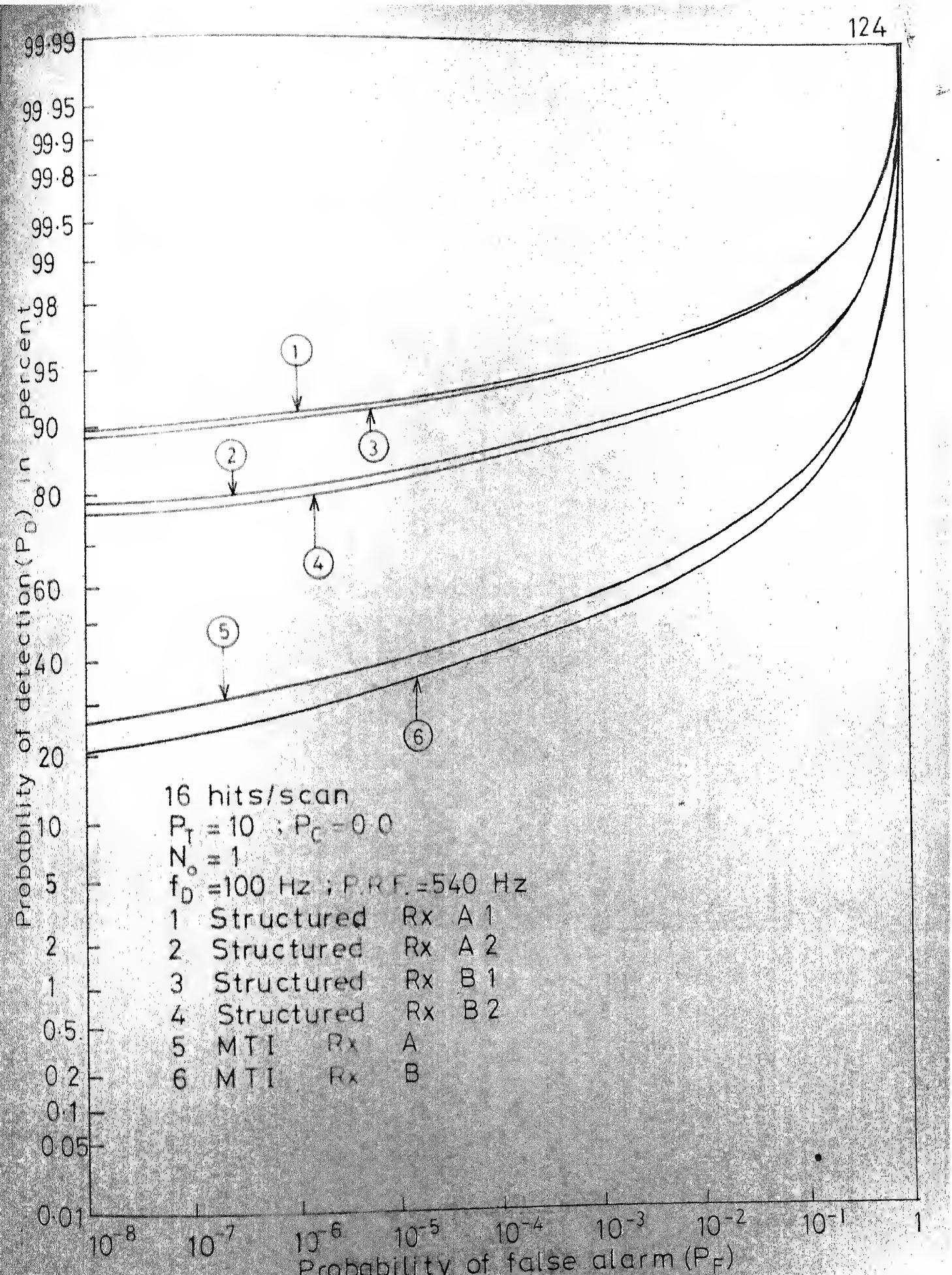

FIG. 5·8 RECEIVER OPERATING CHARACTERISTIC FOR STRUCTURED AND MTI RECEIVERS

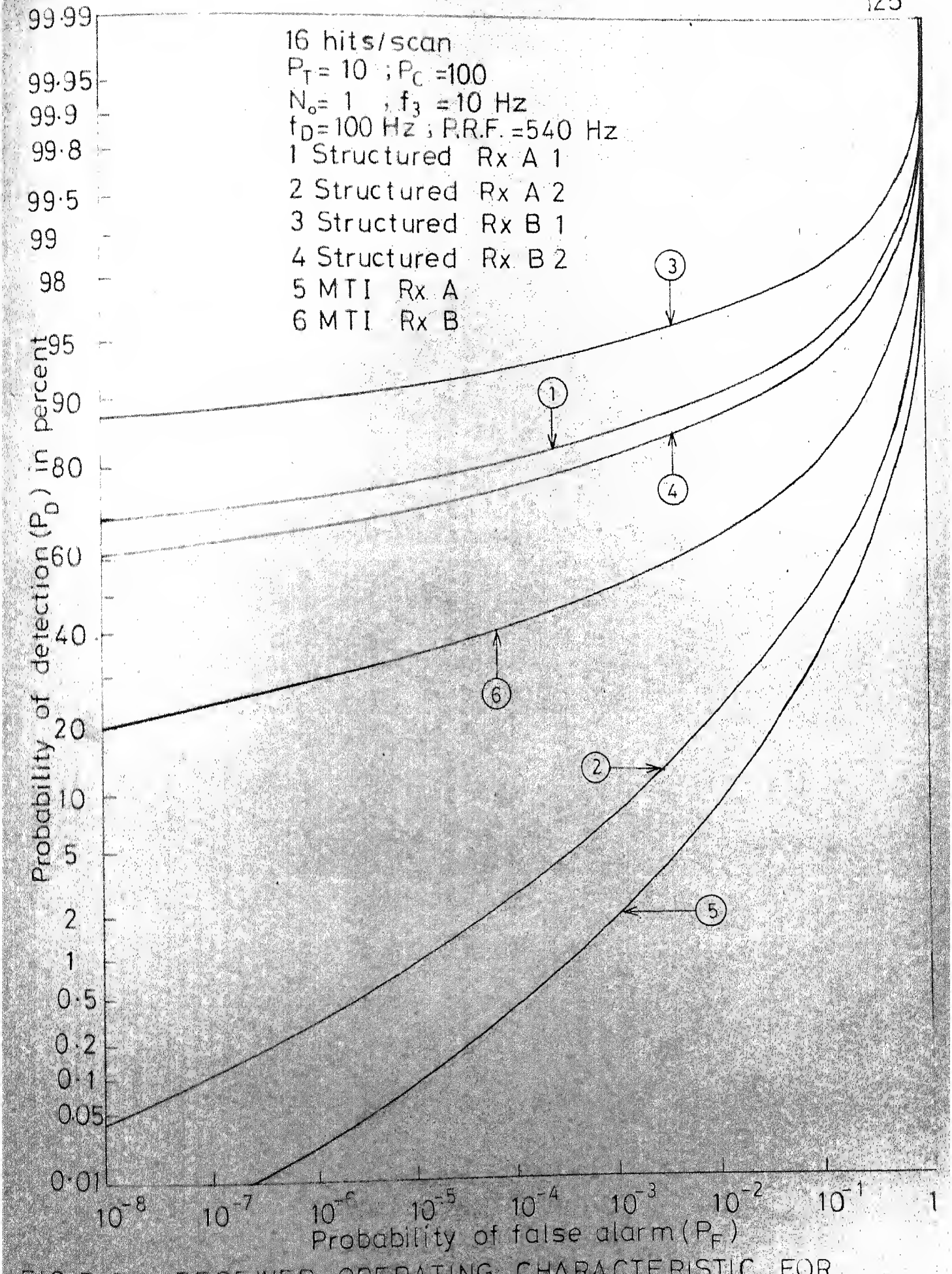

FIG.5·9 RECEIVER OPERATING CHARACTERISTIC FOR STRUCTURED AND MTI RECEIVERS

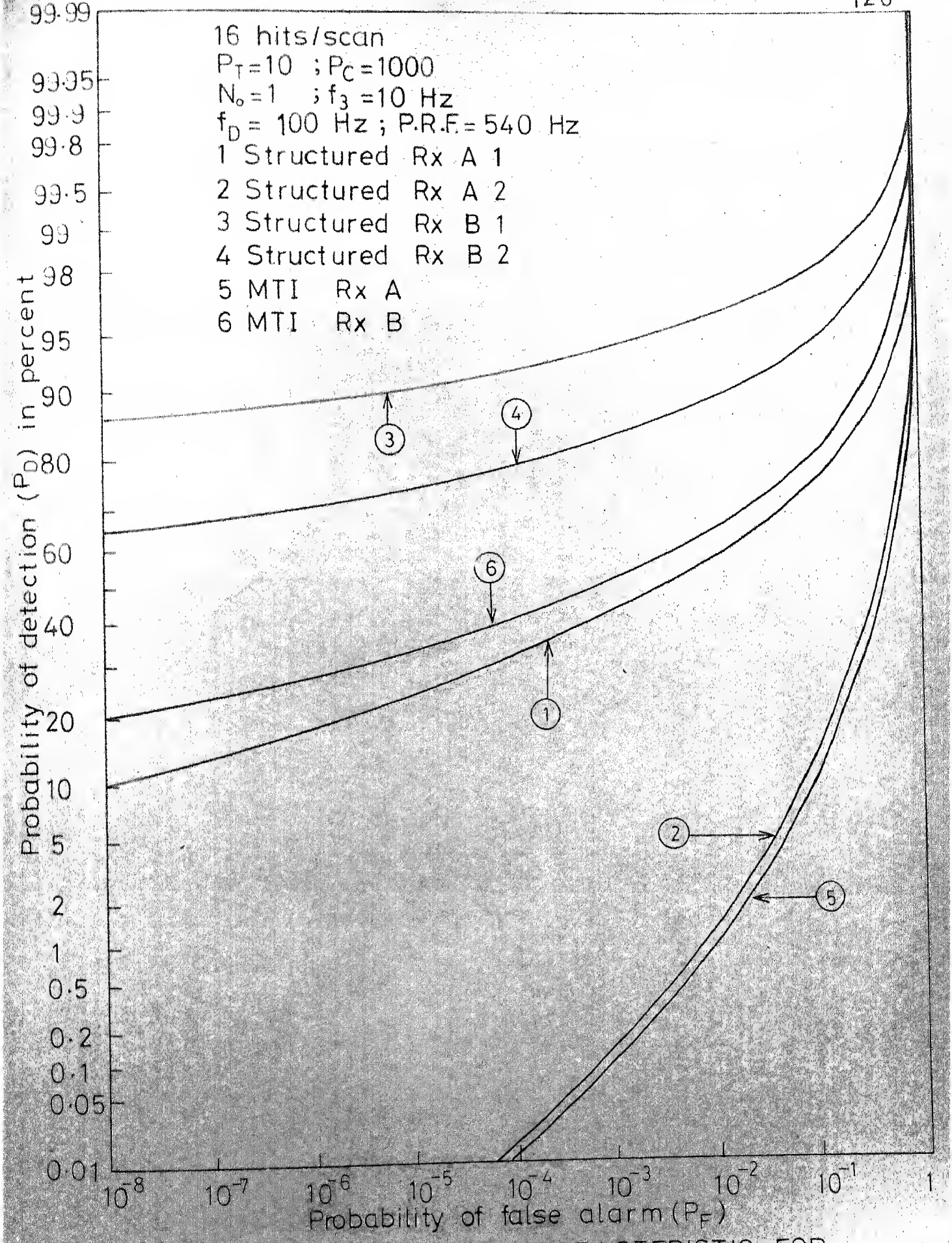

FIG. 5·10 RECEIVER OPERATING CHARACTERISTIC FOR STRUCTURED AND MTI RECEIVERS

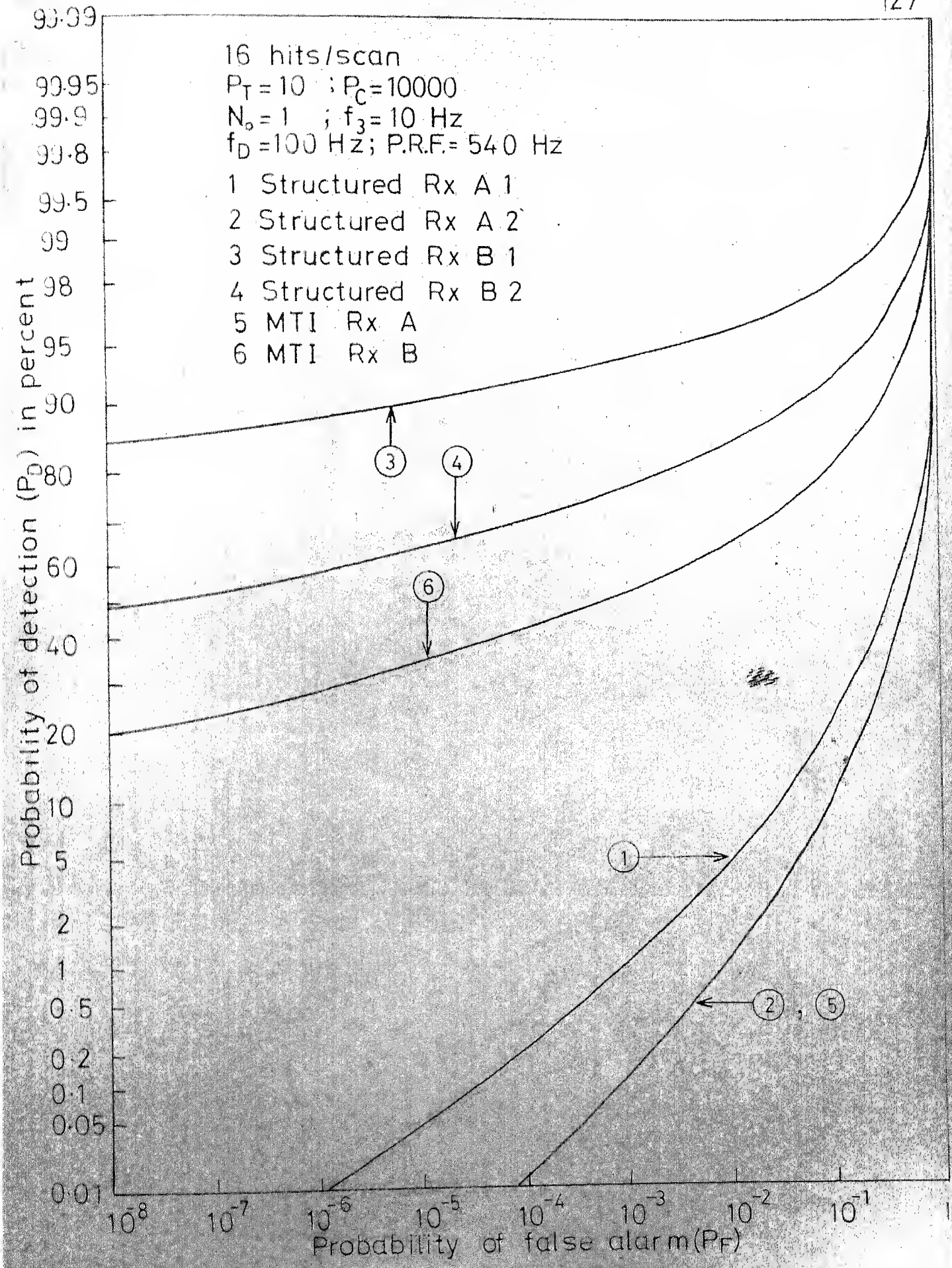

FIG. 5·11 RECEIVER OPERATING CHARACTERISTIC FOR STRUCTURED AND MTI RECEIVERS

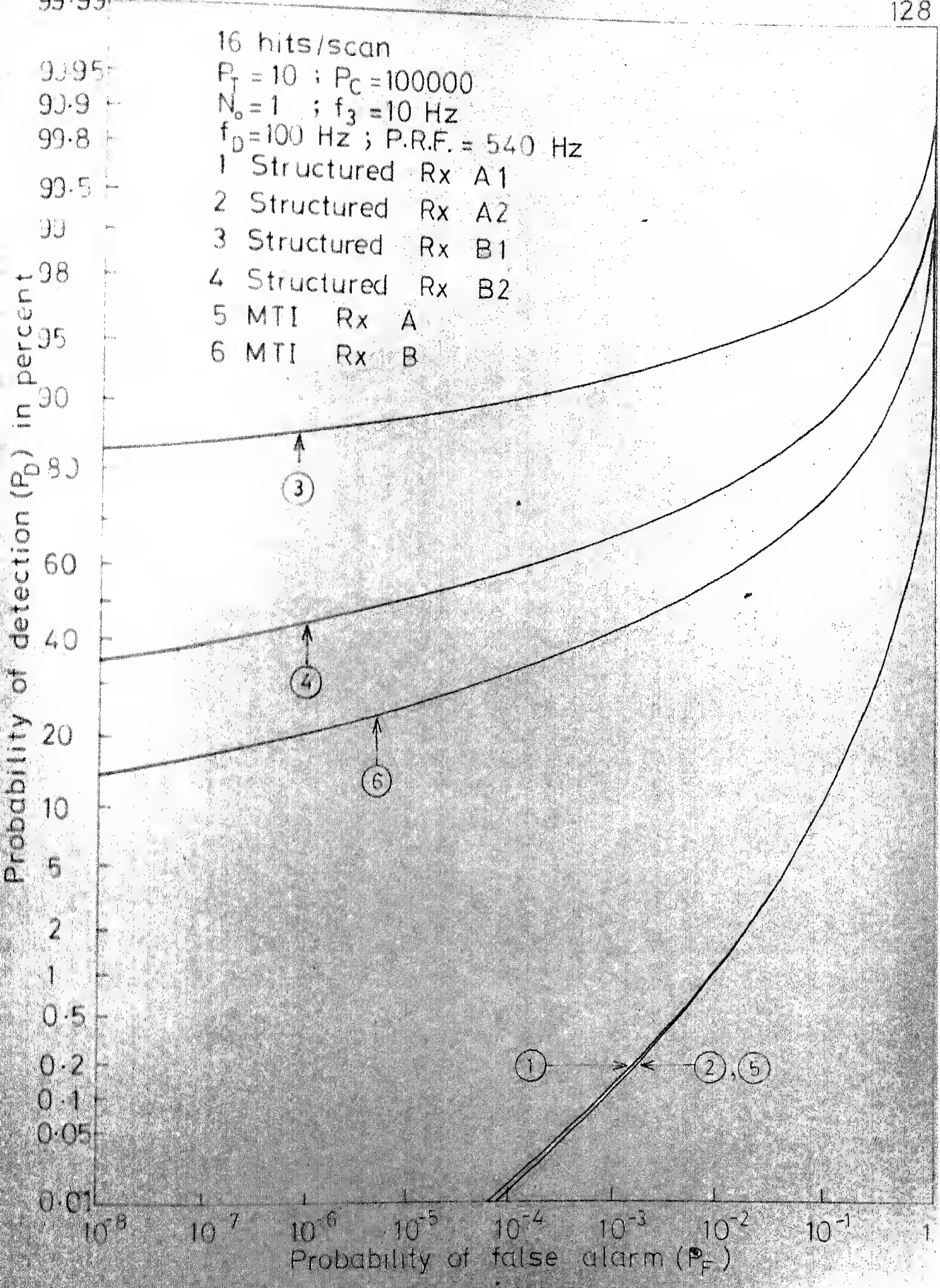

FIG. 5.12 RECEIVER OPERATING CHARACTERISTIC FOR STRUCTURED AND MTI RECEIVERS

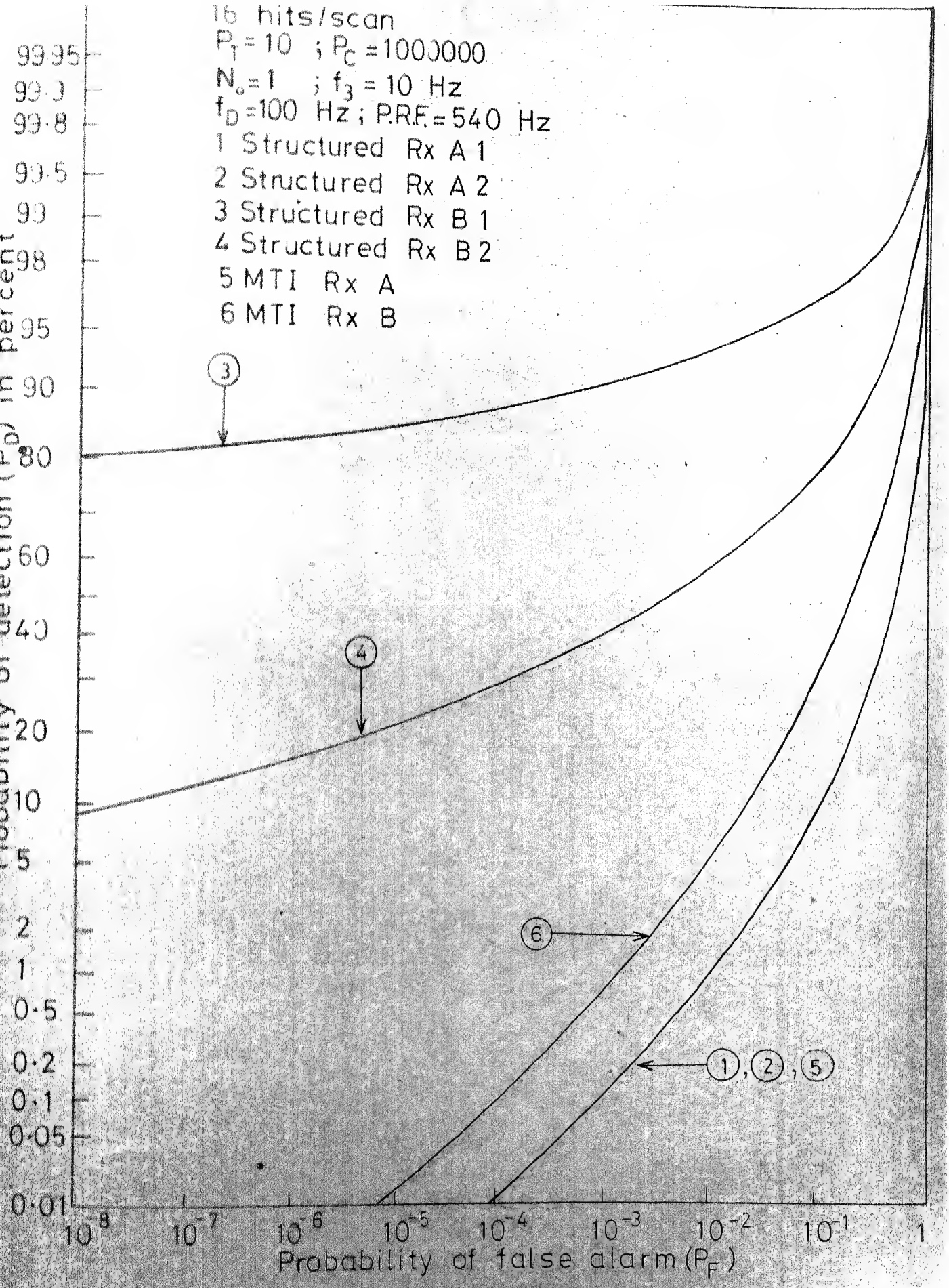

G.5·13 RECEIVER OPERATING CHARACTERISTIC FOR STRUCTURED AND MTI RECEIVERS

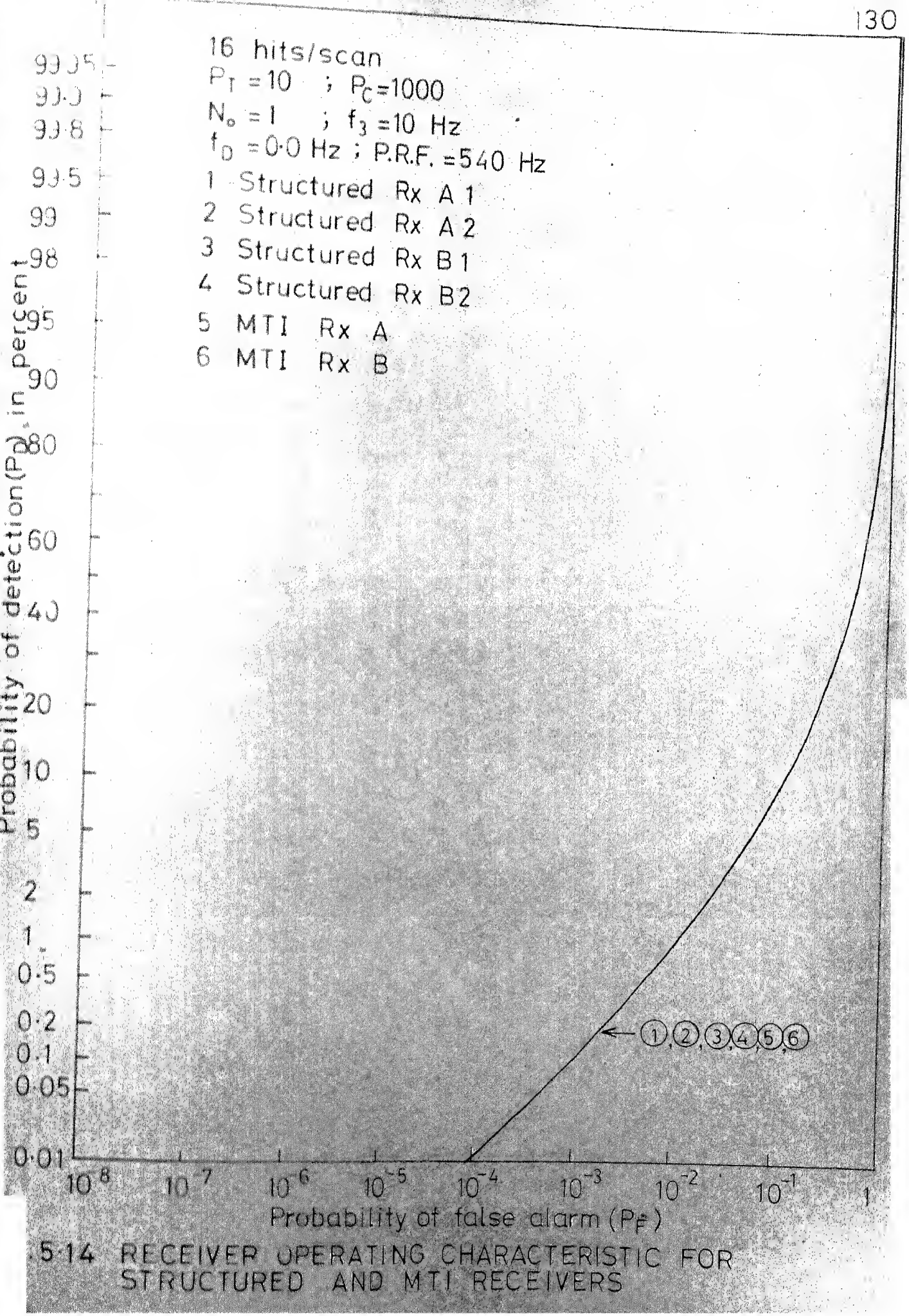

5·14 RECEIVER OPERATING CHARACTERISTIC FOR STRUCTURED AND MTI RECEIVERS

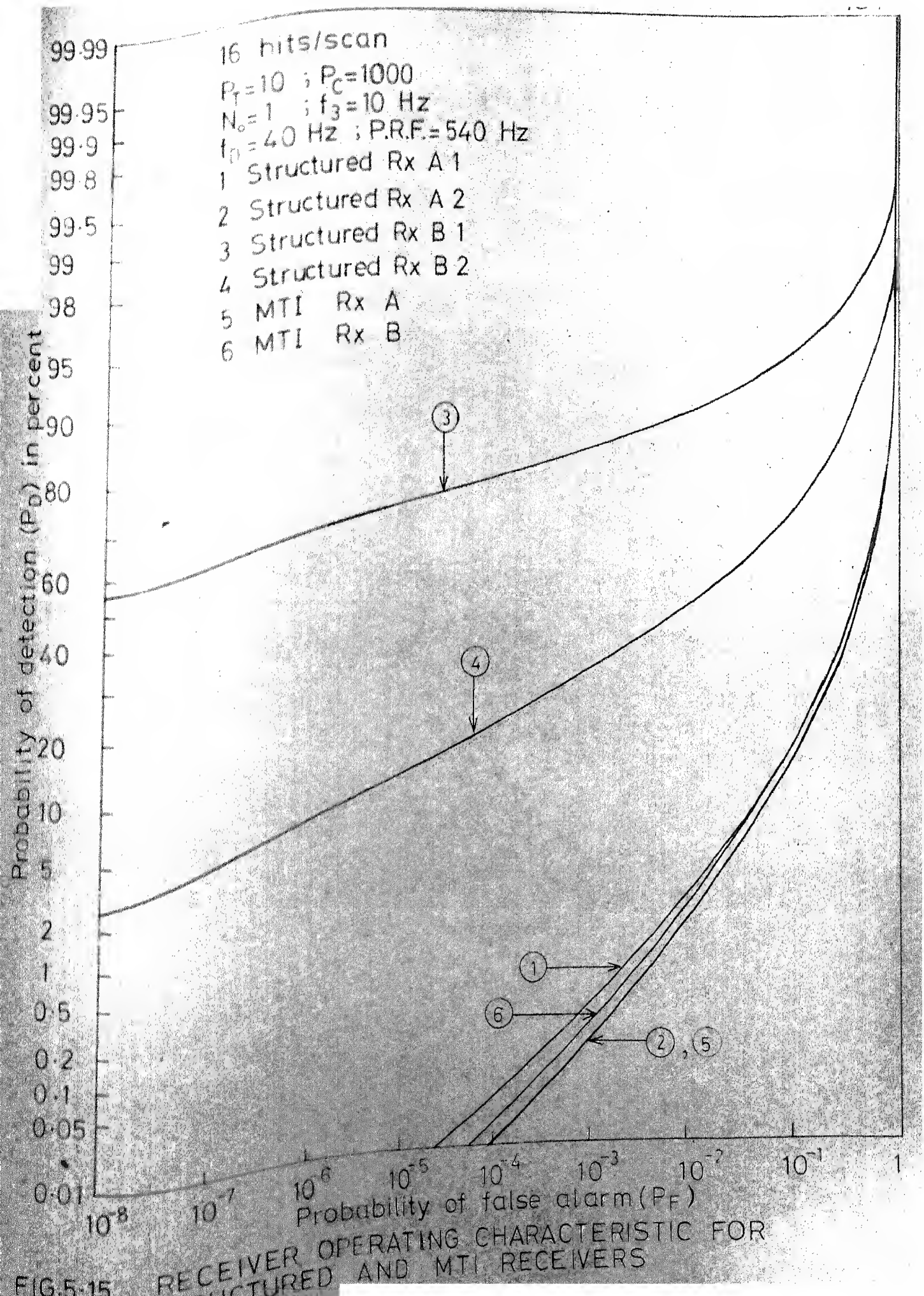

FIG.5·15 RECEIVER OPERATING CHARACTERISTIC FOR STRUCTURED AND MTI RECEIVERS

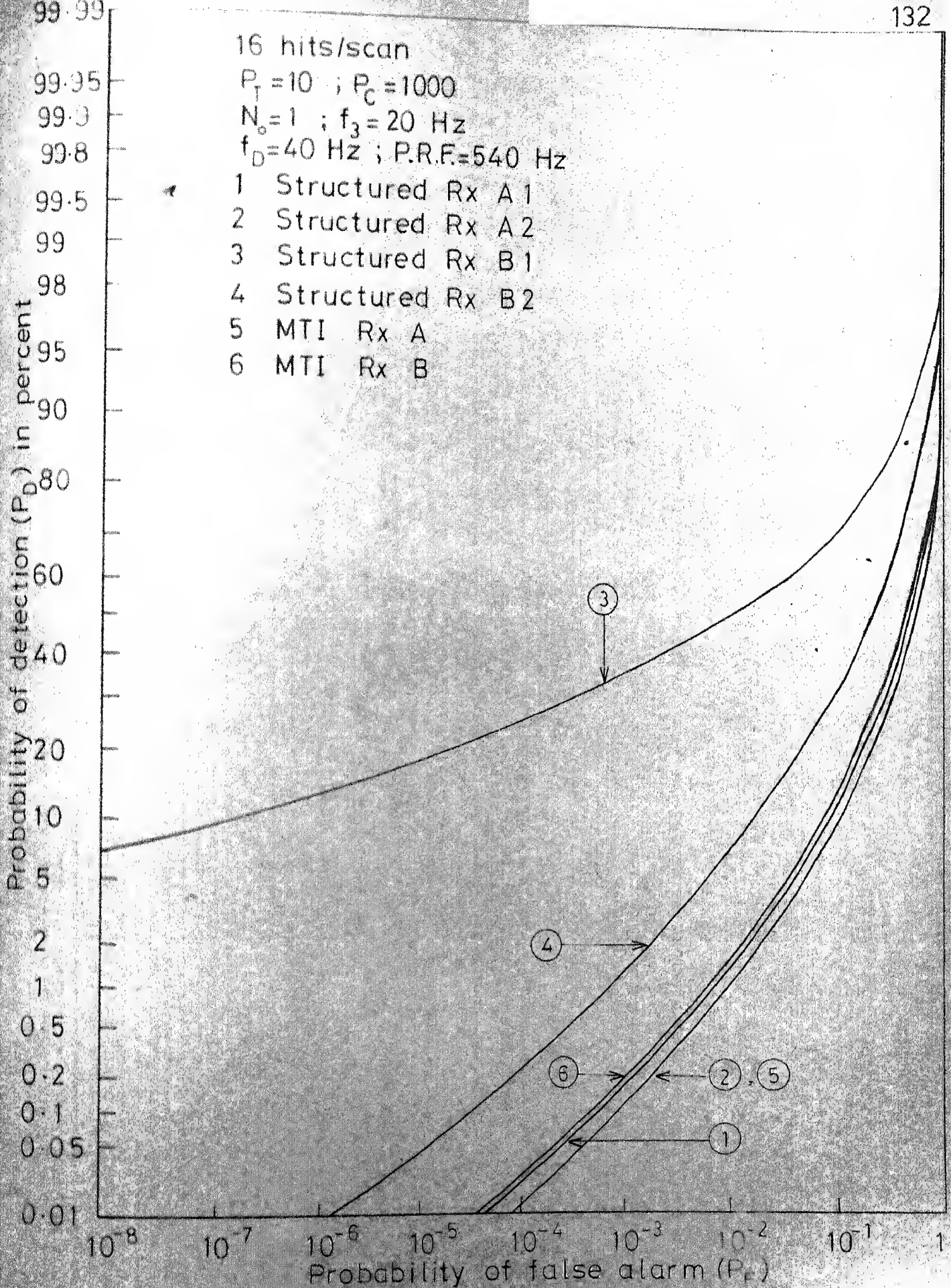

FIG. 5·16 RECEIVER OPERATING CHARACTERISTIC FOR STRUCTURED AND MTI RECEIVERS

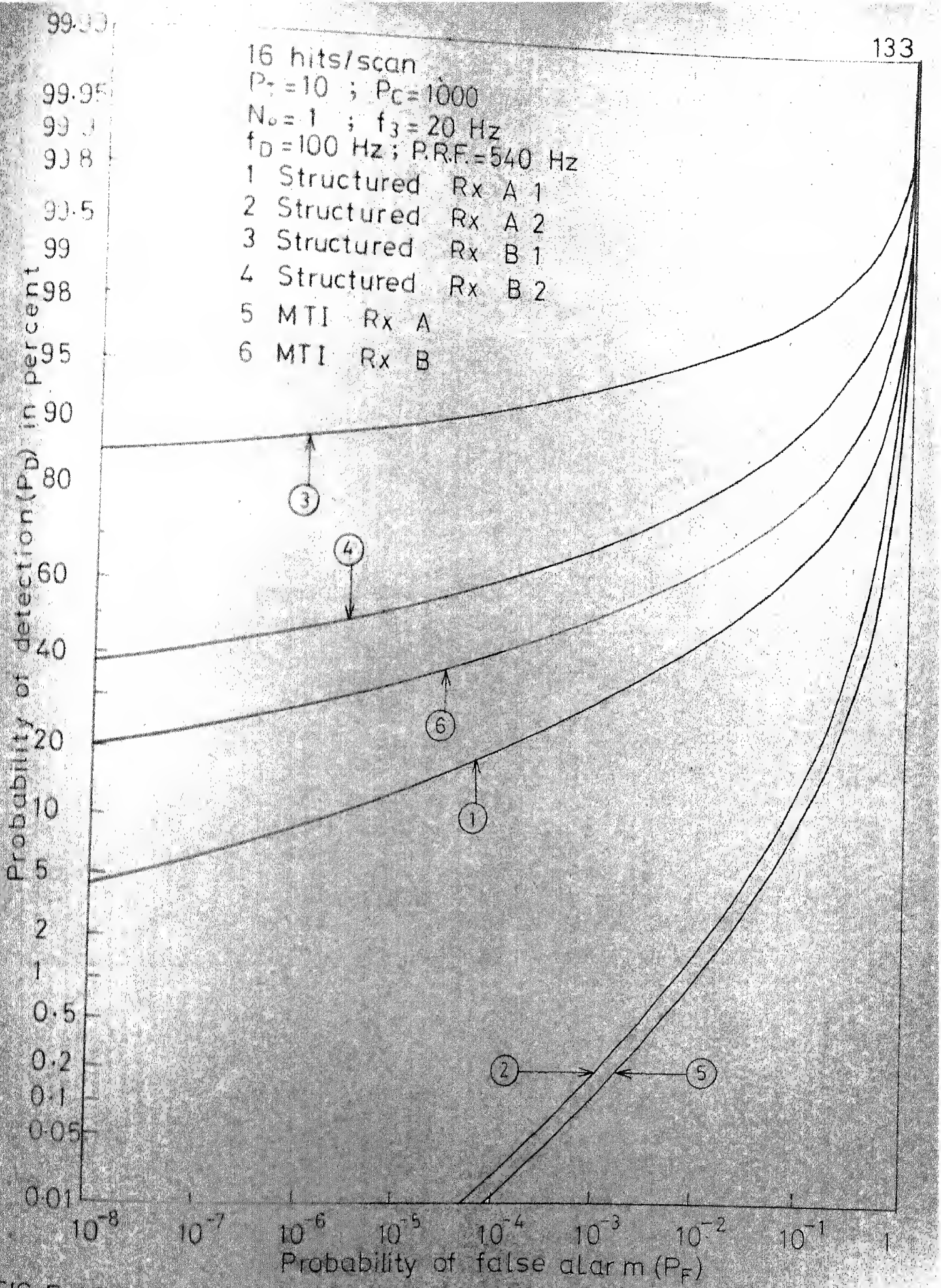

FIG. 5·17 RECEIVER OPERATING CHARACTERISTICS FOR STRUCTURED AND MTI RECEIVERS

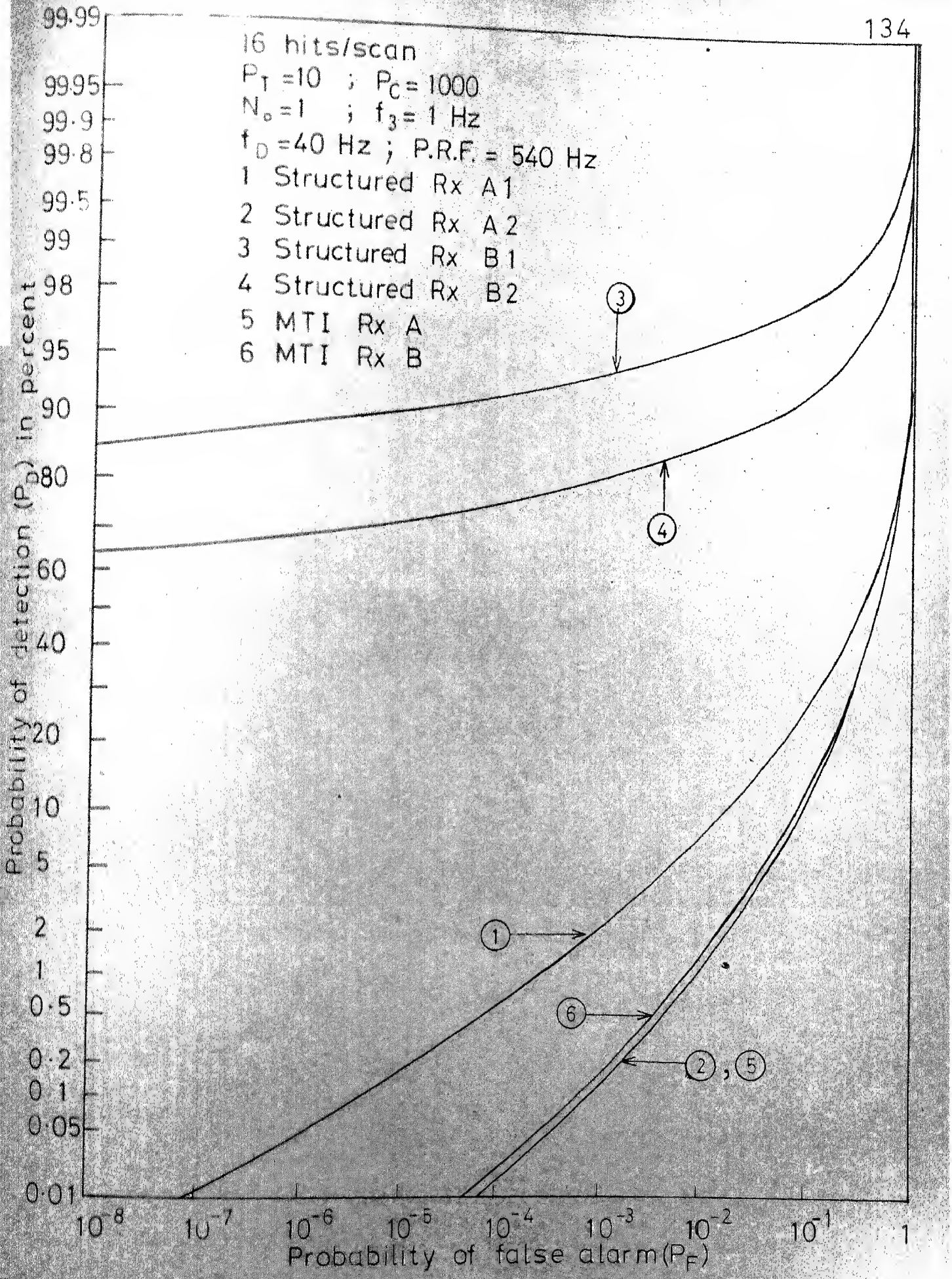

FIG.5.18 RECEIVER OPERATING CHARACTERISTIC FOR STRUCTURED AND MTI RECEIVERS

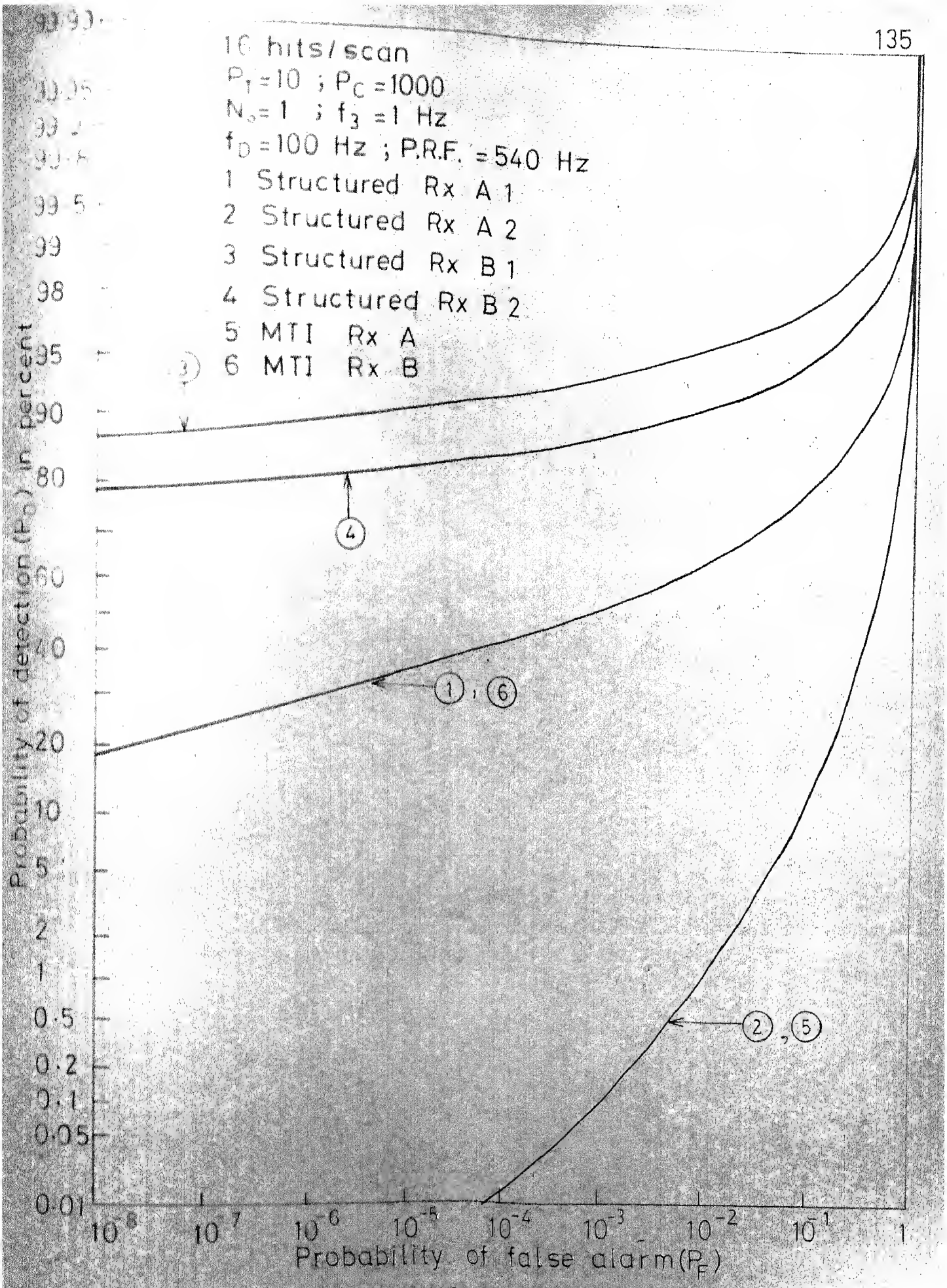

FIG.5-19 RECEIVER OPERATING CHARACTERISTIC FOR STRUCTURED AND MTI RECEIVERS

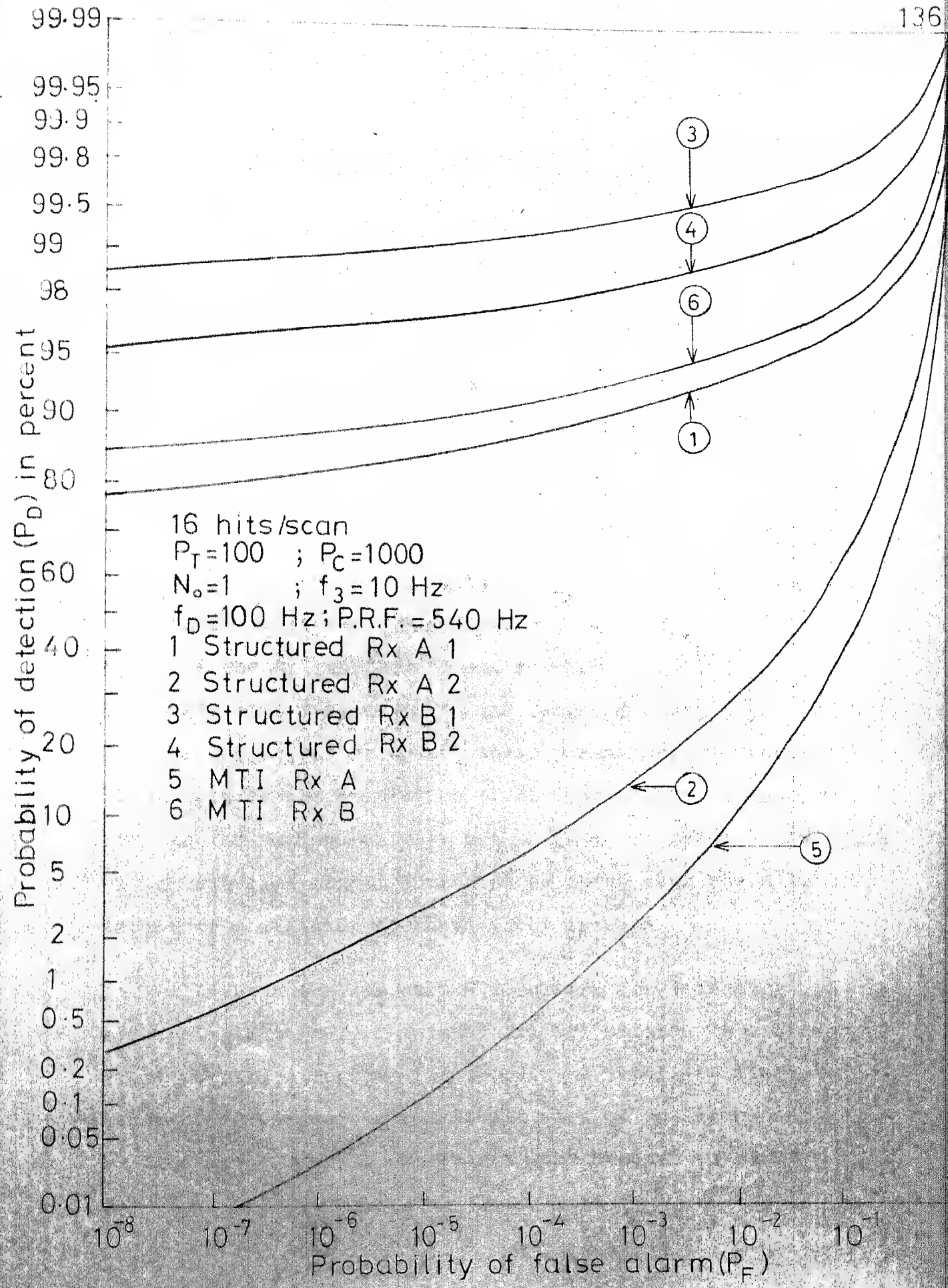

FIG. 5·20 RECEIVER OPERATING CHARACTERISTIC FOR STRUCTURED AND MTI RECEIVERS

CHAPTER 6

CONCLUSIONS

In this thesis, an optimum radar receiver for detecting a Swerling 1 target in the presence of clutter is derived and it is found that implementing this receiver in a changing clutter environment is extremely difficult with present day technology. In view of this, this thesis primarily deals with the design and study of two adaptive suboptimum receivers for detecting a Swerling 1 target in the presence of clutter. These receivers are adaptive in the sense that they estimate the required statistics of clutter and adjust or update their parameters in response to changes in the statistics of clutter. This is achieved through the maximum entropy method (MEM) of spectral analysis of the received signal during those scans when there is no target or a decision to that effect is made.

In both the suboptimum receivers for detecting a Swerling 1 target, a matched filter (matched to a single pulse return) structure is imposed. A matched filter structured receiver is relatively easy to implement and is indeed the optimum receiver in the absence of clutter.

The first suboptimum receiver, termed a Structured Optimum Receiver, is an optimum receiver within the constraints imposed by its matched filter structure. A study is made of how the MEM could be used to estimate the required clutter statistics during those scans when no target is present in the range bin of interest, thereby enabling the parameters of the structured optimum receiver to be determined adaptively. The performance of such a receiver is evaluated for both the cases when the required clutter statistics are a priori known and when the MEM is used to estimate the required statistics of clutter. Performance evaluation studies indicate that the MEM is able to estimate the required clutter statistics 'reasonably well' with only 16 samples. In general, the performance of the structured optimum receiver improves as the clutter spectral width decreases and the target Doppler shift increases. At a target Doppler shift of 100 Hz or more, a pulse repetition frequency (PRF) of 540 Hz and a clutter spectral width of 10 Hz or less, the performance of the structured optimum receiver approaches the maximum attainable limit (when no clutter is present) to within about 20 percent (in terms of signal to interference ratio) even when the clutter power is as high as 50 dB above the thermal noise power. In general, the performance of the structured optimum receiver is far superior to that of a conventional matched filter receiver. However, at low target Doppler shifts (particularly at 20 Hz or less), the performance of both the receivers is poor.

suboptimum receiver is easier to implement than the first suboptimum receiver.

A study of the performance of both the structured optimum and structured receivers carried out at other PRF's - though not reported here - indicates trends similar to those presented in the thesis.

In the procedure followed to estimate the required clutter statistics by MEM, an averaging (as described in Appendix A) over twenty five scans (when no target is present) is done. This procedure ignores the errors due to missing a target during a particular scan and considering the returned signal in that scan to estimate the clutter statistics. To take this error into account, one has to consider the a priori probability of a target being present at the given range bin during any particular scan, as well as the probability of miss of a target. In practice, this apriori probability of a target being present is extremely low, and therefore it is felt that the errors due to missing a target will not be significant when an averaging over a sufficient number of scans is done.

The performance figures of the structured optimum receiver indicate that its performance is 'reasonably good' except at low target Doppler shifts and large clutter spectral widths. At low target Doppler shifts, the performance is

extremely poor. To obtain better performance at low Doppler shifts, it is necessary to search for other implementable receiver structures. One such receiver structure (in the notation of the earlier chapters) that could be tried is shown below.

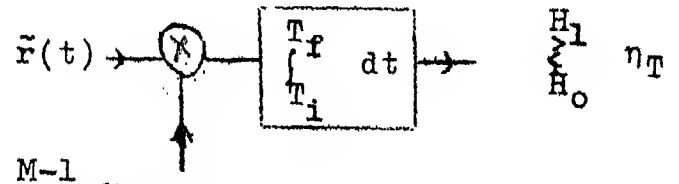

$$\tilde{g}^*(t) = \sum_{m=o}^{M-1} \tilde{f}(t-mT_p) \exp(-j\omega_D t)$$

$$+ \sum_{m=o}^{M-1} \sum_{k=o}^{L} \tilde{\rho}_k^* \exp(-j\omega_D mT_p)\, \tilde{f}^*(t-kT-mT_p)$$

This has the same structure as the optimum receiver except that the coefficients $\tilde{g}_{mk}$'s in the optimum receiver have been replaced by $\tilde{\rho}_k \exp(j\omega_d mT_p)$ terms. $\tilde{\rho}_k$'s could be chosen such that the clutter component in the received signal is completely cancelled. Using the notation of the earlier chapters, $\sum_{k=o}^{L} \tilde{b}_{mk}\, \tilde{f}(t-kT-mT_p)$ is the clutter signal due to the mth pulse, $\tilde{f}(t-mT_p)$, in the transmitted pulse train. When this return is correlated with $\tilde{g}^*(t)$, the output due to the clutter component alone can be written as

$$\sum_{k=o}^{L} \tilde{b}_{mk} \exp(-j\omega_D mT_p)\, \tilde{\varphi}(kT,-\omega_D) + \sum_{k=o}^{L} \sum_{n=o}^{L} \tilde{b}_{mk} \exp(j\omega_D mT_p) \times \tilde{\rho}_n^*\, \tilde{\varphi}((k-n)T,0)$$

where $\tilde{\varphi}(kT,-\omega_D) = \int_{T_i}^{T_f} \tilde{f}(t-kT)\tilde{f}^*(t) \exp(-j\omega_D t)\, dt$

To make this clutter component equal to zero, we can put the above expression to zero and solve for $\tilde{\rho}_k$'s. Or

$$\sum_{n=0}^{L} \tilde{\rho}_n^* \tilde{\varphi}((k-n)T,0) = -\tilde{\varphi}(kT, -\omega_D)$$

for k = 0,1,...,L

We observe that these $\tilde{\rho}_k$'s do not depend on m and choosing $\tilde{\rho}_k$'s in such a fashion would result in the complete cancellation of clutter. However, the power due to the white noise component in the received signal increases at the output of the receiver. One way to compensate for this is to increase the transmitter power or the number of hits/scan. Another way to choose $\tilde{\rho}_k$'s is to maximise the signal to interference ratio and perhaps use a gradient algorithm to recursively compute $\tilde{\rho}_k$'s.

The performance evaluation of the various receivers is done by considering the statistics of the samples at the output of the matched filter. No consideration was given to the design of the basic signal waveform ($\tilde{f}(t)$) to reduce the effects of clutter. By a proper choice of the basic signal waveform ($\tilde{f}(t)$), the clutter power ($2h^2$) at the output of the matched filter itself could be reduced and this would inprove the performance of the structured optimum and structured receivers considerably. Thus if $\tilde{f}(t)$ is so chosen that its ambiguity function ($\tilde{\theta}(\tau, \omega)$) has a low value at small values of ω, the performance of these receivers at low Doppler shifts would improve considerably.

REFERENCES

1. Barton, D.K. (ed.), Radars, Vol. V: Radar Clutter, Artech House, Massachusetts, 1975.

2. Nathanson, F.E., Radar Design Principles, McGraw-Hill, New York, 1969.

3. Skolnik, M.I. (ed.) Radar Handbook, McGraw-Hill, New York, 1970.

4. _____, Introduction to Radar Systems, McGraw-Hill, New York, 1962.

5. Van Trees, H.L., Detection, Estimation and Modulation Theory, Part III, Wiley, New York, 1971.

6. Marcum, J.I., 'A statistical theory of target detection by pulsed radar', IRE Trans. Inform. Theory, Vol.IT-6, No.2, pp. 59-144, April 1960.

7. _____, 'A statistical theory of target detection by pulsed radar, Mathematical Appendix', IRE Trans. Inform. Theory, Vol. IT-6, No.2, pp. 145-267, April 1960.

8. Swerling, P., 'Probability of detection for fluctuating targets', IRE Trans. Inform.Theory, Vol.IT-6, No.2, pp. 269-308, April 1960.

9. _____, 'Recent developments in target models for radar detection analysis', AGARD Conf. Proc. No.66, pp. 7-1-7-21, May 1970.

10. Weinstock, W., 'Target cross section models for radar system analysis', Ph.D. dissertation, University of Pennsylvania, Philadelphia, 1964.

11. Mitchell, R.L., 'Radar cross section statistics of randomly oriented disks and rods', IEEE Trans. Antennas and Propagation, Vol.AP-17, pp.370-371, May 1969.

12. Urkowitz, H., 'Filters for detection of small radar signals in clutter', J. Appl. Phys., Vol.24, pp. 1024-1031, August 1953.

13. Manasse, R., 'The use of pulse coding to discriminate against clutter', M.I.T. Lincoln Lab., Lexington, Mass., Group Rept. 312-12, June 1961.

14. Westerfield, E.C., Prager, R.H.,and Stewart, J.L., 'Processing gains against reverberation (clutter) using matched filters', IRE Trans. Inform. Theory, Vol.IT-6, pp. 342-348, June 1960.

15. Stutt, C.A. and Spafford, L.J., 'A 'best' mismatched filter response for radar clutter discrimination', IEEE Trans. Inform. Theory, Vol.IT-14, pp. 280-287, March 1968.

16. Rummler, W.D., 'Clutter suppression by complex weighting of coherent pulse trains', IEEE Trans. Aerospace and Electronic Systems, Vol. AES-2, pp. 689-699, November 1966.

17. Spafford, L.J., 'Optimum radar signal processing in clutter', IEEE Trans. Inform. Theory, Vol.IT-14, pp. 734-743, September 1968.

18. Delong, D.F.,Jr., and Hofstetter, E.M., 'On the design of optimum radar waveforms for clutter rejection', IEEE Trans. Inform. Theory, Vol. IT-13, pp. 454-463, July 1967.

19. Van Trees, H.L., 'Optimum signal design and processing for reverberation-limited environments', IEEE Trans. Mil. Electronics, Vol. MIL-9, pp.212-229, July 1965,

20. Rummler, W.D., 'A technique for improving the clutter performance of coherent pulse train signals', IEEE Trans. Aerospace and Electronic Systems, Vol. AES-3, pp. 898-906, November 1967.

21. Delong, D.F., Jr., and Hofsteter, E.M., 'The design of clutter-resistant radar waveforms with limited dynamic range', IEEE Trans. Inform. Theory, Vol. IT-15, pp. 376-385, May 1969.

22. Rihaczek, A.W., 'Optimum filters for signal detection in clutter', IEEE Trans. Aerospace and Electronic Systems, Vol. AES-1, pp. 297-299, December 1965.

23. _____,'Radar resolution properties of pulse trains', IEEE Proc., Vol.52, pp. 153-164, February 1964.

24. _____, Principles of High-Resolution Radar, McGraw-Hill, New York, 1969.

25. Wainstein, L.A.,and Zubakov, V.D., Extraction of Signals from Noise, Prentice-Hall, New Jersey, 1962.

26. Muehe, C.E., et.al., 'New techniques applied to air traffic control radars', IEEE Proc., Vol.62, pp. 716-723, June 1974.

27. McClellan, J.H.,and Purdy, R.J., 'Application of digital signal processing to radar', in Applications of Digital Signal Processing, Oppenheim, A. (ed.), Prentice-Hall, New Jersey, 1978, Chap.5.

28. Van Trees, H.L., Detection, Estimation and Modulation Theory, Part I, Wiley, New York, 1968.

29. DiFranco, J.V.,and Rubin, W.L., Radar Detection, Prentice Hall, New Jersey, 1968.

30. Whalen, A.O., Detection of Signals in Noise, Academic Press, New York, 1971.

31. Hawkes, C.D.,and Haykin, S., 'Modelling of clutter for coherent pulse radar', IEEE Trans. Inform. Theory, Vol.IT-21, pp. 703-707, November 1975.

32. Pollon, G.E., 'Statistical parameters for scattering from randomly oriented arrays, cylinders and plates', IEEE Trans. Antennas and Propagation, Vol. AP-18, pp. 68-75, January 1970.

33. Crispin,J.W. Jr., and Maffett, A.L., 'The practical problem of radar cross-section analysis', IEEE Trans. Aerospace and Electronic Systems, Vol.AES-7, pp. 392-395, March 1971.

34. Kailath, T., 'Sampling models for linear time - variant filters', M.I.T. Res.Lab.of Electronics, Cambridge, Mass., Tech. Report 352, May 1959.

35. Burg, J.P., 'Maximum entropy spectral analysis', paper presented at the 37th Annual International SEG Meeting, Oklahoma City, October 1967.

36. _____, 'A new analysis technique for time series data', paper presented at the NATO Advanced Study Institute on Signal Processing, Netherlands, August 1968.

37. Blackman, R.B., and Tukey, J.W., The Measurement of Power Spectra from the Point of View of Communication Engineering, Dover, New York, 1958.

38. Welch, P.D., 'The use of fast Fourier transform for the estimation of power spectra: A method based on the time averaging over short, modified periodograms', IEEE Trans. Audio and Electro-acoust., Vol. AU-15, pp. 70-73, June 1967.

39. Vijay Kumar, B.V.K., 'Power spectrum estimation using maximum entropy method', M.Tech. Thesis, Indian Institute of Technology, Kanpur, 1977.

40. Vijay Kumar, B.V.K., and Mullick, S.K., 'Power spectrum estimation using maximum entropy method', J. IETE, Vol.25, No.5, pp. 181-194, May 1979.

41. Childers, D.G. (ed.), Modern Spectrum Analysis, IEEE, New York, 1978.

42. Ulrych, T.J., and Bishop, T.N., 'Maximum entropy spectral analysis and autoregressive decomposition', Rev. Geophysics and Space Phys., Vol.13, pp. 183-200, February 1975.

43. Kesler, S., and Haykin, S., 'Maximum entropy estimation of radar clutter spectra', IEEE National Telecommunications Conference Record, Vol.2, pp. 18.5.1 - 18.5.5, December 1978.

44. Jaynes, E.T., 'Prior probabilities', IEEE Trans. Systems Sci.Cybern., Vol. SEC-4, pp. 227-241, September 1968.

45. Shanon, C.E., 'A mathematical theory of communication', BSTJ, Vol.27, pp. 379-423, July 1948.

46. Smylie, D.E., Clarke, G.K.C., and Ulrych. T.J., 'Analysis of irregularities in earth's rotation', in Methods in Computational Physics, Vol.13, pp. 391-430, Academic Press, New York, 1973.

47. Levinson, N., 'The Wiener RMS (root mean square) error criterion in filter design and prediction', J. of Math. and Phy., Vol.25, pp. 261-278, 1946.

48. Van Den Bos, A., 'Alternative interpretation of maximum entropy spectral analysis', Trans. IEEE. Inform. Theory, Vol.IT-17, pp. 493-494, July 1971.

49. Haykin, S., and Kesler, S., 'The complex form of the maximum entropy method for spectral estimation', IEEE Proc. Vol. 64, pp. 822-823, May 1976.

50. Anderson, N., 'On the calculation of filter coefficients for maximum entropy spectral analysis', Geophysics, Vol.39, pp. 69-72, February 1974.

51. Akaike, H., 'Fitting autoregressive models for prediction', Ann. Inst. Statist. Math., Vol.21, pp. 243-247, 1969.

52. _____,'Power spectrum estimation through autoregressive model fitting', Ann. Inst. Statist. Math., Vol.21, pp. 407-419, 1969.

53. _____, 'Statistical predictor identification', Ann. Inst. Statist. Math., Vol.22, pp. 203-217, 1970.

54. Jones, R.H., 'Autoregression Order selection', Geophysics, Vol.41, pp. 771-773, August 1976.

55. Kromer, R., 'Asymptotic properties of the autoregressive spectral estimate', Ph.D. Thesis, Stanford Univ., Calif., 1970.

56. Berk, K.N., 'Consistent autoregressive spectral estimate', Ann. Statist., Vol.2, pp. 489-502, May 1974.

57. Hildebrand, F.B., Methods of Applied Mathematics, Prentice-Hall, New Jersey, 1952.

58. Pearson, K., Tables of the Incomplete Gamma Function, Cambridge Univ. Press, London, 1957.

59. Kanter, I., 'A generalisation of the detection theory of Swerling', in Detection and Estimation: Applications to Radar, Haykin, S.S. (ed.), Benchmark Papers in Electrical Engineering and Computer Science, Vol.13, Dowden, Hutchinson and Ross, Inc., Pennsylvania, 1976, pp. 159-166.

60. Mitchell, R.L., Radar Signal Simulation, Artech. House Massachusetts, 1976.

APPENDIX A

PERFORMANCE EVALUATION BY COMPUTER SIMULATION AND NUMERICAL COMPUTATIONS

The performance of the structured optimum, structured, matched filter and moving target indicator (MTI) receivers were evaluated for Swerling 1 target models by computer simulation and numerical computations. The computer used was the DEC-1090 system. This appendix describes the simulation scheme. A flow chart describing the recursive algorithm for the complex form of the maximum entropy method (MEM) is also included.

The objective of the computer simulation was to evaluate the effectiveness of the MEM in estimating the required total interference statistics in the case of the structured optimum receiver, and to estimate the required whitening filter in the case of the structured receiver. As is commonly done in most radar performance evaluations, the clutter returns were assumed to have a Gaussian shaped power spectral density. The number of hits per scan (n) of the radar was taken to be 16.

Complex Gaussian clutter samples ($\tilde{d}_k$'s) were generated on the computer using the method described in [60]. Complex white Gaussian noise samples ($\tilde{w}_k$'s) were also generated on the

computer and these were added to $\tilde{c}_k$'s to obtain the total interference samples ($\tilde{I}_k$'s). These interference samples correspond to the matched filter output for a particular range bin during those scans when no target is present. Then the complex form of the MEM was used to estimate the inverse covariance matrix ($\tilde{A}_I^{-1}$) of the interference samples in the case of the structured optimum receiver and to estimate the whitening filter tap coefficients ($\tilde{\alpha}_k$) and its order (MAX) in the case of the structured receiver. As indicated in Chapter 2, the inverse covariance matrix ($\tilde{A}_I^{-1}$) can be estimated without the need to estimate $\tilde{A}_I$ and then invert it. Also for the reason stated in Chapter 2, the maximum order of the autoregressive (AR) model being fitted, on the samples was restricted to 8.

In order to improve the estimates of $\tilde{A}_I^{-1}$ and the tap coefficients of the whitening filter, twenty five different realisations of the complex Gaussian interference samples (corresponding to those scans when no target is present) were generated on the computer and the following averaging scheme used:

(a) From each realisation of 16 samples, the MEM was used to calculate the AR model coefficients $\tilde{\alpha}_{mk}$'s for $m = 0,1,\ldots,8$ and $k = 0,1,\ldots,m$ by solving equation (2.44) reproduced below in terms of complex envelopes,

$$\sum_{k=0}^{m} \tilde{\alpha}_{mk}\, \tilde{R}(j-k) = P_m\, \delta_{jo} \qquad j = 0,1,\ldots,m$$

$$m = 0,1,\ldots,8$$

$$\tilde{\alpha}_{mo} = 1 \text{ for any } m.$$

m denotes the order of the AR model being fitted, $\tilde{R}(k)$'s denote the element of the interference covariance matrix ($\tilde{A}_I$) and P_m denotes the prediction error power for a prediction error filter of length m+1. These equations are solved using Burg's procedure outlined in Chapter 2. The final prediction error (FPE(m)) as stated in (2.53) was also calculated for $m = 1,2,\ldots,8$. A flow chart of the MEM recursive algorithm for a complex-valued time series is given in Fig. A1.1. The notation used in this figure is that of Chapter 2; only the subscripts are enclosed in parenthesis. MAXORD in Fig. A1.1 indicates the maximum order of the AR model for which the search is to be carried out. In our case MAXORD is set to 8.

(b) These $\tilde{\alpha}_{mk}$'s, P_m and FPI(m) were averaged over twenty five different realisations of the interference samples. Then Akaike's minimum FPE criterion was used to select the AR model order (m = MAX). Then $\tilde{A}_I^{-1}$ was calculated using (2.59). The whitening filter coefficients are given by $\tilde{\alpha}_{kMAX}$ for $k = 0,1,\ldots,MAX$.

The performance of the structured optimum, structured, MTI and matched filter receivers was then evaluated by using the formulae and procedures

described in Chapters 4 and 5. The performance of these receivers was evaluated for a large number of cases by varying the clutter power, clutter spectral width, target power, target velocity and thermal noise power. Appendix B gives a listing of the main program and the subroutines used in the performance evaluation.

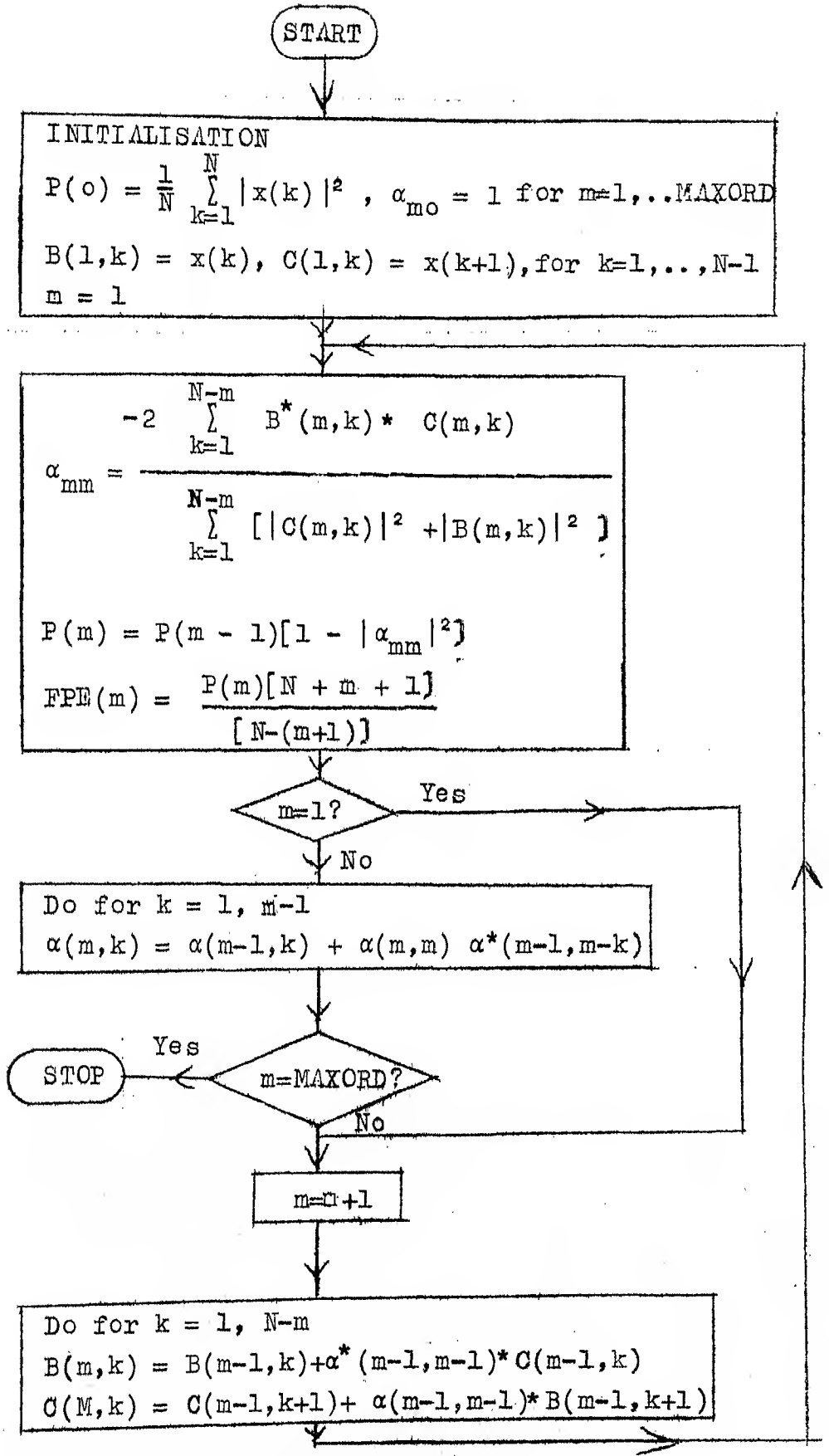

Fig. A1.1 MEM Recursive Algorithm for a Complex-valued Time Series.

APPENDIX A

```
C
C
C
```

```
      ISEED2=34567
      ISEED3=98765
      ISEED4=7654321
      NUMB=200
      FORMAT(100('1'),6X,'TOCP',11X,'TP',16X,'F0',12X,'F3',13X,'NO
     1  ',2X,'NUMB',5X,'PT',14X,'F0')
      PRINT *,' ',TOCP,TP,F0,F3,NO,NUMB,PT,F0
      DO 300 NU=1,NUMB
      NU=NU
C     SUBROUTINE GCWGN GENERATES M COMPLEX WHITE GAUSSIAN SAMPLES
C     EACH POWER NO/SAMPLE.CWGN IS A COMPLEX VECTOR OF DIMENSION M
C     CONTAINING THESE M WHITE NOISE SAMPLES.
      CALL GCWGN(CWGN,ISEED1,M,ISEED2,NO)
C     SUBROUTINE CLUTT GENERATES M COMPLEX GAUSSIAN CLUTTER SAMPLES
C     HAVING A GAUSSIAN SHAPED POWER SPECTRAL DENSITY WITH CENTER
C     FREQUENCY=F0 AND 3DB SPECTRAL WIDTH(TWO SIDED) EQUAL TO F3.
C     D IS A COMPLEX VECTOR OF DIMENSION M CONTAINING THESE M
C     CLUTTER SAMPLES. ARCLUT IS THE M * M COVARIANCE MATRIX
C     (THEORETICAL) OF THESE M SAMPLES.
      CALL CLUTT(D,M,F3,TOCP,TP,F0,ISEED3,ISEED4,NUT,ARCLUT)
C     SUBROUTINE SUMUP ADDS THE M WHITE NOISE SAMPLES TO THE M
C     CLUTTER SAMPLES TO GENERATE M TOTAL INTERFERENCE SAMPLES.
C     INT IS A COMPLEX VECTOR OF DIMENSION M CONTAINING THESE
C     TOTAL INTERFERENCE SAMPLES.
      CALL SUMUP(INT,CWGN,D,M)
C     SUBROUTINE COEM PERFORMS THE MAXIMUM ENTROPY METHOD OF
C     SPECTRAL ANALYSIS ON THE M TOTAL INTERFERENCE SAMPLES(INT).
C     MAXORD DENOTES THE MAXIMUM ORDER OF THE AUTOREGRESSIVE(AR)
C     MODEL FITTED TO THE GIVEN TIME SERIES. T IS AN M** COMPLEX
C     MATRIX CONTAINING THE PREDICTION ERROR FILTER COEFFICIENTS,
C     OR THE AR MODEL COEFFICIENTS FOR ORDERS 1 TO MAXORD. USE
C     THE FIRST SUBSCRIPT OF T DENOTES THE ORDER OF THE AR MODEL
C     FITTED AND THE SECOND SUBSCRIPT DENOTES THE ACTUAL COEFFICIENTS.
C     P IS A VECTOR CONTAINING THE PREDICTION ERROR POWERS WHEN AR
C     MODELS OF ORDER 1 TO ORDER MAXORD ARE FITTED TO THE GIVEN TIME
C     SERIES(M TOTAL INTERFERENCE SAMPLES). P(0) GIVES THE AVERAGE
C     POWER IN EACH SAMPLE IS ALSO EQUAL TO THE PREDICTION ERROR
C     POWER FOR AN AR MODEL OF ORDER ZERO. FPE IS THE FINAL
C     PREDICTION ERROR WHEN AR MODELS OF ORDERS 1 TO MAXORD ARE
C     FITTED TO THE GIVEN TIME SERIES.
      CALL COEM(INT,M,T,P,FPE,MAXORD)
      DO 210 J=1,MAXORD
      DO 220 K=0,J
      TET(NU,J,K)=T(J,K)
220   CONTINUE
210   CONTINUE
      DO 230 J=1,MAXORD
      FPE(NU,J)=FPE(J)
      PP(NU,J)=P(J)
230   CONTINUE
      PP(NU,0)=P(0)
300   CONTINUE
C     SUBROUTINE AVMEM AVERAGES THE RESULTS OBTAINED BY MEM OVER
C     NUMB SCANS.THE AVERAGING PROCEDURE IS DESCRIBED IN APPENDIX A
C     OF THIS THESIS.T,P,FPE ARE THE OUTPUTS AND TET,PP,FFPE,MAXORD,
C     NUMB ARE THE INPUTS.
      CALL AVMEM(TET,PP,FFPE,T,P,FPE,MAXORD,NUMB)
C     SUBROUTINE RCMEM CALCULATES THE INVERSE COVARIANCE MATRIX
C     OF THE TOTAL INTERFERENCE SAMPLES AND THE WHITENING FILTER
C     TAP COEFFICIENTS. AKAIKE'S MINIMUM FPE CRITERION IS USED
C     TO OBTAIN THE OPTIMUM AR MODEL ORDER(MINORD).
```

```
C          ACINV DENOTES THE MEN ESTIMATE OF THE INVERSE COVARIANCE
C          MATRIX OF THE TOTAL INTERFERENCE SAMPLES AND TAP DENOTES A
C          VECTOR CONTAINING THE OPTIMUM FILTER TAP COEFFICIENTS.
C          THIS SUBROUTINE ALSO PRINTS OUTS THE VARIOUS OUTPUTS I.E.,
C          TAP COEFFICIENTS,ACINV ETC.
           CALL SCORE(CH,MAXORD,I,EPE,E,ACINV,TAP,NLORD)
           TYPE 140
 140       FORMAT(1H0,'PERFORMANCE OF STRUCTURED OPTIMUM RECEIVERS')
C          SUBROUTINE PERFA EVALUATES THE PERFORMANCE OF THE STRUCTURED
C          RECEIVER,AND CONVENTIONAL MATCHED FILTER RECEIVERS.WHERE
C          CHAPTER 3,ARINT DENOTES THE THEORETICAL TOTAL INTERFERENCE
C          COVARIANCE MATRIX,ATARG DENOTES THE COVARIANCE MATRIX OF THE
C          TARGET SAMPLES,A SPERLING I TARGET IS ASSUMED.DELOP DENOTES
C          SIGNAL TO TOTAL INTERFERENCE RATIO(SIR) IN THE CASE OF A
C          CONVENTIONAL MATCHED FILTER RECEIVER,DELOP DENOTES THE SIR
C          FOR THE STRUCTURED OPTIMUM RECEIVER S2(REFER CHAPTER 3) ,AND
C          DELST DENOTES THE SIR FOR THE STRUCTURED OPTIMUM RECEIVER S1.
           CALL PERFA(ARCLUT,ACINV,M,TP,PT,FD,TO,APTAT,ATARG)
           TYPE 150
 150       FORMAT(1H0,'PERFORMANCES OF STRUCTURED RX ETC AFTER TOGETHER
          7  INITIAL PULSES ')
C          SUBROUTINE TOTMAT CALCULATES THE COVARIANCE MATRIX(ATOT)
C          OF THE RECEIVED SAMPLES(TARGET PLUS INTERFERENCE) IN
C          HYPOTHESIS H1
           CALL TOTMAT(ARINT,ATARG,ATOT,M)
C          SUBROUTINE PERFBA IS USED IN THE EVALUATION OF THE APT
C          RECEIVER WHEN THE FIRST TWO OUTPUT SAMPLES ARE IGNORED.REFER
C          CHAPTER 5.THIS SUBROUTINE CALCULATES THE EIGENVALUES REQUIRED
C          FOR CALCULATING PF AND PD OF APT RECEIVERS USING DOUBLE DELAY
C          LINE CANCELLERS.ALAM AND AMU ARE VECTORS OF DIMENSION NLBA
C          AND CONTAIN THE PF AND PD EIGENVALUES RESPECTVELY.
           CALL PERFBA(ATOT,ARINT,M,ALAM,AMU,NLTA)
C          SUBROUTINE PERFBB IS USED IN THE EVALUATION OF THE MATCHED
C          FILTER RECEIVER(WHEN USED WITH NONCOHERENT DETECTION),ALAM
C          AND AMU CONTAIN THE PF AND PD EIGENVALUES RESPECTIVELY.
           CALL PERFBB(ATOT,ARINT,M,ALAM,AMU)
C          SUBROUTINE PERFBC IS USED IN THE PERFORMANCE EVALUATION
C          OF THE STRUCTERED RECEIVER(WITH BOTH COHERENT AND
C          NONCOHERENT DETECTION MODES) WHEN THE INITIAL OUTPUT SAMPLES
C          ARE IGNORED.THIS SUBROUTINE CALCULATES THE SIGNAL TO
C          TOTAL INTERFERENCE RATIO(DELSTM) IN THE CASE OF THE
C          STRUCTURED RECEIVER WITH COHERENT DETECTION.IT ALSO
C          CALCULATES THE EIGENVALUES REQUIRED TO CALCULATE PF AND PD
C          FOR STRUCTURED RECEIVERS WITH NONCOHERENT DECTECTION.CLAM AND
C          CMU CONTAIN THESE NLTB EIGENVALUES.
           CALL PERFBC(ATOT,ARINT,M,TAP,MINORD,CLAM,CMU,DELD,FD,TP)
C          SUBROUTINE PRO CALCULATES PD AND PF OF THE VARIOUS RECEIVERS
C          GIVEN THE EIGENVALUES AND THRESHOLDS.
           CALL PRO(ALAM,AMU,CLAM,CMU,NLTA,NLTB,NLA,VTA)
           TYPE 160
 160       FORMAT(1H0,'PERFORMANCES OF STRUCTURED RX ETC WITHOUT IGNORING
          7  INITIAL PULSES')
C          SUBROUTINE PERFTA IS SIMILAR TO PERFBA;ONLY THE INITIAL OUTPUT
C          SAMPLES  ARE NOT IGNORED.
           CALL PERFTA(ATOT,ARINT,M,ALAM,AMU)
C          SUBROUTINE PERFTC IS SIMILAR TO PERFBC;ONLY THE INITIAL
C          OUTPUT SAMPLES ARE NOT IGNORED.DELST DENOTES THE SIR FOR
C          STRUCTURED RECEIVER WITH COHERENT DETECTION.
           CALL PERFTC(ATOT,ARINT,M,TAP,MINORD,CLAM,CMU,FD,TP)
           CALL PRO(ALAM,AMU,CLAM,CMU,M,M,NLB,VTB)
           STOP
```

```
      CALL GGUD
      CALL DGAMMA
      CALL GGNORM
      CALL GGEXP
      CALL GGPOIS
      CALL BGVMSP
      CALL MGAMAC
      CALL MGAMRC
      CALL MGMSSC
      CALL CLUTTP
      CALL CLUTTC
      END
```

```
      SUBROUTINE GCWGN(CWGN,ISEED1,M,ISEED2,N0)
      COMPLEX CWGN,C,S
      REAL N0
      DIMENSION CWGN(0:15)
      DIMENSION R1(16),R2(16),THETA(16),RAYL(16),C(16),S(16)
C     TYPE *,ISEED1
      CALL GGUD(ISEED1,M,R1)
C     TYPE *,ISEED1
      PI=3.14159265
      DO 10 I=1,M
      THETA(I)=2.0*PI*R1(I)
      C(I)=CMPLX(0.0,THETA(I))
10    CONTINUE
      SNO=SQRT(N0)
      AMEAN=1.0
C     TYPE *,ISEED2
      CALL GGEXP(ISEED2,AMEAN,M,R2)
C     TYPE *,ISEED2
      DO 20 I=1,M
      RAYL(I)=(SQRT(R2(I)))*(SNO)
      S(I)=CEXP(C(I))
      CWGN(I-1)=S(I)*RAYL(I)
C     TYPE *,CWGN(I-1)
20    CONTINUE
      RETURN
      END
```

```
      SUBROUTINE CLUTT(D,M,F3,TOCP,TP,F0,ISEED3,ISEED4,N0,ARCLUT)
C THIS GENERATES GAUSSIAN SPECTRUM SAMPLES
```

```
      C) COMPLEX C,CP,SUM,CX,AG,AE,CRSP,ARCLUT,TEMP
      DIMENSION CP(15),RS(5),CP(5),CX(5),ARCLUT(0:15,0:15)
      DIMENSION SIG, TEMP(0:15),SN(5)
      PI=3.141592
      DELF=0.6*F3
      NN=M-1
      A=0.0*PI/180.
      RS(1)=0.1020*PR0
      RS(2)=0.1558*PR0
      RS(3)=0.7503*PR0
      RS(4)=1.1558*PR0
      RS(5)=0.1020*PR0
      N=5
      T3=T3SQRD3
      T4=T3SQRD4
      VAR=1.0
      CALL CRSQCP(CP,T3,N5,T4,VAR)
      T3SQRD3=T3
      T3SQRD4=T4
      DO 20 N=1,5
      CRSN=CMPLX(RSP(N),0.0)
      CX(N)=CP(N)*CRSN
20    CONTINUE
      DO 30 K=0,M-1
      SUM=(0.0,0.0)
      DO 40 N=1,5
      AA=F0+(FLOAT(N)-3.0)*DELF
      AB=AA**K*TP*2.0*PI
      AG=CMPLX(0.0,AB)
      AE=CEXP(AG)
      SUM=SUM+CX(N)*AE
40    CONTINUE
      C(K)=SUM
30    CONTINUE
      IF(10.NE.1)GO TO 700
      TYPE 50,F3,F0
50    FORMAT(1H0,'F3DB=',F6.2,'F0=',F6.2)
      TYPE *,(C(K),K=0,M-1)
C TO CALCULATE COVARIANCE OF CLUTTER SAMPLES BY THEORY
      DO 80 K=0,M-1
      SUM=(0.0,0.0)
      DO 90 N=1,5
      DO 70 I=1,5
      SN(I)=RSN(I)**2
70    CONTINUE
      CRSN=CMPLX(SN(N),0.0)
      AA=F0+(FLOAT(N)-3.0)*DELF
      AB=AA*2.0*PI*TP*K
      AG=CMPLX(0.0,AB)
      AE=CEXP(AG)
      SUM=SUM+AE*CRSN
90    CONTINUE
      TEMP(K)=SUM
80    CONTINUE
      TYPE *,(TEMP(K),K=0,M-1)
      DO 190 J=0,M-1
      DO 100 K=0,J
      ARCLUT(J,K)=TEMP(J-K)
100   CONTINUE
      IF(J.EQ.(M-1))GO TO 190
      DO 110 K=J+1,M-1
```

```
      ARCLUT(J,K)=CONJG(TEMP(K-J))
110   CONTINUE
100   CONTINUE
C     TYPE 120
120   FORMAT(1X,'MATRIX ARCLUT:COVARIANCE MATRIX OF CLUTTER')
      DO 130 J=0,M-1
C     TYPE 130,(ARCLUT(J,K),K=0,J-1)
130   FORMAT(1X,4(E12.5,3X,E12.5,5X))
140   CONTINUE
70    CONTINUE
      END
      SUBROUTINE GENCP(CP,ISEED3,NS,ISEED4,M0)
      COMPLEX CP(NS),C,S
      REAL M0
      DIMENSION R1(5),R2(5),THETA(5),RAYL(5),C(5),S(5)
C     TYPE *,ISEED3
      CALL GGUBS(ISEED3,NS,R1)
C     TYPE *,ISEED3
C     TYPE *,(R1(K),K=1,NS)
      PI=3.14159265
      DO 10 I=1,NS
      THETA(I)=2.0*PI*R1(I)
      C(I)=CMPLX(0.0,THETA(I))
10    CONTINUE
      SM0=SQRT(M0)
      AMEAN=1.0
C     TYPE *,ISEED4
      CALL GGEXP(ISEED4,AMEAN,NS,R2)
C     TYPE *,ISEED4
C     TYPE *,(R2(K),K=1,NS)
      DO 20 I=1,NS
      RAYL(I)=(SQRT(R2(I)))*(SM0)
      S(I)=CEXP(C(I))
      CP(I)=S(I)*RAYL(I)
C     TYPE *,CP(I)
20    CONTINUE
      RETURN
      END
```

```
      SUBROUTINE SUMUP(INT,CWGN,D,M)
      COMPLEX INT(0:15),CWGN(0:15),D(0:15)
      DO 10 J=0,M-1
      INT(J)=CWGN(J)+D(J)
10    CONTINUE
      RETURN
      END
```

```
      SUBROUTINE COEFS(R,N,T,P,PPE,MAXORD)
      COMPLEX R,T,P,C,PNUM,PDEN,CB,CC
      COMPLEX TTT,TT
      DIMENSION R(0:15),T(0:15,0:15)
      DIMENSION B(0:15,0:15)
      DIMENSION C(0:15,0:15),P(0:15),PPE(0:15)
      SUP=0.0
      DO 10 J=0,N-1
      PL=CABS(P(J))
      SUP=SUP+PL*PL
10    CONTINUE
      P(N)=SUP/(FLOAT(M))
      M=1
      DO 20 J=0,N-2
      B(M,J)=P(J)
      C(M,J)=P(J+1)
20    CONTINUE
      DO 25 J=1,MAXORD
      T(J,J)=(1.0,0.0)
25    CONTINUE
100   PNUM=(0.0,0.0)
      PDEN=(0.0,0.0)
      M=N-1-M
      DO 30 J=0,MM
      CB=CONJG(B(M,J))
      PNUM=PNUM+C(M,J)*CB
      CC=CONJG(C(M,J))
      PDEN=PDEN+B(M,J)*CB+C(M,J)*CC
30    CONTINUE
C CALCULATION OF PREDICTION ERROR COEFFICIENTS
      T(M,M)=(2.0,0.0)*PNUM/PDEN
      RL=CABS(T(M,M))
      P(0)=P(0-1)*(1.-RL*RL)
      PPE(M)=P(M)*(FLOAT(M+M+1))/(FLOAT(M-M-J))
      IF(M.EQ.1)GO TO 60
      DO 40 J=1,M-1
      TTT=CONJG(T(M-1,M-J))
      T(M,J)=T(M-1,J)+T(M,M)*TTT
40    CONTINUE
60    IF(M.EQ.MAXORD)GO TO 1000
      M=M+1
      DO 90 J=0,M-1-M
      TT=CONJG(T(M-1,M-1))
      B(M,J)=B(M-1,J)+TT*C(M-1,J)
      C(M,J)=C(M-1,J+1)+T(M-1,M-1)*B(M-1,J+1)
90    CONTINUE
      GO TO 100
1000  RETURN
      END
```

```
      SUBROUTINE AVMEM(TET,PP,FFPE,T,P,FPE,MAXORD,MINO3)
      COMPLEX TET,T,ASUM,AA
      DIMENSION TET(30,0:15,0:15),PP(30,0:15),FFPE(30,0:15)
      DIMENSION PPE(0:15), P(0:15),T(0:15,0:15)
      DO 300 J=1,MAXORD
      ASUM=0.0
      NUMB=0.0
      DO 310 K=1,NUMB
      SUM=SUM+FFPE(K,J)
      ASUM=ASUM+PP(K,J)
310   CONTINUE
      FPE(J)=(SUM)/(FLOAT(NUMB))
      P(J)=(ASUM)/(FLOAT(NUMB))
300   CONTINUE
      SUM=0.0
      DO 320 J=1,NUMB
      SUM=SUM+PP(J,0)
320   CONTINUE
      P(0)=(SUM)/(FLOAT(NUMB))
      DO 330 J=1,MAXORD
      DO 340 K=0,J
      ASUM=(0.0,0.0)
      DO 350 I=1,NUMB
      ASUM=ASUM+TET(I,J,K)
350   CONTINUE
      A=FLOAT(NUMB)
      AA=CMPLX(A,0.0)
      T(J,K)=(ASUM)/(AA)
340   CONTINUE
330   CONTINUE
      RETURN
      END
```

```
      SUBROUTINE RCMEM(M,MAXORD,T,FPE,P,ACINV,TAP,MINORD)
      COMPLEX T,TAP,AC,ACINV
      COMPLEX PHI,ASUM,PT,TM,TMTC,PDM,CPW,TMP
      DIMENSION T(0:15,0:15),TAP(0:15)
      DIMENSION AC(0:15,0:15),ACINV(0:15,0:15)
      DIMENSION P(0:15),FPE(0:15),PHI(0:15)
      DIMENSION TM(0:15,0:15),TMTC(0:15,0:15),PDM(0:15,0:15)
      DIMENSION TMP(0:15,0:15)
      FMIN=0.100E+20
      MINORD=0
      TAP(0)=(1.0,0.0)
      DO 500 N=1,MAXORD
      IF(FPE(N).GE.FMIN)GO TO 500
      FMIN=FPE(N)
      MINORD=N
      PMIN=P(N)
500   CONTINUE
```

```
C GENERATION OF TAP COEFFICIENTS
      DO 520 I=1,MINORD
      PAP(I)=T(MINORD,I)
520   CONTINUE
C GENERATION OF COVARIANCE MATRIX
100   PHI(0)=CMPLX(P(0),0.0)
      DO 110 I=1,MINORD
      ASUM=(0.0,0.0)
      DO 120 K=1,I
      ASUM=ASUM+PHI(I-K)*T(I,K)
120   CONTINUE
      PHI(I)=ASUM
110   CONTINUE
      DO 130 I=MINORD+1,M-1
      ASUM=(0.0,0.0)
      DO 140 K=1,MINORD
      ASUM=ASUM+PHI(I-K)*T(MINORD,K)
140   CONTINUE
      PHI(I)=ASUM
130   CONTINUE
      TYPE *,(PHI(J),J=0,M-1)
      DO 150 J=0,M-1
      DO 160 K=0,J
      AC(J,K)=PHI(J-K)
160   CONTINUE
      IF(I.EQ.(M-1))GO TO 150
      DO 170 K=I+1,M-1
      PT=CONJG(PHI(K-I))
      AC(I,K)=PT
170   CONTINUE
150   CONTINUE
C GENERATION OF INVERSE COVARIANCE MATRIX
C  FIRST GENERATE TM MATRIX
C  FIRST INITIALISE TO ZERO
      DO 190 J=0,M-1
      DO 200 K=0,M-1
      TM(K,J)=(0.0,0.0)
200   CONTINUE
190   CONTINUE
C ACTUAL GENERATION OF TM MATRIX
      DO 210 J=0,M-1-MINORD
      DO 220 K=0,MINORD
      TM(K+J,J)=T(MINORD,K)
220   CONTINUE
210   CONTINUE
      T(0,0)=(1.0,0.0)
      NNN=MINORD
      DO 230 J=M-MINORD,M-1
      NNN=NNN-1
      DO 240 K=0,NNN
      TM(K+J,J)=T(NNN,K)
240   CONTINUE
230   CONTINUE
C GENERATE TMTC MATRIX
      DO 250 J=0,M-1
      DO 260 K=0,M-1
      TMTC(J,K)=CONJG(TM(K,J))
260   CONTINUE
250   CONTINUE
C GENERATION OF POWER(POW) MATRIX
      DO  270 J=0,M-1
```

```
      DO 280 K=0,K=1
      PROD(I,K)=(0.0,0.0)
280   CONTINUE
270   CONTINUE
      DO 290 J=0,M=1-MINORD
      CPJ=CMPLX(P(I+MINORD),0.0)
      DO (I,J)=(1.0,0.0)/CPJ
290   CONTINUE
      J=M-MINORD
      DO 300 I=M-MINORD,M=1
      J=J+1
      CPJ=CMPLX(P(J+M),0.0)
      DO(I,J)=(1.0,0.0)/CPJ
300   CONTINUE
C MATRIX MULTIPLICATION TO GIVE INVERSE COVARIANCE MATRIX ACINV=INV(AC)
      DO 310 I=0,M=1
      DO 320 J=0,M=1
      TMP(I,J)=(0.0,0.0)
      DO 330 K=0,M=1
      TMP(I,J)=TMP(I,J)+PM(I,K)*PROD(K,J)
330   CONTINUE
320   CONTINUE
310   CONTINUE
C ACINV=TMP*INVC
      DO 360 I=0,M=1
      DO 350 J=0,M=1
      ACINV(I,J)=(0.0,0.0)
      DO 360 K=0,M=1
      ACINV(I,J)=ACINV(I,J)+TMP(I,K)*INVC(K,J)
360   CONTINUE
350   CONTINUE
340   CONTINUE
C OUTPUTTING RESULT OF MEM ANALYSIS
1085  TYPE 1090,MINORD,PMIN,FMIN,M
1090  FORMAT(1H ,'MINORD=',I2,5X,'PMIN=',E15.8,5X,'FMIN=',
     1 E15.8,5X,'NO OF HITS/SCAN=',I3)
      TYPE 1100
1100  FORMAT(1H ,'THE TAP COEFFICIENTS ARE')
      TYPE 1110,(TAP(J),J=0,MINORD)
1110  FORMAT(1H0,E15.8,5X,E15.8)
      TYPE 1130
1130  FORMAT(1H0,'THE T(N,K) MATRIX IS')
      DO 1140 J=0,MINORD
      TYPE  1020,(T(J,K),K=0,J)
1140  CONTINUE
1142  TYPE 1150,P(0)
1150  FORMAT(1H0,'P(0)=',E15.8)
      TYPE 1160
1160  FORMAT(1H0,'ORDER',20X,'FPE',20X,'P')
      DO 1066 J=1,MAXORD
      TYPE 1170,J,FPE(J),P(J)
1170  FORMAT(1H0,10X,I2,10X,E15.8,10X,E15.8)
1066  CONTINUE
      TYPE 1025
1025  FORMAT(1H0,'COVARIANCE MATRIX AC')
      DO 1030 J=0,M=1
      TYPE 1020,(AC(J,K),K=0,M=1)
1020  FORMAT(1H0,4(E12.5,3X,E12.5,5X))
1030  CONTINUE
      TYPE 1035
1035  FORMAT(1H0,'INVERSE COVARIANCE MATRIX ACINV')
```

```
      DO 1045 J=0,M-1
      TYPE 1020,(ACINV(J,K),K=0,M-1)
1040  FORMAT(/)
      TYPE 1035
1035  FORMAT(100,'MATRIX TM')
      DO 1050 J=0,M-1
      TYPE 1020,(TM(J,K),K=0,M-1)
1050  FORMAT(/)
      TYPE 1055
1055  FORMAT(100,'MATRIX TMTC')
      DO 1045 J=0,M-1
      TYPE 1020,(TMTC(J,K),K=0,M-1)
1045  FORMAT(/)
1500  RETURN
      END
```

```
      SUBROUTINE PFREA(ARCLUT,ACINV,M,PP,PT,FD,RD,ARINT,ATARG)
      REAL RD
      COMPLEX ARCLUT,ACINV,ATARG,U,V,AC,AD,TEMPA,TEMPB,TEMP
      COMPLEX ARINT,SUM,DELWF,DELOK,DELTU,ACTTU
      DIMENSION ARCLUT(0:15,0:15),ACINV(0:15,0:15),ARINT(0:15,0:15)
      DIMENSION TEMP(0:15),ATARG(0:15,0:15),V(0:15),U(0:15)
      DIMENSION ACTTU(0:15,0:15),ATEMP(16,16),ATEMP(16,16)
      DIMENSION WKAREA(350)
      PI=3.14159265
      PD=2.0*PI*FD
      AA=PD*PP
      DO 10 J=0,M-1
      AB=AA*FLOAT(J)
      AC=CMPLX(0.0,AB)
      U(J)=CEXP(AC)
10    CONTINUE
C     TYPE *,(U(J),J=0,M-1)
      DO 50 J=0,M-1
      AD=CMPLX(PT,0.0)
C     TYPE *,U(J)
      DO 60 K=0,J
      ATARG(J,K)=(U(J-K))*AD
60    CONTINUE
      IF(J.EQ.(M-1))GO TO 50
      DO 70 K=J+1,M-1
      ATARG(J,K)=CONJG(U(K-J))*AD
70    CONTINUE
50    CONTINUE
      DO 100 J=0,M-1
      DO 110 K=0,M-1
      ARINT(J,K)=ARCLUT(J,K)
110   CONTINUE
100   CONTINUE
      AD=CMPLX(RD,0.0)
      DO 120 JL=0,M-1
      ARINT(JL,JL)=ARCLUT(JL,JL)+AD
```

```
120     CONTINUE
C       FOR MATCHED FILTER CALCULATIONS
        CALL AMALT(ATARG,U,TEMP,M)
        SUM=(0.0,0.0)
        DO 150 JJ=0,M-1
        SUM=SUM+(TEMP(JJ))*(CONJG(U(JJ)))
150     CONTINUE
        TEMPA=SUM
        CALL AMALT(ARINT,U,TEMP,M)
        SUM=(0.0,0.0)
        DO 160 JJ=0,M-1
        SUM=SUM+TEMP(JJ)*(CONJG(U(JJ)))
160     CONTINUE
        TEMPB=SUM
        DELMF=TEMPA/TEMPB
        TYPE *,TEMPA,TEMPB
        TYPE 170,DELMF
170     FORMAT(100,'DELMF=',E15.8,10X,E15.8)
C       FOR ST. OPT RX. CALCULATIONS
        CALL AMALT(ACINV,U,V,M)
        CALL AMALT(ATARG,V,TEMP,M)
        SUM=(0.0,0.0)
        DO 210 J=0,M-1
        SUM=SUM+TEMP(J)*(CONJG(V(J)))
210     CONTINUE
        TEMPA=SUM
        CALL AMALT(ARINT,V,TEMP,M)
        SUM=(0.0,0.0)
        DO 220 J=0,M-1
        SUM=SUM+TEMP(J)*(CONJG(V(J)))
220     CONTINUE
        TEMPB=SUM
        DELOF=TEMPA/TEMPB
        TYPE *,TEMPA,TEMPB
        TYPE 230,DELOF
230     FORMAT(100,'DELOF='E15.8,10X,E15.8)
        DO 300 J=0,M-1
        DO 310 K=0,M-1
        ATEMP(J+1,K+1)=REAL(ARINT(J,K))
310     CONTINUE
300     CONTINUE
        IDGT=0
        CALL LINV2F(ATEMP,M,M,AITEMP,IDGT,WKAREA,IER)
        TYPE *,IDGT,IER
        DO 400 J=0,M-1
        DO 410 K=0,M-1
        ACTIN(J,K)=CMPLX(AITEMP(J+1,K+1),0.0)
410     CONTINUE
400     CONTINUE
        CALL AMALT(ACTIN,U,V,M)
        CALL AMALT(ATARG,V,TEMP,M)
        SUM=(0.0,0.0)
        DO 250 J=0,M-1
        SUM=SUM+TEMP(J)*(CONJG(V(J)))
250     CONTINUE
        TEMPA=SUM
        CALL AMALT(ARINT,V,TEMP,M)
        SUM=(0.0,0.0)
        DO 260 J=0,M-1
        SUM=SUM+TEMP(J)*(CONJG(V(J)))
260     CONTINUE
```

```
      TEMPA=SUM
      DELTH=TEMPA/TEMPB
      TYPE *,TEMPA,TEMPB
      TYPE 270,DELTH
270   FORMAT(1H0,'DELTH=',E15.8,10X,E15.8)
700   RETURN
      END
      SUBROUTINE AMALT(AMAT,VECT,RES,M)
      COMPLEX AMAT,VECT,RES,SUM
      DIMENSION AMAT(0:15,0:15),VECT(0:15),RES(0:15)
      DO 10 J=0,M-1
      SUM=(0.0,0.0)
      DO 20 K=0,M-1
      SUM=SUM+AMAT(J,K)*VECT(K)
20    CONTINUE
      RES(J)=SUM
10    CONTINUE
      RETURN
      END
```

```
      SUBROUTINE TOTMAT(ARINT,ATARG,ATOT,M)
      COMPLEX ARINT,ATARG,ATOT
      DIMENSION ARINT(0:15,0:15),ATARG(0:15,0:15),ATOT(0:15,0:15)
      DO 10 J=0,M-1
      DO 20 K=0,M-1
      ATOT(J,K)=ARINT(J,K)+ATARG(J,K)
20    CONTINUE
10    CONTINUE
      RETURN
      END
```

```
      SUBROUTINE PERFBA(ATOT,ARINT,M,ALAM,AMU,NLT)
      COMPLEX ATOT,DMTI,CMTI,ATEMP,BTEMP,ARINT,TMTI,TCMTI
      DIMENSION ATOT(0:15,0:15),ALAM(0:15),AMU(0:15),ARINT(0:15,0:15)
      DIMENSION DMTI(0:15,0:15),CMTI(0:15,0:15),ATEMP(0:15,0:15)
      DIMENSION BTEMP(0:15,0:15),TMTI(0:15,0:15)
C     PF AND PD FOR AN NTI RECEIVER SYSTEM
      NLT=14
      DO 30 J=0,M-1
      DO 40 K=0,M-1
      DMTI(J,K)=(0.0,0.0)
40    CONTINUE
30    CONTINUE
```

```
      DMTI(0,0)=(1.0,0.0)
      DMTI(1,0)=(-2.0,0.0)
      DMTI(1,1)=(1.0,0.0)
      DMTI(2,0)=(1.0,0.0)
      DMTI(2,1)=(-2.0,0.0)
      DMTI(2,2)=(1.0,0.0)
      DO 50 J=3,M-1
      DO 60 K=J-2,J
      DMTI(J,K)=DMTI(J-1,K-1)
60    CONTINUE
50    CONTINUE
      DO 85 J=0,NLT-1
      DO 86 K=0,M-1
      TMTI(J,K)=DMTI(J+2,K)
86    CONTINUE
85    CONTINUE
      DO 87 J=0,NLT-1
      DO 88 K=0,M-1
      DMTI(J,K)=TMTI(J,K)
88    CONTINUE
87    CONTINUE
      DO 92 J=0,M-1
      DO 93 K=0,NLT-1
      CDMTI(J,K)=CONJG(DMTI(K,J))
93    CONTINUE
92    CONTINUE

C     FOR PF EIGENVALUES, BTEMP=DMTI*ARINT*CDMTI
      CALL TMULT(DMTI,ARINT,ATEMP,M,NLT,M)
      CALL TMULT(ATEMP,CDMTI,BTEMP,M,NLT,NLT)
      CALL FINDE(BTEMP,NLT,ALAM)
      TYPE 100
100   FORMAT(1H0,'EIGENVALUES FOR PF USING MTI RECEIVER SYSTEM ARE')
      TYPE *,(ALAM(J),J=0,NLT-1)
C     FOR PD EIGENVALUES,BTEMP=DMTI*ATOT*CDMTI
      CALL TMULT(DMTI,ATOT,ATEMP,M,NLT,M)
      CALL TMULT(ATEMP,CDMTI,BTEMP,M,NLT,NLT)
C     FIND EIGENVALUES OF BTEMP
      CALL FINDE(BTEMP,NLT,AMU)
      TYPE 200
200   FORMAT(1H0,'EIGENVALUES FOR PD USING MTI RECEIVER SYSTEM ARE')
      TYPE *,(AMU(J),J=0,NLT-1)
      RETURN
      END
```

```
      SUBROUTINE PERFBB(ATOT,ARINT,M,ALAM,AMU)
      COMPLEX ATOT,ARINT
      DIMENSION ATOT(0:15,0:15),ALAM(0:15),AMU(0:15),ARINT(0:15,0:15)
C     PF AND PD FOR A MATCHED FILTER RECEIVER
C     FOR PF FIND EIGENVALUES OF ARINT
      CALL FINDE(ARINT,M,ALAM)
```

```
      TYPE 100
100   FORMAT(1H0,'EIGENVALUES FOR PF USING MATCHED FILTER BY ARE')
      TYPE *,(CLAM(J),J=0,M-1)
C     FOR PD FIND EIGENVALUES OF ATOT
      CALL EIGOE(ATOT,M,CMU)
      TYPE 200
200   FORMAT(1H0,'EIGENVALUES FOR PD USING MATCHED FILTER BY ARE')
      TYPE *,(CMU(J),J=0,M-1)
      RETURN
      END

      SUBROUTINE PEREBC(ATOT,ARINT,M,TAP,MINORD,CLAM,CMU,NLT,PD,PF)
      COMPLEX ATOT,ARINT,TAP,ATEMP,BTEMP,CTEMP,DTEMP,TMTI,CONJG
      COMPLEX AC,UT,RT,SUM,ADEN,ANUM,PELSTR
      DIMENSION ATOT(0:15,0:15),ARINT(0:15,0:15),TAP(0:15)
      DIMENSION CLAM(0:15),CMU(0:15),ATEMP(0:15,0:15)
      DIMENSION BTEMP(0:15,0:15),CTEMP(0:15,0:15),DTEMP(0:15,0:15)
      DIMENSION TMTI(0:15,0:15),UT(0:15),RT(0:15)
C     PF AND PD FOR STRUCTURED RECEIVER
      NLT=M-MINORD
      DO 10 J=0,M-1
      DO 20 K=0,M-1
      ATEMP(J,K)=(0.0,0.0)
20    CONTINUE
10    CONTINUE
      DO 30 J=0,MINORD
      DO 40 K=0,J
      I=J-K
      ATEMP(J,K)=TAP(I)
40    CONTINUE
30    CONTINUE
      DO 50 J=MINORD+1,M-1
      DO 60 K=J-MINORD,J
      ATEMP(J,K)=ATEMP(J-1,K-1)
60    CONTINUE
50    CONTINUE
      DO 85 J=0,NLT-1
      DO 86 K=0,M-1
      TMTI(J,K)=ATEMP(J+MINORD,K)
86    CONTINUE
85    CONTINUE
      DO 87 J=0,NLT-1
      DO 88  K=0,M-1
      ATEMP(J,K)=TMTI(J,K)
88    CONTINUE
87    CONTINUE
      DO 96 J=0,M-1
      DO 97 K=0,NLT-1
      BTEMP(J,K)=CONJG(ATEMP(K,J))
97    CONTINUE
96    CONTINUE
```

```
C       FOR  PERF. OF THIS ST. RX WITH CURRENT DETECTION
        PI=3.14159265
        WD=2.0*PI*FD
        AA=WD*TD
        DO 610 J=0,NLT-1
        AB=AA*FLOAT(J)
        AC=CMPLX(0.0,AB)
        UT(J)=CEXP(AC)
610     CONTINUE
C       DTEMP=ATEMP*ARINT*BTEMP
        CALL TMULT(ATEMP,ARINT,CTEMP,M,NLT,M)
        CALL TMULT(CTEMP,BTEMP,DTEMP,M,NLT,NLT)
        CALL VECT(DTEMP,UT,RT,NLT)
        SUM=(0.0,0.0)
        DO 620 J=0,NLT-1
        SUM=SUM+RT(J)*(CONJG(UT(J)))
620     CONTINUE
        ADEN=SUM
C       FIND EIGENVALUES OF DTEMP, FOR PF
        CALL FINDE(DTEMP,NLT,CLAM)
        TYPE 100
100     FORMAT(1H0,'EIGENVALUES FOR PF USING STRUCTURED RECEIVER ARE')
        TYPE *,(CLAM(J),J=0,NLT-1)
C       DTEMP=ATEMP*ATOT*BTEMP
        CALL TMULT(ATEMP,ATOT,CTEMP,M,NLT,M)
        CALL TMULT(CTEMP,BTEMP,DTEMP,M,NLT,NLT)
        CALL VECT(DTEMP,UT,RT,NLT)
        SUM=(0.0,0.0)
        DO 630 J=0,NLT-1
        SUM=SUM+RT(J)*(CONJG(UT(J)))
630     CONTINUE
        ANUM=SUM
C       FIND EIGENVALUES OF DTEMP, FOR PD
        CALL FINDE(DTEMP,NLT,CMU)
        TYPE 200
200     FORMAT(1H0,'EIGENVALUES FOR PD USING STRUCTURED RECEIVER ARE')
        TYPE*,(CMU(J),J=0,NLT-1)
        DELSTM=(ANUM-ADEN)/ADEN
        TYPE *,ANUM,ADEN
        TYPE 642,DELSTM
642     FORMAT(1H0,'DELSTM=',E15.8,10X,E15.8)
        RETURN
        END
```

```
        SUBROUTINE PERFTA(ATOT,ARINT,M,ALAM,AMU)
        COMPLEX ATOT,DMTI,CDMTI,ATEMP,BTEMP,ARINT
        DIMENSION ATOT(0:15,0:15),ALAM(0:15),AMU(0:15),ARINT(0:15,0:15)
        DIMENSION DMTI(0:15,0:15),CDMTI(0:15,0:15),ATEMP(0:15,0:15)
        DIMENSION BTEMP(0:15,0:15)
C       PF AND PD FOR AN MTI RECEIVER SYSTEM
        DO 30 J=0,M-1
```

```
      DO 50 K=0,M-1
      DMTI(J,K)=(0.0,0.0)
40    CONTINUE
30    CONTINUE
      DMTI(0,0)=(1.0,0.0)
      DMTI(1,0)=(-2.0,0.0)
      DMTI(1,1)=(1.0,0.0)
      DMTI(2,0)=(1.0,0.0)
      DMTI(2,1)=(-2.0,0.0)
      DMTI(2,2)=(1.0,0.0)
      DO 50 J=3,M-1
      DO 60 K=J-2,J
      DMTI(J,K)=DMTI(J-1,K-1)
60    CONTINUE
50    CONTINUE
      DO 70 J=0,M-1
      DO 80 K=0,M-1
      CDMTI(J,K)=CONJG(DMTI(K,J))
80    CONTINUE
70    CONTINUE
C     FOR PF EIGENVALUES, BTEMP=DMTI*ARINT*CDMTI
      CALL TMULT(DMTI,ARINT,ATEMP,M,M,M)
      CALL TMULT(ATEMP,CDMTI,BTEMP,M,M,M)
C     FIND EIGENVALUES OF BTEMP
      CALL FINDE(BTEMP,M,ALAM)
      TYPE 100
100   FORMAT(1H0,'EIGENVALUES FOR PF USING MTI RECEIVER SYSTEM ARE')
      TYPE *,(ALAM(J),J=0,M-1)
C     FOR PD EIGENVALUES,BTEMP=DMTI*ATOT*CDMTI
      CALL TMULT(DMTI,ATOT,ATEMP,M,M,M)
      CALL TMULT(ATEMP,CDMTI,BTEMP,M,M,M)
C     FIND EIGENVALUES OF BTEMP
      CALL FINDE(BTEMP,M,AMU)
      TYPE 200
200   FORMAT(1H0,'EIGENVALUES FOR PD USING MTI RECEIVER SYSTEM ARE')
      TYPE *,(AMU(J),J=0,M-1)
      RETURN
      END
```

```
      SUBROUTINE PERFTC(ATOT,ARINT,M,TAP,MTNORD,CLAM,CMU,PD,PF)
      COMPLEX ATOT,ARINT,TAP,ATEMP,BTEMP,CTEMP,DTEMP
      COMPLEX AC,AD,SUM,UT,RT,APEN,AMBA,DELST
      DIMENSION ATOT(0:15,0:15),ARINT(0:15,0:15),TAP(0:15)
      DIMENSION CLAM(0:15),CMU(0:15),ATEMP(0:15,0:15)
      DIMENSION BTEMP(0:15,0:15),CTEMP(0:15,0:15),DTEMP(0:15,0:15)
      DIMENSION AD(0:15),UT(0:15),RT(0:15)
C     PF AND PD FOR STRUCTURED RECEIVER
      DO 10 J=0,M-1
      DO 20 K=0,M-1
      ATEMP(J,K)=(0.0,0.0)
20    CONTINUE
10    CONTINUE
      DO 30 J=0,MTNORD
      DO 40 K=0,J
      I=J-K
```

```
      ATEMP(J,K)=TAP(I)
40    CONTINUE
30    CONTINUE
      DO 50 J=MINORD+1,M-1
      DO 60 K=J-MINORD,J
      ATEMP(J,K)=ATEMP(J-1,K-1)
60    CONTINUE
50    CONTINUE
      DO 70 J=0,M-1
      DO 80 K=J,M-1
      ATEMP(J,K)=CONJG(ATEMP(K,J))
80    CONTINUE
70    CONTINUE
C     FOR  PEPE, OF THIS SF. RX WITH COHERENT DETECTION
      PI=3.14159265
      PD=2.0*PI*FD
      AA=PD*TP
      DO 710 J=0,MINORD
      AB=AA*FLOAT(J)
      AC=CMPLX(0.0,AB)
      AD(J)=CEXP(AC)
710   CONTINUE
      DO 720 J=0,M-1
      IF(J.GT.MINORD)GO TO 715
      SUM=(0.0,0.0)
      DO 730 K=0,J
      SUM=SUM+TAP(K)*AD(J-K)
730   CONTINUE
      UT(J)=SUM
      GO TO 720
715   AB=AA*FLOAT(J-MINORD)
      AC=CMPLX(0.0,AB)
      UT(J)=(CEXP(AC))*(UT(MINORD))
720   CONTINUE
C
      DTEMP=ATEMP*ARINT*BTEMP
      CALL TMULT(ATEMP,ARINT,CTEMP,M,M,M)
      CALL TMULT(CTEMP,BTEMP,DTEMP,M,M,M)
      CALL VECT(DTEMP,UT,RT,M)
      SUM=(0.0,0.0)
      DO 760 J=0,M-1
      SUM=SUM+RT(J)*(CONJG(UT(J)))
760   CONTINUE
      ADEN=SUM
C     FIND EIGENVALUES OF DTEMP, FOR PP
      CALL FINDE(DTEMP,M,CLAM)
      TYPE 100
100   FORMAT(1HO,'EIGENVALUES FOR PP USING STRUCTURED RECEIVER ARE')
      TYPE *,(CLAM(J),J=0,M-1)
C     DTEMP=ATEMP*ATOT*BTEMP
      CALL TMULT(ATEMP,ATOT,CTEMP,M,M,M)
      CALL TMULT(CTEMP,BTEMP,DTEMP,M,M,M)
      CALL VECT(DTEMP,UT,RT,M)
      SUM=(0.0,0.0)
      DO 780 J=0,M-1
      SUM=SUM+RT(J)*(CONJG(UT(J)))
780   CONTINUE
      ANUM=SUM
C     FIND EIGENVALUES OF DTEMP, FOR PD
      CALL FINDE(DTEMP,M,CLAM)
      TYPE 200
200   FORMAT(1H0,'EIGENVALUES FOR PD USING STRUCTURED RECEIVER ARE')
```

```
      TYPE*,(CMU(J),J=0,M-1)
      DELST=(ANUM-ADEN)/ADEN
      TYPE *,ANUM,ADEN
      TYPE 820,DELST
820   FORMAT(1X,'DELST=',E15.8,10X,E15.8)
      RETURN
      END
      SUBROUTINE TMULT(AT,BT,CT,M,NLT,NUX)
      COMPLEX AT,BT,CT
      DIMENSION AT(0:15,0:15),BT(0:15,0:15),CT(0:15,0:15)
      DO 10 I=0,NLT-1
      DO 20 J=0,NUX-1
      CT(I,J)=(0.0,0.0)
      DO 30 K=0,M-1
      CT(I,J)=CT(I,J)+AT(I,K)*BT(K,J)
30    CONTINUE
20    CONTINUE
10    CONTINUE
      RETURN
      END
      SUBROUTINE FINDE(BTEMP,M,TLAM)
      COMPLEX BTEMP,XTEMP,VTEMP,XLAM
      DIMENSION XTEMP(16,16),VTEMP(16,16),XLAM(16)
      DIMENSION BTEMP(0:15,0:15),WK(600),TLAM(0:15)
      NCN=1
      IJOB=0
      IZ=16
      DO 10 J=0,M-1
      DO 20 K=0,M-1
      JJ=J+1
      KK=K+1
      XTEMP(JJ,KK)=BTEMP(J,K)
20    CONTINUE
10    CONTINUE
      CALL EIGCC(XTEMP,NCN,IZ,IJOB,XLAM,VTEMP,IZ,WK,IER)
      DO 30 J=0,M-1
      TLAM(J)=REAL(XLAM(J+1))
30    CONTINUE
      RETURN
      END
      SUBROUTINE VECT(AT,BT,CT,M)
      COMPLEX AT,BT,CT,SUM
      DIMENSION AT(0:15,0:15),BT(0:15),CT(0:15)
      DO 10 J=0,M-1
      SUM=(0.0,0.0)
      DO 20 K=0,M-1
      SUM=SUM+AT(J,K)*BT(K)
20    CONTINUE
      CT(J)=SUM
10    CONTINUE
      RETURN
      END
```

```
      SUBROUTINE PROD(ALAM,AMU,CLAM,CMU,PLTA,BLTB,BL,VT)
      DOUBLE PRECISION XLAM,XMU,YLAM,YMU,PFA,PDA,PFB,PDB,TEMP,VT
      DIMENSION XLAM(0:15),XMU(0:15),YLAM(0:15),YMU(0:15)
      DIMENSION PFA(100),PDA(100),PFB(100),PDB(100),TEMP(0:15),VT(100)
      DIMENSION ALAM(0:15),AMU(0:15),CLAM(0:15),CMU(0:15)
      M=16
      DO 990 J=0,15
      XLAM(J)=ALAM(J)
      XMU(J)=AMU(J)
      YLAM(J)=CLAM(J)
      YMU(J)=CMU(J)
990   CONTINUE
C     FOR PF OF MTI RECEIVER
      CALL PROD(XLAM,TEMP,NLTA)
      CALL CALC(XLAM,VT,TEMP,PFA,NLTA,NL)
C     FOR PD OF MTI RECEIVER
      CALL PROD(XMU,TEMP,NLTA)
      CALL CALC(XMU,VT,TEMP,PDA,NLTA,NL)
C     FOR PF OF STRUCTURED RECEIVER
      CALL PROD(YLAM,TEMP,NLTB)
      CALL CALC(YLAM,VT,TEMP,PFB,NLTB,NL)
C     FOR PD OF STRUCTURED RECEIVER
      CALL PROD(YMU,TEMP,NLTB)
      CALL CALC(YMU,VT,TEMP,PDB,NLTB,NL)
      TYPE 100
100   FORMAT(1H0,10X,'VT',20X,'PF(MTI)',15X,'PD(MTI)',15X,'PF(ST)',15X
     &,'PD(ST)')
      DO 60 J=1,NL
      TYPE 200,VT(J),PFA(J),PDA(J),PFB(J),PDB(J)
200   FORMAT(1H0,5X,5(D15.8,5X))
60    CONTINUE
      RETURN
      END
      SUBROUTINE PROD(ALAM,TEMP,M)
      DOUBLE PRECISION ALAM,TEMP,ATEMP,AL,BL
      DIMENSION ALAM(0:15),TEMP(0:15)
      DO 10 J=0,M-1
      ATEMP=1.0
      DO 20 K=0,M-1
      IF(K.EQ.J)GO TO 20
      AL=ALAM(K)/ALAM(J)
      BL=1.0-AL
      ATEMP=ATEMP*BL
20    CONTINUE
      TEMP(J)=ATEMP
10    CONTINUE
      RETURN
      END
      SUBROUTINE CALC(XM,VT,TEMP,PR,M,NL)
      DOUBLE PRECISION XM,VT,TEMP,PR,ATEMP,AL,BL,CL
      DIMENSION XM(0:15),TEMP(0:15),VT(100),PR(100),BL(0:15),CL(0:15)
      DO 10 K=1,NL
      ATEMP=0.0
      DO 20 J=0,M-1
      AL=-(VT(K)/XM(J))
      BL(J)=DEXP(AL)/TEMP(J)
20    CONTINUE
      DO 30 J=0,14,2
      CL(J)=BL(J)+BL(J+1)
30    CONTINUE
      DO 40 J=0,12,4
```

A 66003

CD 6.72.9

EE-1980-M-VIS-ADA